CHARLES UNIVERSITY IN PRAGUE
2ND MEDICAL SCHOOL

AGE RELATED CHANGES IN VESTIBULO-OCULAR REFLEX

Ph.D. Thesis

2006 Richard Brzezny

CHARLES UNIVERSITY IN PRAGUE
2ND MEDICAL SCHOOL

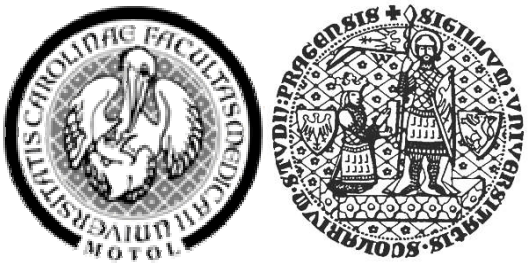

AGE RELATED CHANGES IN VESTIBULO-OCULAR REFLEX

Ph.D. Thesis

Richard Brzezny

Prague 2006

CHARLES UNIVERSITY IN PRAGUE - 2ND MEDICAL SCHOOL

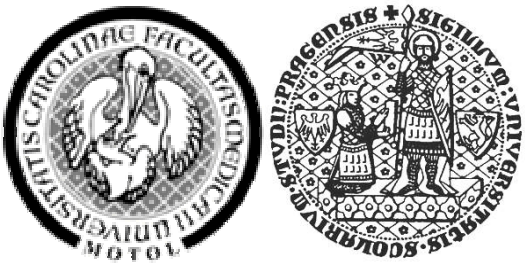

AGE RELATED CHANGES IN VESTIBULO-OCULAR REFLEX

Richard Brzezny

Ph.D. Thesis in Neurosciences, September 2006

Thesis supervisor: Doc.MUDr. Jaroslav Jeřábek, CSc.

Department of Neurology, Charles University in Prague - 2nd Medical School, The Motol University Hospital, Czech Republic.

Usus magister est optimus
(Cicero, Pro C. Rabirio Postumo)

Médeis ageómtrétos eisitó
(Accademia Platonica)

Brevis esse laboro, obscurus fio
(Horatius, De arte poetica)

Acknowledgements

Having glanced through a fair number of doctoral dissertations myself, I believe the acknowledgements to be one of the most widely read sections. It is where the author, for a brief moment, can stray away from the dryness of academic writing to explicate his way to acquired experiences, the years of toil, to explain frustrations or achievements, and, above the all, to express the accumulated gratitude.

My years of vestibular research had begun during my 9th semester of my medical studies. Neuroothology lab of the Department of Neurology, 2nd School of Medicine at the Charles University was looking for new pre-gradual scientific colleagues. I found this topic most intriguing among other exciting issues of neuroscience—the keenest to my interests. I began to work as a member of an enduring and seasoned team, enriching myself greatly with the key fundamentals of neurosciences and neurology especially.

First of all, there would be no great concern with the vestibular questions on my part without permanent effect of the enduring discussions, stimulating appeals and memorable exchanges with my supervisor Dr. Jaroslav Jeřábek, to whom I hereby wish to express my greatest gratitude. Thanks to the other team constituent member, Dr. Rudolf Černý, I began understand the importance of other scientific areas in the medical research, like algebra or physics, to name the few, and also the meaning of the word "detail". Many highly intelligent and dedicated people have joined the group over the years. In particular, I wish to recognize and thank my very good friend and a believer in my work, Dr. Martin Vyhnálek, whose neuroscientific thinking (and a great academic future for that matter) is undoubted.

Most of my research was performed at the laboratories of the Department of Neurology at the University Hospital Munich-Grosshadern (Ludwig-Maximilians University). My visiting study and training there proved crucial to my thesis. My stays were supported by the Charles University, the Charta 77 Foundation, the hosting institution, and most notably by the European Commission via the Marie Curie Fellowship Training Program. In Munich, I received the best possible in the vestibular research: Munich's Center proved to be a highly-ranked scientific center with attributes of a world leading institution in sensorimotor research, with a long-established tradition of scientific training involving the home-grown and foreign researchers alike. Training in Grosshadern provided me with the knowledge of leading the whole process of scientific work—from a hypothesis to the publication.

Of all people on the Munich's team, my gratitude goes first and foremost to my supervisor prof. Dr. Büttner who accepted me generously as a member of his group, providing me with a full research support, free access to all required matters, and, what was especially desirable, his time whenever it was needed. I most appreciated his never-ending encouragement to a regular laboratory work leading me to be a responsible and a conscious

researcher. With my friend and closest of co-workers, Dr. Otmar Bayer, we recorded the data. Dr. Thomas Eggert showed me how to deal with the recording hardware and taught me the fundamentals of data handling instructing me in programming and data analyzing in Matlab® software. Special thanks also go to Dr. Stefan Glassauer, the superior of the Sensorimotor Center, for his continuous scientific assistance in addition to his autorship of the core analyzing programs used in this thesis.

Two very special people deserve particular mention and thanks; without them, this thesis would unlikely exist. Firstly, the thanks go to my brother, Dr. Alexander Brzezny, M.D., M.P.H. Many publications I wrote (including parts of this thesis) and many grants I applied for were checked over and tidied up by him, frequently adding essential suggestions and ideas to the mix. Certainly, our common fraternity is indubitable. I must add that his courage and fortitude have always been on my mind. Most importantly, there would be no research without a full support from my loving and devoted wife Alexandra. She has been the source of an indispensable and ever-present encouragement for me. She has been there literally forcing me to "sit-and-work" for which her I am entirely grateful. Her work on copy-editing of my scientific texts likewise deserves a notable mention here.

I also wish to acknowledge my co-workers who have been helpful during my career and during the work on this manuscript. Special thanks and appreciation go to my current superiors, Dr. Michal Tichý and Dr. Lubomír Pekař, my former supervisors, former or current colleagues and friends, and in particular supervisors at the Neurology wards at Motol, Dr. Martin Bojar and Dr. Lenka Kinštová, as well as Dr. Martin Bláha from the Neurosurgery Department, and colleagues from the Munich's lab -Xiaofang Tang, Justus Kleine, Jan Nedvídek and Sigrid Langer.

Last but not least, my wholehearted gratitude goes to my prodigious parents Jiřina and Alois for their faith and support.

The space offered here is limited. Hence, I wish to recognize and apologize to all those great men and women whose names have been omitted from the honorable mention here. Please, know, your omission has occurred through a mere coincidence. You have enriched me and helped my scientific career through your patient interactions with me. For that I cannot thank you enough.

> *...Again, one preparing for a voyage and about to traverse the wild waves cries out to wood more unsound than the boat that bears him. For the urge for profits devised this latter, and Wisdom the artificer produced it. But your providence, O Father! guides it, for you have furnished even in the sea a road, and through the waves a steady path, showing that you can save from any danger, so that even one without skill may embark. But you will that the products of your Wisdom be not idle; therefore men trust their lives even to frailest wood, and have been safe crossing the surge on a raft...[Wis 14:1-5].*

Abstract and Overview

It stands to reason, that with increasing age there is an evident rise in vestibular system abnormalities what successively lead in balance disorders. Current evidence shows that age dependent anatomical changes in the vestibular endorgans, as well as in their central pathways, inexactly reflect age related behavior of the sense of balance. However, the vestibular system performance has never been tested under natural circumstance. In my work, using a novel approach that quantitatively simulates common locomotion I aimed to describe how a function of the balance system, best represented by the vestibulo-ocular reflex (VOR) deteriorates with age.

MATERIAL AND METHODS: 38 normal human subjects divided into 3 groups according to age were studied (twelve in the young age group with age up to 30, thirteen in the middle age group: age 30-60, thirteen in the elderly group: age over 60). Subjects were tested using manually delivered, passive, in timing and direction unpredictable low amplitude (10-20°), high acceleration (>1000°/s^2) head rotations in the directions of the vestibulo-ocular reflex (VOR) – the head impulse tests. Angular displacement of the head and eye in the yaw, pitch and roll planes were recorded using the search-coil technique. The real spatial ratio of head and eye velocities, the so called γ-gain, was computed. Repeated measures analysis of variance (ANOVA) was performed.

RESULTS: I have identified an age-related deterioration in measured characteristics of function of the VOR with special effect in the roll and pitch planes with increased responses in middle-aged in compare with other age groups.The repeated measures ANOVA revealed statistically highly significant age related changes in γ-gain in pitch-plane [$F(2,26)=13.6$; $p<0.0001$] and highly significant age related changes in γ-gain in roll-plane [$F(2,31)=9.8$; $p<0.001$].

DISCUSSION AND CONCLUSION: Increase in age leads to observable histological changes in nearly all anatomic structures involved in the VOR. Even though the anatomic loss is in accordance with my results, the pattern of histological changes differs. Most of the anatomical decrease is gradient or step-like neuronal or fiber deterioration with age. In my study, the relation of γ-gain and age shows an inverse U-shaped curve indicating age dependency. Continuous central mechanisms that facilitate inputs from peripheral vestibular structures are suspected. Subsequently, in contrary to previous studies, I suggest a critical threshold age after which these essential central mechanisms are not able to serve any more resulting in decrease of VOR performance — age after which the system collapses.

Table of contents

List of figures

List of tables

I Introduction

I.1 Eye Movements

The eye movements allow us to keep and maintain the orientation in the space. To accomplish this, the brain orientates the eyes, head and body pointing the gaze towards a specific direction. The pointed gaze alone, however, would not suffice in the world where everything moves, even the viewer, and where reaction to the moving target is vital. Therefore, the second, even more important effort of the brain is to stabilize the projected picture of the observed scene on the retina, thus preventing a blurry vision. This is most efficiently realized by quick corrective eye movements. Of course, the head and body movements continue to play an important role for visual information to flow undisturbed. However, most animals, including the primates, are critically dependent on the excellent visual acuity provided by a small but neurally over-represented part of the retina—the fovea (Land, 1999;Leigh RJ, 1999;Angelaki, 2003).

Thanks to the eye-movements, viewer percepts the scene flawlessly, even when his head or the vicinity are moving. The generated impression of the surrounding environment as stationary, permitting a smooth and clear tracking of any object, is truly overwhelming. In the words of a book: “She let her eyes wander over his clipped tawny hair...” (Allen, 2003). But is it really a “wander movement” what the eyes do? No, they jump around with the frequency of up to 3Hz (Land, 1999).

So how does it work? There are several kinds of eye movements, varying between each other based on their main characteristics (velocity, latency of reaction, duration, accuracy), or the central pathways involved during their action. Nevertheless, they can be simply divided into the fast and slow eye movements (**Table I-A**.) (Land, 1999). Their coordination and organization is an integral part of *the oculomotor system*.

The fast eye movements, or *saccades*, have angular velocity of the eyeball movement over 500°/sec, and quickly re-orientate the eyes. Saccades are either voluntary (pointing the gaze towards an object of interest), or involuntary, as a resetting mechanism for the eye (e.g. quick phase of the nystagmic jerk). While saccade movement is performed, the visual perception is suppressed.

The slow eye movements are: optokinetic eye movements (OKN), convergence (VE) and smooth pursuit (ETT). *The optokinetic system* is needed for tracking of the environment, when large part of the visual field is moving, i.e. during the slow movement of the subject. It

complements other reflexive eye movements, especially, when a subject moves with a constant velocity. *The smooth pursuit* is utilized for following small targets traveling across a stationary background. *The (con)vergence* can move the eyes the opposite direction, making it unique among the other eye movements. Its work is to compensate for the angular discrepancy between targets of different distance in order to keep the clearest picture on the viewer's both foveae [for review, see (Leigh RJ, 1999)].

More complex eye movements are applied during the *fixational eye movements*. This group consists of small saccades called *microsaccades*, a quick *tremor* of small amplitude, and a slow *drift*. The combination of these movements seems to be crucial for optimal viewing conditions while fixating a target, otherwise the visual perception would likely fade, probably as a consequence of a neural adaptation (Engbert & Kliegl, 2003;Gerrits & Vendrik, 1970;Leigh RJ, 1999;Martinez-Conde, Macknik et al., 2002;Moller, Laursen et al., 2002).

Velocity	Type	Role
Fast	Saccades	Fast reorientation of the gaze
	VOR	Eye movements compensating the locomotion
	Fixational eye movements	Complex of microsaccades, tremor and drift during fixation
Slow	OKN system	Compensatory eye movements during a slow locomotion
	Smooth pursuit	Foveal tracking of small targets
	Vergence	Foveal tracking in depth

Table I-A: Types and roles of human eye movements.
VOR – vestibulo-ocular reflex. OKN – optokinetic eye movements.

I.2 Vestibulo-ocular Reflex

The vestibulo-ocular reflex (VOR) has a particular place amongst the eye movements. This reflex is of the highest importance for a steady vision during head perturbations – during locomotion. Mechanoreceptors located in the inner ear react to the angular or linear accelerations and percept the change of the head movement. In quick three-neuron arc, called the *elementary vestibulo-ocular reflex arc*, respond by generating eye movements to correct the head displacement for steady picture on fovea (Leigh RJ, 1999).

I.2.1 Histological and Anatomical Properties of the VOR

I.2.1.1 The Sensory Organs

The organs responsible for detecting of quick head accelerations are located in the inner ear [for review, see (James, 1991;Druga & Petrovický, 1991)]. The inner ear is also called *the labyrinth*. It has its *bony* and *membranous* parts and lies bilaterally in the temporal

bones of the skull. The membranous labyrinth is encased in the bony labyrinth and between them is *perilymph*, fluid that originates from plasma, and acts as a mechanical buffer. Its ionic composition is similar to the cerebro-spinal fluid—it is thought that perilymph is secreted by the arterioles of the bony labyrinth periosteum. The membranous labyrinth is made up of a simple epithelium and in specialized regions specializes into a sensory epithelium serving as a transducing structure for audition or acceleration. According to their function the labyrinth is divided into the auditory and *vestibular portion* (**Figure I-1**).

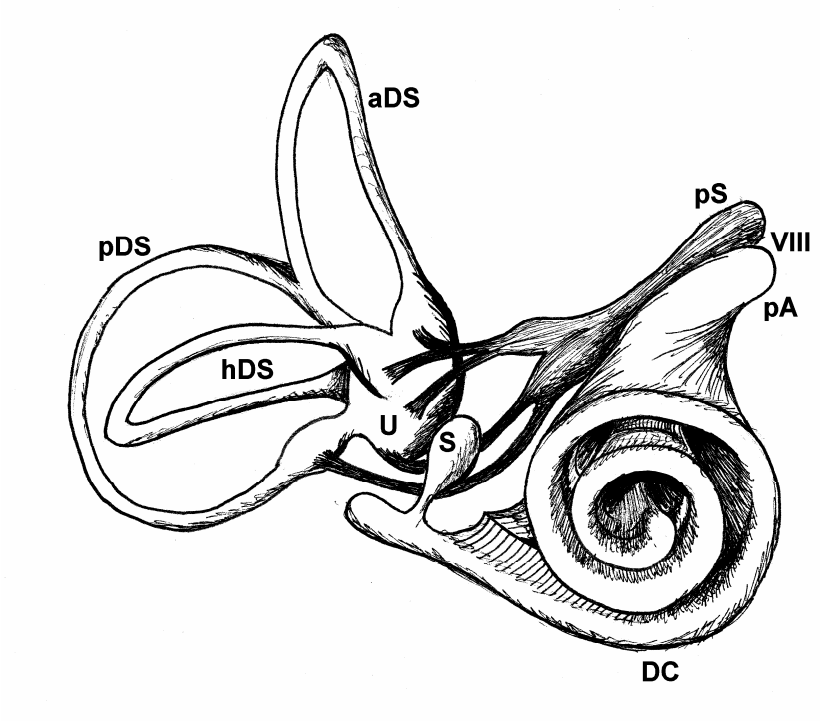

Figure I-1: The membranous labyrinth.
Vestibular portion: U – utricle, S – saccule, pDS – posterior semicircular duct, aDS – anterior semicircular duct, hDS – lateral semicircular duct (horizontal),
Auditory portion: DC – cochlear duct,
VIII – vestibuloauditory nerve, pS – vestibular part, pA – cochlear part. Redrawn from: (Feneis, 1974).

The vestibular portion of the membranous labyrinth consists of two principal sets of structure:

1. *Otolith sense organs* – pair of sac-like eminences called the *utriculus* and the *sacculus* responsible for linear acceleration perception.
2. *Semicircular ducts* – three directionally sensitive canal structures responsible for rotational acceleration perception - *lateral semicircular duct* (horizontal duct), *anterior semicircular duct* and *posterior semicircular duct* (vertical ducts).

Sacculus and utriculus are located in the middle part of the labyrinth and closely abut on the cochlear duct. Semicircular ducts lie in bony semicircular canals (SCCs) which forms the posterior part of labyrinth. SCCs are arranged in a specific manner so they can detect efficiently the movements of the head during common locomotion. The 3D reconstructions of vestibular end-organs in the temporal bones demonstrate that the angles between them are about 100° (see **Table I-B**, **Figure I-2**). This arrangement, especially between the vertical ducts,

provides larger sensitivity for *vertical (pitch)* head movements, at the expense of a lower sensitivity for *torsional (roll)* head movements (Muller & Verhagen, 2002). Left and right vertical SCC's are aligned diagonally with respect to the head. Although they are not parallel (the angle between them is around **23°-24°**), they form two approximately co-planar pairs:

- the left anterior / right posterior SCC (*LARP*) pair,
- the right anterior / left posterior SCC (*RALP*) pair,

which are approximately **45°** diagonal to head median plane – lying in the midway between planes of pitch and roll movements. Additionally, the mean measured angle between right and left horizontal canal planes is about **19 degrees**; the horizontal canals form an angle of **25 degrees** with the *Reid horizontal plane* (canthomeatal line) (Blanks, Curthoys et al., 1975;Cremer, Halmagyi et al., 1998).

Angle between			
LSD and ASD	109.9°	111.7°	101.8°
ASD and PSD	108.6°	86.2°	108.2°
PSD and LSD	96.7°	95.8°	101.3°
	(Rother, Schrock-Pauli et al., 2003)	(Blanks, Curthoys, & Markham, 1975)	(Takagi, Sando et al., 1989)

Table I-B: Angles between the planes of individual semicircular ducts.
LSD – lateral semicircular duct, ASD – anterior semicircular duct, PSD – posterior semicircular duct.

The membranous labyrinth is filled with the *endolymph*. It originates from the perilymph, and is produced mostly by the dark cells that surround the sensory epithelia. The endolymph is an unusual extracellular fluid because its ion composition is rich in potassium (and week in natrium and calcium), and is very similar to the composition of the intracellular fluids. Ionic pumps in the membranous labyrinth maintain this unique concentration, which can vary somewhat in different portions of the labyrinth but generate a potential difference between the endolymph and perilymph of less then 80mV (a bit smaller relatively to the cochlear duct). The potential serves as a battery charging a large extracellular driving force of 140 mV across the tops of the hair cells; the extracellular space is +80mV, while resting potential of receptive cells is 60mV. This driving force causes ionic current flow through channels of these cells when they are opened. Threshold responses of the cells can be directly affected by changes in extracellular potentials (James, 1991;Milhaud, Nicolas et al., 1999;Sterkers, Ferrary et al., 1988).

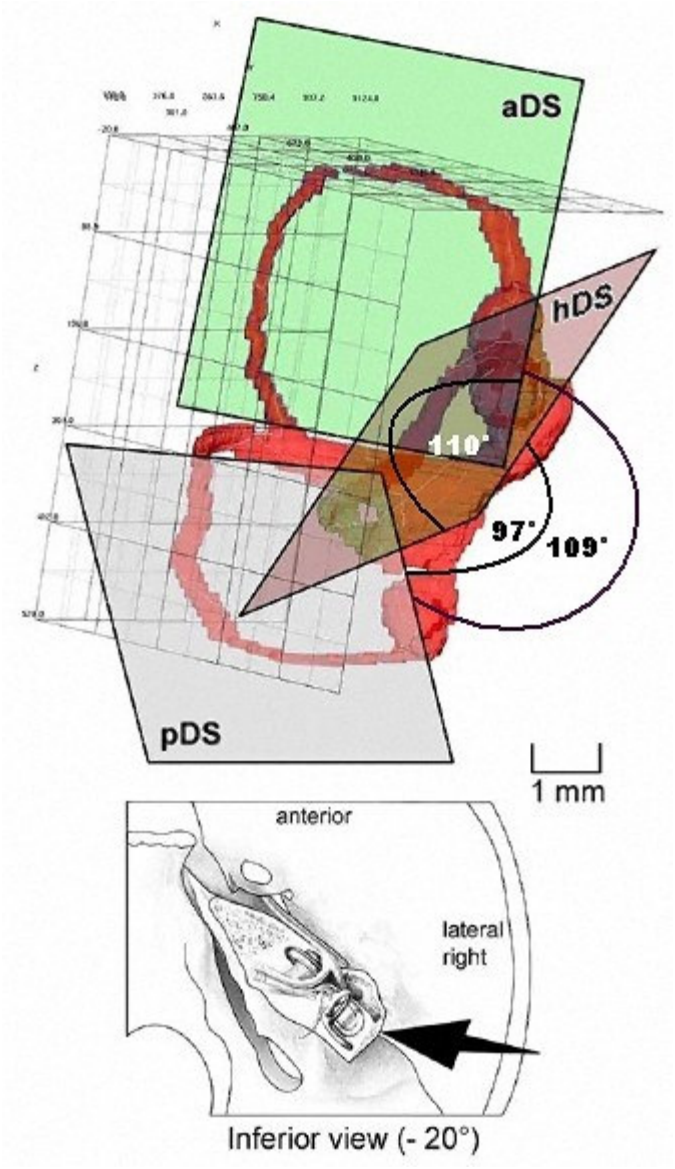

Figure I-2: Average angular measurements between the semicircular ducts.
Upper part of the figure depicts 3-D reconstruction of the labyrinth from pathological specimens of the temporal bone sectioned in the horizontal plane. In the lower part, the perspective arrow shows the line of sight from which the 3-D model is seen.
Each semicircular duct is assigned to its own plane.
pDS – posterior semicircular duct, aDS – anterior semicircular duct, hDS – lateral semicircular duct (horizontal).
From (Rother, Schrock-Pauli, Karmody, & Bachor, 2003).

A sensory epithelium—the mechanoreceptors of the membranous labyrinth—lies in its specialized regions. One set of the mechanoreceptors lies in the semicircular canals. Anatomically, all endings of the semicircular canals terminate in the utricle, although one limb of the superior duct fuses with the posterior duct into *crus commune* before joining the utricle. One end of each duct dilates before joining the utricle. Inside this dilatation, called *ampulla,* the epithelium thickens into a region called the *ampullary crest (crista ampullaris).* This region of the epithelium is concentrically organized (zones I – III – peripheral, intermediate, central region) and contains a peculiar set of receptors – the *vestibular hair cells.* Semicircular ducts are hydrodynamically interconnected. During head movements endolymph in semicircular ducts is displaced and in specific manner affects the hair cells of all three ampullar crests (see chapter “I.2.2 Mechanical Properties of the Sensory Organs”)

(Muller & Verhagen, 2002;Muller & Verhagen, 2002). The ampulary crest is covered by a gelatinous, diaphragm-like mass called *cupula* that stretches to the roof of ampula. It seems that cupula is a quite floppy substance, which is indirectly responsible for the transfer of the forces exerted by endolymph on the sensors. There are many theories about the cupula functioning [Swinging door (Steinhausen, 1933), Diaphragm (Hillman & McLaren, 1979), Moving piston (Rusch & Thurm, 1989)] but it is most likely that endolymph passes through the cupular part smoothly under. Cupula serves more less as a buffer during higher excitations of endolymph movements and by closing the path of the subcupular space prevents damage to the hair cell region (Jijiwa, Watanabe et al., 2001;Dohlman, 1971;Muller, 1994;Dohlman, 1981). Each hair cell bears a *hair bundle* that is composed of a single *kincocilium,* with a length of about 60 µm, and about 25-100 hexagonally arranged *stereovilli*. The kinocilium is always found on one side of the hair bundle. The longest of villi are in direct neighborhood of the kinocilium and decrease at a greater distance. Both give each hair cell a *morphological axis of polarity.* Kinocilium and stereovilli are interconnected together by fibrillar strands and behave mechanically as a single unit. The kinocilium is flexible and often sinusoidally bent in microscopic pictures. It can actively move in flagella-like motion using its 9+2 filament structure. The latter movement can only be induced by mechanical stimulation and not by a potential difference over the cell membrane. The stereovilli are much stiffer than the kinocilium because they are reinforced by a system of connections where main role is played by the actin microfilaments. The kinocilia cross the subcupular space and penetrate into the cupula [for review, see (Muller, 1994)]. A deflection of the hair bundle modulates current flow through the mechanoelectrical transduction channels, which are present on the kinocilia, generating a receptor potential. Bundle deflection is believed to gate the *transduction channels* by changing the tension in *tip links*, which connect adjacent stereocilia. The change in the intracellular Ca^{2+} during the deflection mediates the adaptation of tip links – high endolymphal flow leads to the decrease of resting tip link tension, and vice versa (Holt, Corey et al., 1997). The hair cell release excitatory transmitter *glutamate* even the hair bundle is not bent. Bending of the hair bundle toward the kinocilium opens the transduction channels leading to a depolarization of the hair cell, an increase in the release of transmitter, and an increase in the firing of the afferent fibers. Conversely, bending away from the kinocilium closes the transduction channels causing a hyperpolarization of the hair cell, a decrease in the release of transmitter, and a decreased firing in the afferent fibers. The hair cells of the semicircular ducts are arranged in an orderly pattern. For instance, in the horizontal duct the morphological axis of polarity points toward the utricle, and therefore bending of the hairs in

the direction of the utricle is excitatory (videlicet during ampullofugal flow of the endolymph) (Dohlman, 1971;James, 1991;Muller, 1994).

Hair cells on the semicircular cristae come in two types:

- *type I cells* are flasked shaped cells found mainly in the central zones of the cristae,
- *type II cells* are cylindrical cells which dominate in the peripheral region.

Both differ in shapes, more subtle ultrastructural differences are in the diameters of mitochondria and stereocilia (larger in hair cells I), in the distribution of nuclear chromatin (round pale nuclei located at the top with diffused nucleoli in hair cells II) and in presence of typical afferent endings (for more, see chapter "I.2.1.2 The Peripheral Vestibular Connections"). Hair cells are embedded into a layer of *supporting cells.* Their apical region is armed with microvilli, they have electron-dense cytoplasm, small, abundant secretory granules and basally situated nuclei. The hair cells to the supporting cells ratio is about 2.4:1 in pigeons. It seems that supporting cells serve as precursors for hair cells. A presence of the immature hair cells and their precursors in the sensory epithelium suggest the possibility of regeneration of the hair cell layer. Unfortunately, this spontaneous regeneration in mammalian vestibular systems appears to be limited (Lopez, Honrubia et al., 1997;Eatock, Rusch et al., 1998;Kevetter, Blumberg et al., 2000;Leigh RJ, 1999;Goldberg, 2000;Matsui & Cotanche, 2004).

A second set of mechanoreceptors of the membranous labyrinth is present in the detectors of linear acceleration – the saculus and the utriclus. Both are sac-like structures and inlay bony structures of the same name. Only parts of these sacs bear receptive cells (the hair cells, as seen in semicircular ducts). Those innervated sections of epithelium are called *maculae.* Hair cells are covered by three consecutive layers of morphologically separable meshwork called the *otolith membrane* (Jaeger, Takagi et al., 2002). The topmost one—the *otoconia layer*—is a strongly connected filament matrix containing calcium carbonate crystals known as *otoconia* (Lins, Farina et al., 2000). The size and asymmetry of these crystals is not genetically coded: they grow according to the size and direction of the *gravitational force* (the most important acceleration). Animal models of the lower vertebrates show, that this happens during early phases after the fertilization, before the macular epithelium is differentiated (Wiederhold, Harrison et al., 2003;Ibsch, Anken et al., 2004;Anken, Beier et al., 2004).

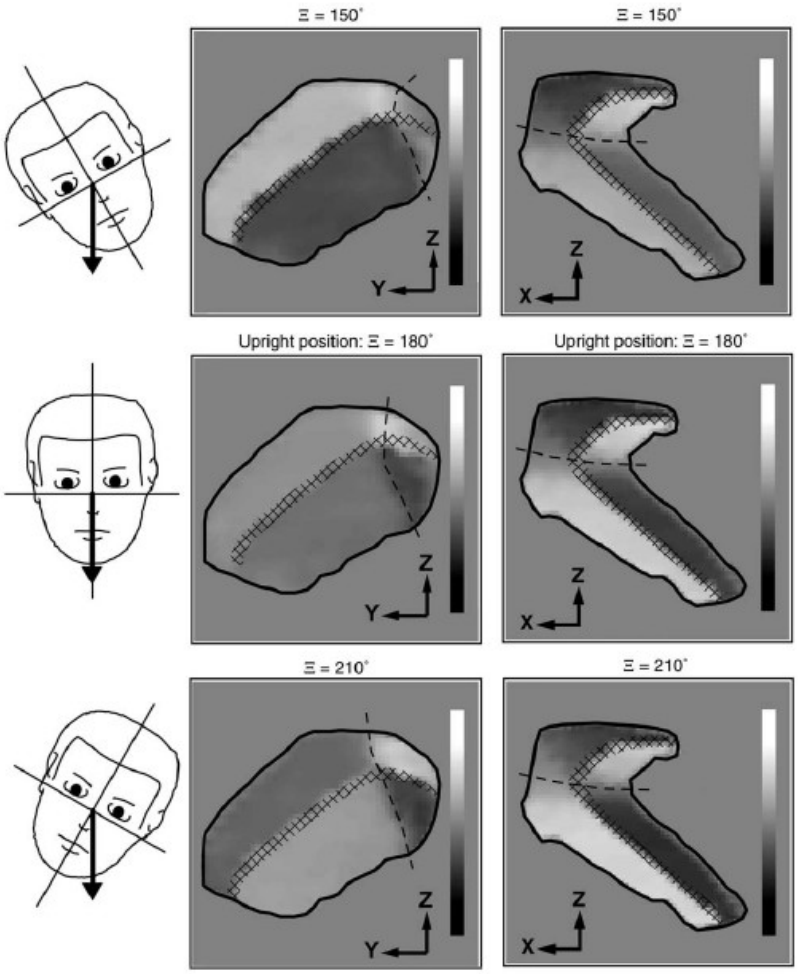

Figure I-3: Excitation maps of left utricle and saccule for three directions of acceleration.
The background color represents zero polarization, while white and black indicate depolarization and hyper-polarization, respectively. The maps are projections onto the main head planes (Jaeger, Takagi, & Haslwanter, 2002)

Middle layer, called *mesh-layer* is stiffer than the otolith membrane (Kondrachuk, 2000). Structurally it consists of a densely and randomly interconnected filament matrix. Its function is probably to distribute the forces acting on the otoconia in a more homogenous fashion. Visco-elastic properties of the most low layer resemble those of a gel, and it is therefore called the *gel-layer* (Grant, Huang et al., 1994). In comparison with the mesh-layer the structure is columnar.

Reception is, as well as in semicircular ducts, mediated by hair cells, and they also occur in two types:

- *type I cells* are mainly found in the central part of the macula. This part is also called the *striola.*
- *type II cells* are found in the *juxta- and extrastriola* region.

Both cell types have a constitution similar to the hair cells of cristae of the semicircular ducts, including the typical stereocilia-kinocilium arrangement. Nevertheless, the projections of the macula hair-cells are embedded into the gel-layer: Kinocilia of the extra-

striola area are attached to the mesh layer (Kachar, Parakkal et al., 1990) or even protrude into the otoconia-layer above (Ross, Komorowski et al., 1987) [for review, see (Jaeger, Takagi, & Haslwanter, 2002)]. The polarization properties (influence of the hair bundles deflection on the hair cells depolarization) are somehow analogous to the crista hair cells. However, unlike in the semicircular canals, their morphological axis of polarity is not constant throughout the otolith macula, showing a distinct pattern (James, 1991). The mechanism of action of the otoliths is an inertia-generated shearing movement of the otoconial layer, parallel to the underlying surface of the sensory epithelium. The shape and orientation of the otolith maculae is rather complicated (see **Figure I-6**). Both maculae have pronounced curvature so that dorsoventral shear forces will stimulate regions of both the utricular and saccular maculae (**Table I-C**, **Figure I-3**) (Curthoys, BETTS et al., 1999;Sato, Sando et al., 1992;Takagi & Sando, 1988;Jaeger, Takagi, & Haslwanter, 2002). This kind of profile is necessary for detecting of any acceleration /position of the head in space.

Utricular macula				
Length (mm)	2.59	3.15	2.71	2.80
Width (mm)	2.09	2.03	2.07	2.20
Transverse angle	35.01°	-	-	-
Longitudinal angle	37.70°	-	-	-
Saccular macula				
Length (mm)	2.26	2.60	2.58	2.60
Width (mm)	1.63	1.43	1.23	1.20
Transverse angle	37.7°	-	-	-
Longitudinal angle	82.7°	-	-	-
Intermacular angle	52°-127°	77.0°	-	-
	(Rother, Schrock-Pauli, Karmody, & Bachor, 2003)	(Takagi & Sando, 1988)	(Sato, Sando, & Takahashi, 1992)	(Rosenhall, 1972)

Table I-C: Values of the measured otolithic structures.

I.2.1.2 The Peripheral Vestibular Connections

Every hair cell receives both the *efferent* and *afferent* innervations.

Based on the morphology of the peripheral terminal arbors, three kinds of afferents can be recognized in the vestibular endorgans.

- *Calyx fibers* provide calyx endings to 1-3 neighboring type-I hair cells,
- *Bouton fibers* give rise to 15-100 bouton endings contacting type-II hair cells,
- *Dimorphing fibers* provide a mixed innervation of 1-4 calyx endings to type-I hair cells and 1-50 bouton endings to type II hair cells.

With respect to distribution of the hair cells, calyx units are largely confined to a central zone and bouton units to a concentrically arranged peripheral zone, while dimorphic units are found throughout the sensory epithelium. Similarly, dimorphic units are also distributed throughout the otolithic macula, calyx units are restricted to the striola and very few bouton units found in the peripheral juxta- and extrastriola [for review,see (Goldberg, 2000)].

Efferent fibers are *bouton-like* nerve terminals. They are in direct contact with type II sensory hair cells or with the afferent nerve calices surrounding one ore more bodies of type I hair cells. The efferent endings show *acetylcholinergic* (ACh) activity (Kong, Hussl et al., 1998).

Nerve fibers from the cristae and maculae pass as dendrites and axons through the perforations of the *lamina cribrosa* of the *petrosal bone* to reach *Scarpa's ganglion* at the lateral aspect of the *internal auditory canal*. In the Scarpas ganglion, somas of primary *vestibular bipolar neurons* of the afferent vestibular pathway are located. The *vestibular nerve* is divided into two branches (respectively, the ganglion itself is divided into two accordant portions connected by the *isthmus ganglionaris*): the *superior division*, which innervates the anterior and lateral semicircular canals and the utricle, and the *inferior division*, which innervates the posterior semicircular canal and saccule. The superior branch runs with the *facial nerve*, and the inferior branch runs with the *cochlear nerve*. A small number of vestibular fibers may also run in the cochlear division. From Scarpa's ganglion, the vestibular nerve passes medially, traversing the *cerebellopontine angle*. It then lies posterior to the cochlear nerve and below the facial nerve, entering the brain stem between the *inferior cerebellar peduncle* and the *spinal trigeminal tract*, to synapse in the *vestibular nuclei* (Leigh RJ, 1999;Bergstrom, 1973).

Vestibular nerves consist of heterogeneous set of fibers. About 10 percent of them are non-myelinated (Nagai, Goto et al., 1999). Those with a myelin cover differ in calibers. The number of thicker fibers diverges between approximately 2 and 20 percent (calibers and rates fluctuate depending on age and respective primary nerves [for more, see chapter “I.3.2 Degenerative Patterns in the Vestibular System”]) (Bergstrom, 1973;Bergstrom, 1973).

I.2.1.3 The Central Vestibular Connections

As discussed above, the otholits and the semicircular ducts generate sensory signals which, relayed through the *vestibular nuclei* (VNs), act on the extraocular motoneurons in the

cranial nerve nuclei III, IV and VI. This is called the elementary vestibulo-ocular reflex arc and its function is known as VOR.

The VOR bipolar afferent neurons of Scarpa's ganglion finish their axons mainly in the vestibular nuclei. In humans, the volume of VNs is about 67mm^3 containing approximately 200 000 neurons. Larger neurons in the vestibular nuclei receive labyrinthine input from axons of a larger caliber; smaller neurons receive input from smaller-caliber axons. There is a considerable divergence of single primary afferents within VNs, with the rate of 15 neurons of vestibular nuclei per axon. A single axon from lateral semicircular canal can influence all VNs. The reason is in multifaceted function of VNs. Neurons in the vestibular nuclei that receive input from primary vestibular afferents encode not only head velocity but also an eye position, and varying amounts of smooth pursuit and saccadic signals. In response to this, there are several cell types in the vestibular nuclei which receive primary afferents. A common and important cell type is the *position-velocity-pause (PVP) neuron*. It encodes head velocity and eye position and becomes silent (pauses) during saccades. Another cell type is the *floccular target neuron (FTN)*, which also receives projection from the *cerebellar flocculus* and may be important in the VOR adaptation. Additional cell types include those showing a sensitivity to eye and head velocities – the *EH neurons*, to head velocity alone, and to eye velocity and eye position – the *burst-position (BP) neurons.*

There are four major vestibular nuclei and several smaller accessory subgroups (Suarez, Diaz et al., 1997):

- *medial vestibular nucleus (MVN),* greatest in volume and the longest,
- *lateral vestibular nucleus (LVN),*
- *inferior (descending) vestibular nucleus (DVN),*
- *superior vestibular nucleus (SVN),*
- *interstitial nucleus (IN),*
- *y-group (Y),*
- other accessory subgroups *(f-group, m-group, x-group, z-group, ncl.subventricularis, ncl.supravestibularis)*.

Their space arrangements and lengths are depicted in **Figure I-4**.

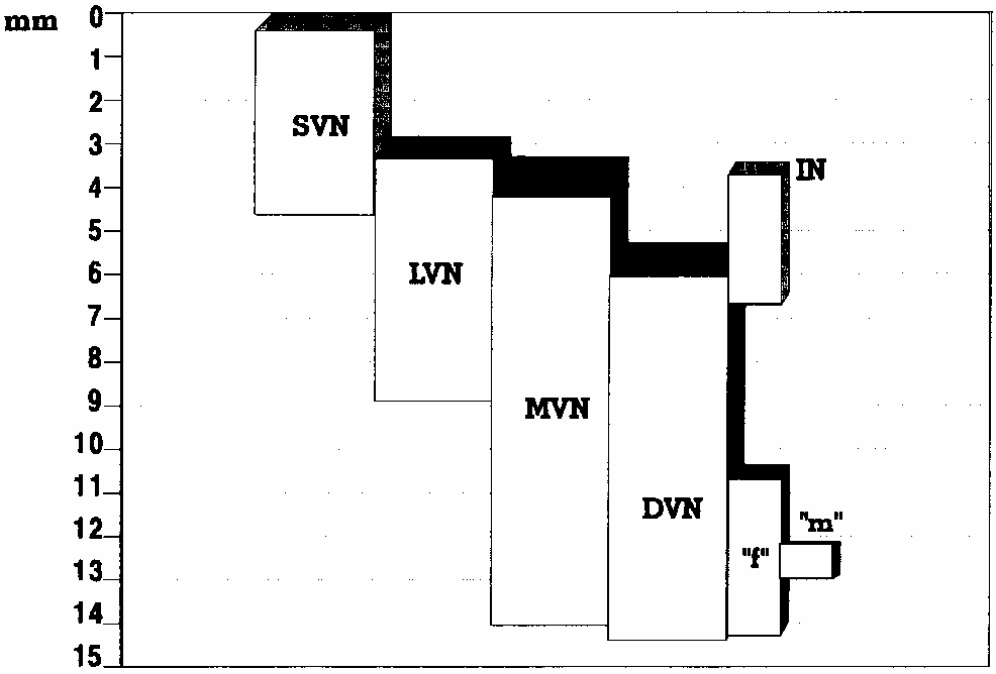

Figure I-4: Space arrangement and length of the vestibular nuclei.
from (Suarez, Diaz, Tolivia, Alvarez, Gonzalez, & Navarro, 1997)

All canals and otoliths project to *zone 1* which lies around the borders of the ventromedial LVN, medial MVN, and dorsomedial DVN. All canals also converge on a small patch in the ventromedial SVN. These two areas contain the secondary vestibulo-ocular neurons that project to the abducens, oculomotor and trochlear nuclei.

Canal afferents also converge on the IN of the vestibular nerve, which projects to the *flocculus.* Recent single-cell reconstructions of identified otolith primary afferents have revealed that utricular afferents terminate mainly in the DVN, innervating the LVN and MVN and even the abducens nucleus sparsely. In comparison, the saccule fibers terminate mainly in LVN and DVN, sometimes in SVN (Buttner-Ennever, 1999). Some projections from the otoliths overlap with those from semicircular canals, presumably reflecting their common roles in detecting similar head movements.

Projections of vestibular nuclei neurons do not aim just to motoneurons, they also send axon collaterals to the *nucleus prepositus hypoglossi (NPH)*, to the *nucleus of Roller*, to the cell groups of the *paramedian tracts (PMT),* and to the *nucleus of Cajal (iC).* The NPH and adjacent medial vestibular nucleus (the NPH-MVN region) have a crucial role in holding gaze steady (neural integration). The cell groups of the PMT may be important for relaying an internal or efference copy of the eye movement signals to the *flocculus of the cerebellum*. In addition, certain cells in NPH that receive vestibular inputs project to burst neurons in the *paramedian pontine reticular formation (PPRF)* to trigger quick phases of *nystagmus* (i.e.,

abnormal oscillations of the eyes with fast, resetting, and slow, tonic component that may be initiated by central or peripheral vestibular asymmetry). iC receives axon collaterals from all secondary vestibular afferents that supply the oculomotor nucleus and sends reciprocal projections, predominantly ipsilateral, to the vestibular nuclei. Its function is needed for vertical eye movements and vertical-torsional neural integration (Glasauer, Dieterich et al., 2001;Glasauer, Dieterich et al., 2001). Finally, many secondary vestibular axons have dual projections, both rostrally, as the VOR neurons, and caudally, as the *vestibulocollic neurons.*

Most of the VOR projections from the VNs come from zone 1 and center of SVN. Zone 1 predominantly carries excitatory PVP cells, and is under little direct cerebellar influence. Center zone in the SVN contains burst-position cells (neurons that discharge with eye velocity and eye position).

For the **anterior canal system**, **excitatory PVP** cells lie in the MVN or adjacent *ventral lateral vestibular nucleus (VLVN)*. Their projections, after crossing, ascend in or just below the *medial longitudinal fasciculus (MLF)* to contact the ipsilateral superior rectus and the contralateral inferior oblique subdivisions of the oculomotor complex. Axon collaterals of these fibers project to the iC, to cell groups of the PMT, and to the perihypoglossal nuclei, including NPH. **Inhibitory neurons for the anterior canal system** lie in the SVN. Their axons exit to the ipsilateral MLF to contact the contralateral superior oblique motoneurons in the trochlear nucleus and the ipsilateral inferior rectus neurons in the oculomotor nucleus. Axon collaterals project to the NPH and to cell groups of the PMT. The neurotransmitter of these inhibitory vestibular neurons seems to be the *gamma-aminobutyric acid (GABA).*

For the **posterior canal system, excitatory PVP cells** are also found at the junction of the MVN and VLVN. After crossing the midline, the projections enter the MLF and continue rostrally to the contralateral trochlear nucleus (the ipsilateral superior oblique muscle) and the ipsilateral inferior rectus subdivision of the oculomotor complex. Axon collaterals also pass, via the MLF, to the NPH and PMT cell groups and to the iC. In addition, the posterior semicircular canal also projects to the contralateral abducens nucleus (contralateral lateral rectus muscle). **Inhibitory posterior canal neurons** are found in the SVN and rostral MVN. Their axons project through the pontine reticular formation to reach the ipsilateral MLF and thus contact the contralateral superior rectus and the ipsilateral inferior oblique subdivisions of the oculomotor complex. These neurons also contact PMT cell groups and the iC. Like the inhibitory neurons of the anterior canal system, these cells most probably use GABA as an inhibitory neurotransmitter.

For the **lateral (or horizontal) canals, excitatory PVP neurons** are located in the ventral part of the MVN and adjacent VLVN. Most of these excitatory neurons course rostrally and medially and cross the midline at the level of the abducens nucleus or slightly rostral to it. Soon after crossing the midline, these axons give collaterals that either enter and terminate in the contralateral abducens nucleus (the contralateral lateral rectus muscle) or project to the NPH and PMT cell groups. Some PVP neurons project rostromedially, and run in the ATD (ascending Deiter's tract) to terminate in the ipsilateral medial rectus subdivision of oculomotor complex, some of these axons send collaterals to the PMT cell groups. The functional significance of the pathway through the ATD is uncertain, but it may relate to vestibulo-ocular responses associated with *translation*. **Inhibitory pathways for the lateral canals** pass from the MVN to the adjacent abducens nucleus (the ipsilateral lateral rectus muscle). These neurons may use *glycine* as a neurotransmitter. The contralateral medial rectus neurons are peculiar in having no known disynaptic inhibitory input, although a multisynaptic, extra-MLF pathway may play a role [for review, see(Leigh RJ, 1999)].

The pathways for central otolith connections are not known as well as those for the canal links. Experimental stimulation of the **utricular nerve** causes eye movements that suggest contraction of the ipsilateral superior oblique, superior rectus, and medial rectus, and the contralateral inferior oblique, inferior rectus, and lateral rectus muscles (Suzuki, Tokumasu et al., 1969). A disynaptic input from the utricle to the ipsilateral abducens motoneurons are known. Secondary ipsilateral abducens-projecting cells are localized to the LVN and rostral DVN. The pathway carrying the disynaptic utricular signal to the medial rectus motoneurons is suggested to be the ATD (combined with a canal signal ipsilaterally). There is no evidence for a direct monosynaptic input to the trochlear motoneurons (the superior oblique muscle), implying that it is multisynaptic (Buttner-Ennever, 1999).

There are VN otolith afferents to the **cerebellum** (nodulus and uvula) and cerebellar nuclei (the fastigial nucleus) going either directly or indirectly through the *inferior olive (IO)* (from the MVN and DVN) and the *lateral reticular nucleus (LRN)* (from the LVN and SVN). Efferents of the nodulus and the uvula project in a topographic fashion back onto the vestibular nuclei (e.g. the lateral nodulus to the caudal MVN, and the medial nodulus to the middle part of MVN). Efferent pathways from the fastigial nucleus terminate in the ipsilateral and contralateral LVN and DVN [for review, see (Buttner-Ennever, 1999)].

The cell bodies of **vestibular endorgans efferents** are located primarily in a closely-spaced group of small cells confined to a region dorsolateral to the facial genu, and ventromedial to the MVN, called the *efferent vestibular nucleus (EVN)*. Efferent innervation

pattern is diffuse with individual fibers terminating onto multiple hair cells and onto afferents that arise from different vestibular endorgans. The axon collaterals of vestibular efferents project to the cerebellar flocculus (Leigh RJ, 1999). There is an evidence of an excitatory action of the efferent onto the afferent discharge. Also a strong relationship between the efferent responses and discharge regularity is seen for both the canal and otolith afferent fibers (Marlinski, Plotnik et al., 2004). The real function of vestibular efferents is not quite clear yet.

I.2.2 Mechanical Properties of the Sensory Organs

I.2.2.1 Semicircular Canals

The classical representation of the semicircular duct system consists of three separate duct circuits. The ducts are, however, in reality, hydrodynamically interconnected. The flow of the endolymph in this system fundamentally deviates from flow in models of three separate single-duct circuits. The endolymph moves from one duct into another and into other parts of the vestibular system [for review, see (Muller & Verhagen, 2002)]. Although, hydrodynamically interconnected labyrinth, in general, does not produce a biologically distinctive behavior compared to the system with separated ducts (the endolymph cannot be dragged away from a given duct by a large flow in the other interconnected duct), in special cases during pure movement in one SCC plane, two ampullae might be somewhat affected. These simultaneous ampullar signals probably represents an advantage to the nervous system, avoiding ambiguous information when a pool of brain cells would be silent [for explanation, see (Muller & Verhagen, 2002a;Muller & Verhagen, 2002b;Muller & Verhagen, 2002c) Undoubtedly, above fact could be significant in combined head movements (roll-yaw-pitch) that stimulate all cristae at one time.

There are many **mechanical problems** affecting the flow of the endolmyph in the semicircular ducts to consider. Some are more important than the others. The cupula is obviously an essential element of the mechano-electrical transduction part of the system. It is, however, an extremely flabby structure and, therefore, unimportant for the fluid mechanics of the semicircular duct system. Making the cupula 1000 times stiffer then its actual value has hardly any influence on endolymph movement in the physiological range of interest. Therefore, we can omit it in considerations of endolymph flow. Similarly, in open, unobstructed ducts, the effects of wall-elasticity can be neglected.

From the geometrical point of view, **three** (Rabbitt, 1999) or **two-duct** (Muller & Verhagen, 2002) **theories** can be taken into account. Unfortunately, the flow in a three-duct labyrinth leads into unsurvayable formulae for endolymph movement, while a two-duct consideration provides for a simpler yet realistic review, along with keeping the essentials of a hydrodynamically interconnected duct system intact.

Should we consider the **stimuli to the duct system** characteristic of those in daily life, we would end up with step-like turning movements of the head, rather than gradual or sinusoidal ones (Muller, 1994;St George, Lord et al., 2003;Grossman, Leigh et al., 1988;Grossman, Leigh et al., 1989;Leigh & Brandt, 1993) [see chapter "I.2.4.2 Physiology of the VOR During Locomotion"]. The result of the equation for the motion of the semicircular duct system for a step-like input stimulus leads to formulae of the type:

$$x_{max} \approx \dot{x}(0) T_2 \qquad (1)$$

x_{max} is the maximal endolymph displacement, $\dot{x}(0)$ is the initial endolymph velocity after the stimulus, T_2 is the short time constant of the system. For a two-duct system, two short time constants exist – T_{21} and T_{22}. First provides a characteristic of the flow through a duct and crus commune, the latter is dependent on the radius of the anterior and posterior ducts, and is equal to T_2 of a single –duct system:

$$T_{22} = T_2 = r^2/(8v) \qquad (2)$$

where v is kinematic viscosity of the endolymph and r the radius of a duct. Derivation of the equation of motion and the time constants is called *the internal dynamics*. The maximum endolymph displacement (x_{max}) occurs at about $5T_2$.

The force balance in a flow circuit of a **single closed duct** can be described by this equation:

$$M\ddot{x} + F\dot{x} + Sx = 0 \qquad (3)$$

in which M is the mass of the endolymph fluid, F is a friction constant originating from Poiseuille's law, S is an elasticity constant of the mechano-electrical transducer system in the ampulla, and $\ddot{x}$, $\dot{x}$, x are endolymph displacements, - velocity and -acceleration, respectively. The mean velocity over the period $5T_2$ is:

$$\dot{x}_m = x_{max}/(5T_2) \qquad (4)$$

and the mean acceleration is:

$$\ddot{x}_{m} = 2x_{max}/(25T_2) \tag{5}$$

The general form of the equation of motion for a **three-duct system** is:

$$\begin{bmatrix} [A1] & [B1] & [C1] \\ [A2] & [B2] & [C2] \\ [A3] & [B3] & [C3] \end{bmatrix} \begin{bmatrix} X_a \\ X_p \\ X_h \end{bmatrix} = 0 \tag{6}$$

As mentioned above a **two-duct consideration** is simpler, along with keeping the essentials of a hydrodynamically interconnected duct system intact:

$$\begin{bmatrix} [A1] & [B1] \\ [A3] & [B3] \end{bmatrix} \begin{bmatrix} X_a \\ X_p \end{bmatrix} = 0 \tag{7}$$

applicable for two vertical ducts (anterior and posterior) and the crus commune, and:

$$\begin{bmatrix} [A2] & [C2] \\ [A3] & [C3] \end{bmatrix} \begin{bmatrix} X_a \\ X_h \end{bmatrix} = 0 \tag{8}$$

for the vertical duct, the horizontal duct and the utriculus. Closer explanation of formulae (6-8) exceeds the scope of this thesis and can be found in (Muller & Verhagen, 2002).

The lengths of the crus commune and the two ducts can be optimally attuned to each other only when the areas enclosed by the duct circuits can be maximized. This is the cause for circle- or elipse-like duct circuits. Although the shapes of natural morphologies of duct circuits can be irregular, those subtle asymmetries are not affecting impulses and endolymph flow (Muller & Verhagen, 2002).

For arrangement of the semicircular ducts it the skull, see chapter “I.2.1.1 The Sensory Organs”. Three-dimensional orientation vectors of human semicircular canals are leading to an asymmetry (Blanks, Curthoys, & Markham, 1975). The angle between *left posterior (LP)* and *right posterior (RP)* is larger than between *left anterior (LA)* and *right anterior (RA)*. Thus, an upward head movement would result in a VOR weaker than a downward head movement VOR (upward gain of 0.85, downward gain of 1.15, see **Figure I-5**, for explanation about gains, see chapter “I.2.4.5 Quantitative Aspects of the VOR”). The vector sum of resting discharges, therefore, would lead to an upward drift of the eyes, which is

physiologically canceled by inhibitory pathways of the flocculus and the paraflocculus (Ito, Nisimaru et al., 1977).

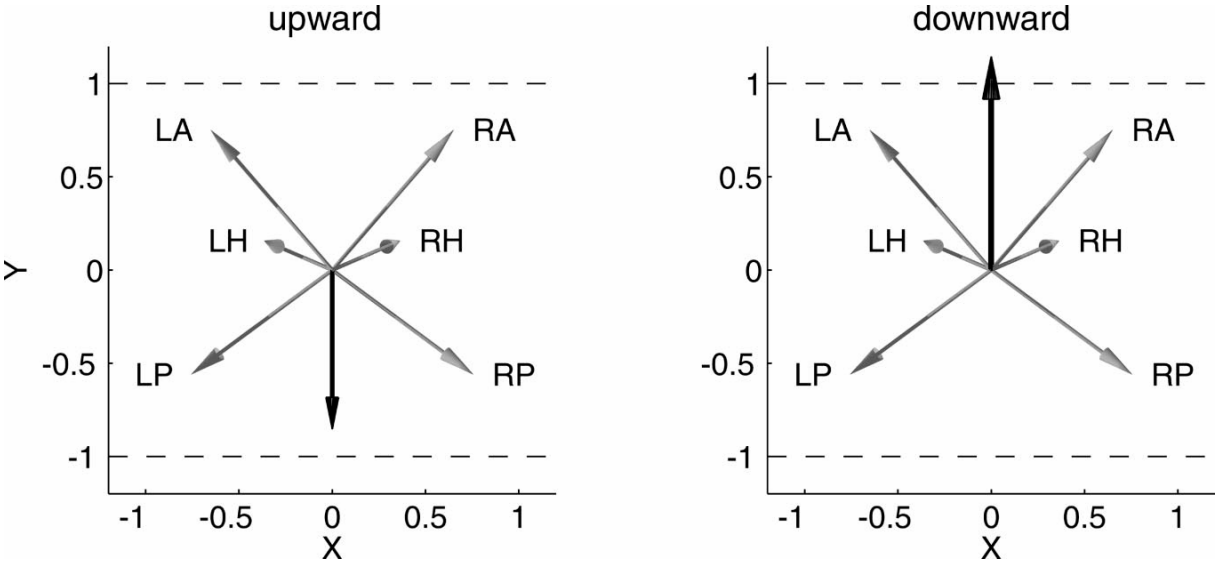

Figure I-5: Three-dimensional orientation vectors of human semicircular canals as seen from above. (gray arrows; L - left; R - right; P - posterior; A - anterior; H - horizontal). LH arrows point toward the reader, RH arrows away from the reader. The angle between LP and RP is larger than between LA and RA, leading to an asymmetry. (Left) Black arrow shows resultant angular velocity vector due to upward head rotation. (Right) Black arrow shows resultant angular velocity vector due to downward head rotation. The length of the black arrows corresponds to the expected gain. Thus, an upward head movement would result in a vestibulo-ocular reflex (VOR) gain of 0.85 and a downward head movement in a VOR gain of 1.15 (Glasauer, von Lindeiner et al., 2004).

The internal diameter of the semicircular canals (0.58±0.04 mm) is small relative to their radius of the curvature (2.96±0.11 mm) (Rother, Schrock-Pauli, Karmody, & Bachor, 2003). Thus, given the hydrodynamic properties of the endolymph, the motion of endolymph caused by a head rotation is approximately proportional to head velocity. In such way, the semicircular canals mechanically integrate the angular head acceleration that they sense, allowing them to provide the brain with a head-velocity signal. The flow of the endolymph affects the hair cells and cupula. Return of the system to its resting position has an exponentially decaying time course, and has been estimated to be about 6 sec (Cohen, Henn et al., 1981). Brain has ability to prolong this time, so that the head motion can be perceived for an extended period. The central background of this phenomenon is mentioned in chapter "I.2.1.3 The Central Vestibular Connections" and is called the *velocity storage mechanism.*

Before concluding this section, it is important to mention two empiric laws that rule the SC mechanics:

1) Each canal produces movements of the eyes in the plane of that canal (*Flourens' law*),
2) The excitation (of the hair cells in SC cupulae) is a relatively better vestibular stimulus than the inhibition (*Ewald's second law*) [for review, see (Leigh RJ, 1999)].

I.2.2.2 Otholiths

Physical properties of the otolith maculae are more difficult to analyze than those of the semicircular canals, but basic properties can be established. If constant linear acceleration is applied, for example head tilt (the acceleration of gravity), the otoconia will move until the floating force acting on them is counterbalanced by elastic forces that originate in the otolith membrane. A displacement of the otoconia, with concurrent shearing of the gel-layer, leads to a deflection of the stereocilia embedded in the gel-layer, which in turn causes the sensory hair cells to change their excitation in the same manner like the hair cells of cristae. In this way, the otoliths can sense both translational head movements (i.e., linear accelerations), and static tilts of the head (with respect to the pull of gravity). Human sensitivity to linear acceleration has been measured to be 0.002 g. This acceleration leads to a deflection in the order of 1 nm, which is the minimum magnitude the hair cells can detect.

Important to the function of the otolith receptors is the elasticity of the mesh- and otoconia-layers. It has often been postulated that the otolith membrane is continuous elastic material and so its movement has to obey the Cauchy's equation of motion:

$$\rho \frac{\partial^2 u_i}{\partial t^2} = \rho B_i + \sum_j \frac{\partial T_{ij}}{\partial x_j} \qquad \text{with } i,j = 1,2,3 \tag{9}$$

where ρ represents the *effective material density*, u_i the *displacements* along the *i*-axis, B_i the components of *body force per unit volume* (e.g. gravity or inertial forces), and $T_{i,j}$ the *Couchy stress components*. The x_j represents coordinates. Equation (9) can be simplified to:

$$0 = \rho B_i + (\lambda + \mu) \frac{\partial e}{\partial x_i} + \mu \sum_j \frac{\partial^2 u_i}{\partial x_j^2} \tag{10}$$

where μ and γ are *Lamé constants,* μ being identical to the shear modulus. For further explanation see (Jaeger, Takagi, & Haslwanter, 2002). Since one can assume that otolith membrane is either homogenous material or a material with low elasticity, it is suggested, that this composition of a membrane resets local irregularities in the otolith arrangement and the hair cells react to the otolith membrane displacements. However, if the higher elasticity of the mesh layer is present, this must lead to a transduction of the local inhomogenity of the otoconia layer to the hair cells. Although we can speculate, that the otolith membrane has evolved in the way that ensures non-interaction of parts with different orientation (Jaeger, Takagi, & Haslwanter, 2002) it seems nonetheless, that a development of the otolith crystals is an important, unambiguous, gravitation-dependent process (Wiederhold, Harrison, & Gao, 2003;Ibsch, Anken, Beier, & Rahmann, 2004;Anken, Beier, & Rahmann, 2004).

Unfortunately, such complex behavior of the otolith membrane system has never been modeled or closely studied; it appears that more important to the function of the receptor system that rules the otolith perception is the complex orientation of the hair cells. As explained in chapter "I.2.1.1 The Sensory Organs", otolith maculae are curved structures and their hair cells represent polarized elements with distinct pattern (see **Figure I-6**). Both leads to the assertion that even purely horizontal accelerations can induce significant vertical displacements, and that different parts are displaced with diverse magnitudes and directions (see **Figure I-3**). Small regions can be found, where the excitation level changes rapidly over a short distance. The location and shape of these regions might provide an important cue for the determination of head orientation (Jaeger, Takagi, & Haslwanter, 2002). Earlier findings reflecting the otolith function pointed out the complementary function of both maculae (Leigh RJ, 1999). Unfortunately, this is not the case, and it seems that both maculae are sending overlapping information. The reasons for this, as well as the reasons for the otolith crystals irregularity, are still unclear.

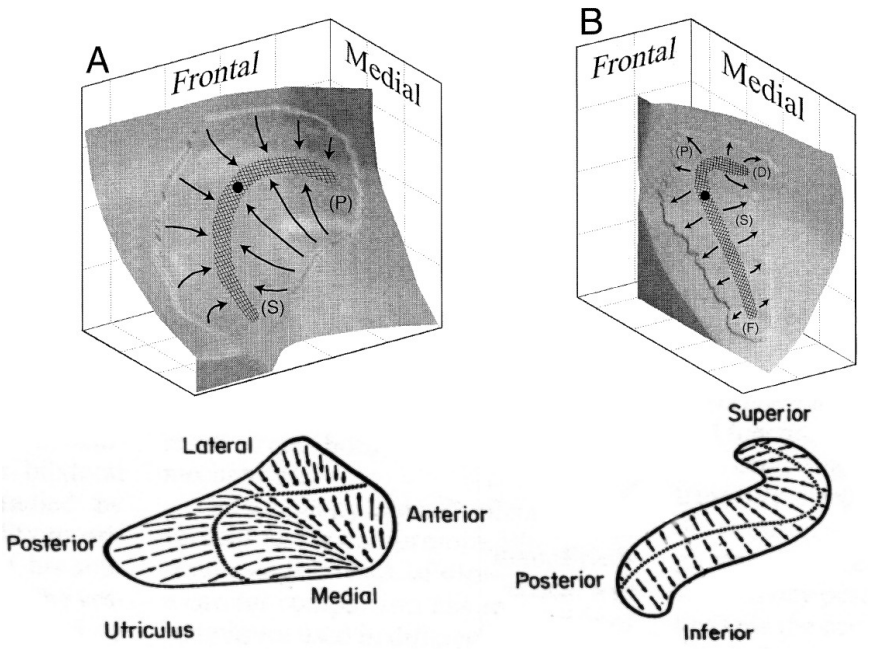

Figure I-6: Orientation of the maculae and their hair cells in the otolith organs.
(A) utriculus, (B) sacculus. The arrows indicate the directional sensitivities of the hair cell receptors. Deflection of the hair cells towards the arrowhead, i.e. of the stereocilia towards the kinocilium, by acceleration in the opposite direction, is excitatory. Revised from (Gresty, Bronstein et al., 1992;Jaeger, Takagi, & Haslwanter, 2002).

I.2.3 Neural Activity in the Vestibular Afferents

The vestibular nerve afferent fibers, that project to neurons within the vestibular nuclei mediating the VOR responses, have been classified as having *regular or irregular spacing action potentials*. Fibers classified as regularly or irregularly discharging differ in several other respects as well. It seems that inputs from the **regular afferents** dominate the vestibular response during *higher-frequency vestibular stimulation*. Their inputs may also play a role in

the *VOR adaptation*. Regular afferents have *tonic response dynamics*, resembling the displacement of the hair cells, and have a low sensitivity to head rotations or linear forces. The *caliber of their axons is medium to small* and they end as dimorphic units and bouton units in intermediate and peripheral zones of the cupula or macula. The **irregular afferents** have *phasic-tonic response dynamics*, including sensitivity to the velocity of the cupula and the otolithic membrane displacement, and hence show *acceleration sensitivity*. Their *axons are medium to large*. The irregular afferents in the central zone of the cristae and striolar regions have low rotational sensitivities and terminate as calyx endings onto the type I hair cells. The irregular afferents located away from the center have high rotational sensitivities and terminate as dimorphic endings onto both the type I and type II hair cells. The irregular afferents have also much larger responses to electrical activation of *efferent pathways* than do regular afferents [for review, see (Goldberg, 2000;Leigh RJ, 1999)]. **Table I-D** summarizes some of the differences among the afferents and afferent endings.

Afferents	Irregular		Regular
Fibres	Calyx	Dimorphic	Bouton
Hair cells	Type I		Type II
Macula	Striola	All	Extrastriola
Crista	Central	Intermediate	Peripheral
Axons caliber	Large	Medium	Small
Axons	Myelinated		Non-myelinated
Cancellation	Canceled at VNC		Not canceled at VNC
Rotational sensitivity	Low	High	Low
Sensitivity	Acceleration-velocity		Displacement
Galvanic stimulation	Low threshold		High threshold
Dynamics	Phasic-tonic response		Tonic response
Dominates at	Lower frequency		Higher frequency

Table I-D: Characteristics of regularly and irregularly discharging afferents in vestibular nerve. Adopted from (Goldberg, 2000;Leigh RJ, 1999).

To contribute to the chapter "I.2.1.3 The Central Vestibular Connections", after familiarizing ourselves with the above information, we can report that most of the connections that terminate in the LVN are irregular. Individual regular and irregular fibers innervate overlapping regions of the SVN, MVN and DVN. The irregular, in comparison with regular fibers, have fewer, thicker, and longer preterminal collaterals, with each collateral containing fewer, but larger boutons (on average 2-3x as many boutons on regular fibers). The proximal innervation of neurons with the largest cell bodies is derived almost exclusively from the irregular fibers; smaller neurons may receive their proximal innervation from the regular or

irregular afferents. However, in general, most secondary neurons appear to receive a mixed input.

We can speculate that irregular afferents (myelinated large axons) relay the information faster from the parts of sensory organs with the best reception (center parts of maculae and cristae), and they are more sensitive to acceleration. Therefore, it is quite surprising that the functional ablation of irregular afferents does not affect either the horizontal or vertical angular vestibulo-ocular reflex (rVOR, for explanation about types of VOR see chapter ”I.2.4 Physiology and Function of the Vestibulo-Ocular Reflex”) tested during sinusoidal head rotations as well as rapid head turns (Minor & Goldberg, 1991). This implies that direct rVOR pathways do not receive irregular ipsilateral vestibular-nerve inputs. Most probably, the polysynaptic inhibitory pathways (e.g. from the VN, cerebellum or otholits) could cancel the irregular monosynaptic inputs on the secondary neurons. However, the above effect of functional ablation was not seen during *studies of rVOR with respect of target distance*, and during *off-vertical-axis body rotations (OVAR)* when responses were reduced. We can suggest that these reactions are more dependent on irregular input than VOR. Another reflex that probably also receives irregular input is the *vestibulocollic reflex (VCR)*.

I.2.4 Physiology and Function of the Vestibulo-Ocular Reflex

The VOR compensates the movements of the head by generating appropriate eye movements, which keep the image steady on the retina. To be more precise, eye rotations must counterbalance for movements of the orbits. The movement of the head is sensed by the vestibular organs: an angular acceleration by the semicircular canals, a linear acceleration by the otoliths. The response to the angular (rotational) component of head motion is called the *r-VOR*, and the response to the linear (translational) component of head motion is called the *t-VOR* (see tab.5.). The r-VOR in response to the three possible directions of head rotations produces horizontal (around the rostral-caudal, *yaw*, or z-axis), vertical (around the interaural, *pitch*, or y-axis) and torsional (around the naso-occipital, *roll*, or x-axis) eye movements (see **Figure I-7**). Similarly, the t-VOR responds to three possible directions of head translation, producing horizontal (*heave*, along the interaural axis), vertical (*bob*, along the dorsal-ventral axis) and vergence (*surge*, along the naso-occipital axis) eye movements.

Table I-E: Types of vestibulo-ocular reflex. r-VOR - rotational vestibulo-ocular reflex, t-VOR - translational vestibulo-ocular reflex.

Movement	Peripheral structure	Reflex
Rotational (angular)	Semicircular canals	r-VOR
Translational (linear)	Otoliths	t-VOR

Sometimes a separate third type of the VOR is considered: an *ocular counterrolling*. This is also mediated by the otoliths and responds to linear acceleration. In this case, however, the stimulus is a change in the static orientation of the head with respect to the pull of gravity. In response to a sustained tilt of the head to one side, there is change in static torsion (counterrolling) of the eyes in the opposite direction to the head tilt.

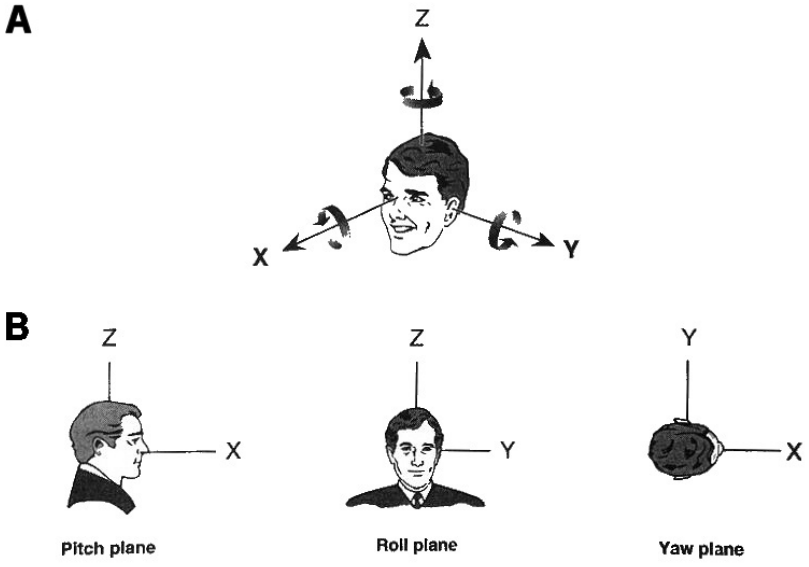

Figure I-7: Head-fixed, right-handed coordinate system used to express angular eye position and eye velocity vectors. **A**: Positive directions of eye rotation are designated by the direction of the arrows. **B**: Pitch plane is orthogonal to the interaural (Y) axis; roll plane is orthogonal to the nasooccipital (X) axis; yaw plane is orthogonal to the rostrocaudal (Z) axis.

I.2.4.1 Features of the VOR Function

Head movements in roll appear set apart from the horizontal and vertical head movements. A subject views straight ahead do not displace images from the fovea, so, from a visual standpoint, the torsional VOR need not be as efficient as its horizontal and vertical counterparts. This observation is consistent with experimental results of the VOR responses in roll (Aw, Haslwanter et al., 1996;Brzezny, Glasauer et al., 2003).

It is important in the understanding the VOR function that since the eyes are horizontally separated and the axis of rotation of the head is usually behind the eyes, rotational head movements invariably produce translations, or linear displacements, of the orbits. Even if the axis of rotation is centered on one orbit, the other eye will still be translated during a head rotation. A compensation for translation of the orbits during both head rotations and pure head translations is a function of the distance between the point of regard from the

head (the viewing distance). The closer the object of interest, the larger the compensatory response must be to prevent unwanted motion of images on the retina. Furthermore, depending upon the locations of the axis of head rotation relative to the two eyes (e.g., closer to one eye than the other), and the location of the object of interest relative to the location of the two eyes (e.g., on the midline or off to one side), the brain must adjust the movements of each eye independently, so that they can both remain pointed at the object of regard during any pattern of head motion [for review, see (Leigh RJ, 1999)].

It is also significant to highlight the three-dimensional instantaneous function of the VOR. It is obvious that common perturbations of the head do not occur only in the planes of VOR function or in the SCC planes. Although, the whole system is best ready for pitch plane perturbations (Muller & Verhagen, 2002;Blanks, Curthoys, & Markham, 1975) any head movement in three-dimensions will lead (thanks to cooperation of all the SCC's and central integration of their function) to corrective eye movement also in a three-dimensional space and time (Aw, Haslwanter, Halmagyi, Curthoys, Yavor, & Todd, 1996;Brzezny, Glasauer et al., 2003) (see also chapter "I.2.2.1 Semicircular Canals" and "*the Flourens' law"*)

I.2.4.2 Physiology of the VOR During Locomotion

To keep the vision steady during locomotion, not only the VOR is active, but also other systems contribute to the gaze stabilization. Body vibrations from sudden heel-toe strikes (with components up to 75 Hz) are absorbed by head inertia or, for instance, by flexion of the legs during walking. Further, motor behavior of the head and body can be modulated during locomotion (Mulavara & Bloomberg, 2002;Grossman, Leigh, Bruce, Huebner, & Lanska, 1989), as well as other complementary reflexes than the VOR can contribute (e.g., VCR or *cervico-collic reflex* - *CCR*) (Leigh & Brandt, 1993;Hirasaki, Moore et al., 1999). Nevertheless, common head perturbations are still of a high *speed* (rotational speed typically from 20 deg.sec^{-1} during walking to 170 deg.sec^{-1} during running), *frequency* (from 0.5 to 8 Hz and more), and *acceleration* (up to 5000 deg.sec^{-2}.) (see **Figure I-8** & **Figure I-9**) (Muller, 1994;St George, Lord, & Fitzpatrick, 2003;Leigh RJ, 1999;Hirasaki, Moore, Raphan, & Cohen, 1999;Crane & Demer, 1997;Grossman, Leigh, Abel, Lanska, & Thurston, 1988;Grossman, Leigh, Bruce, Huebner, & Lanska, 1989). So, how does the locomotion, the typical "activity of daily living", affect it all in more detail? Most of the head movements during walking and running consist of combined horizontal and vertical head rotations and translations. Rotational head movements disturbs visual acuity at any circumstances,

translational perturbations require compensatory eye rotations to hold images steady on the retina only when viewing a near target (Viirre, Tweed et al., 1986). Head perturbations during locomotion are characterized by their randomness. Horizontal and vertical rotational **velocities** rise maximally up to 90 deg.sec^{-1}, while the same movements during running can reach up to 590 deg.sec^{-1} in horizontal velocity and 240 deg.sec^{-1} in vertical velocity. Predominant **frequencies** are in the 0.5 – 8 Hz range, whereas vertical movements and running are of higher values. Furier spectra show harmonics of up to 20 Hz range (in vertical movements, lower number of harmonics in horizontal). **Amplitudes** during all movements and conditions are all within 20° (Grossman, Leigh, Abel, Lanska, & Thurston, 1988). Maximal derived **accelerations** are approximately 4800 deg.sec^{-2} large. Generally, it is the frequency and acceleration of the head rotation that presents the main threat to a clear vision.

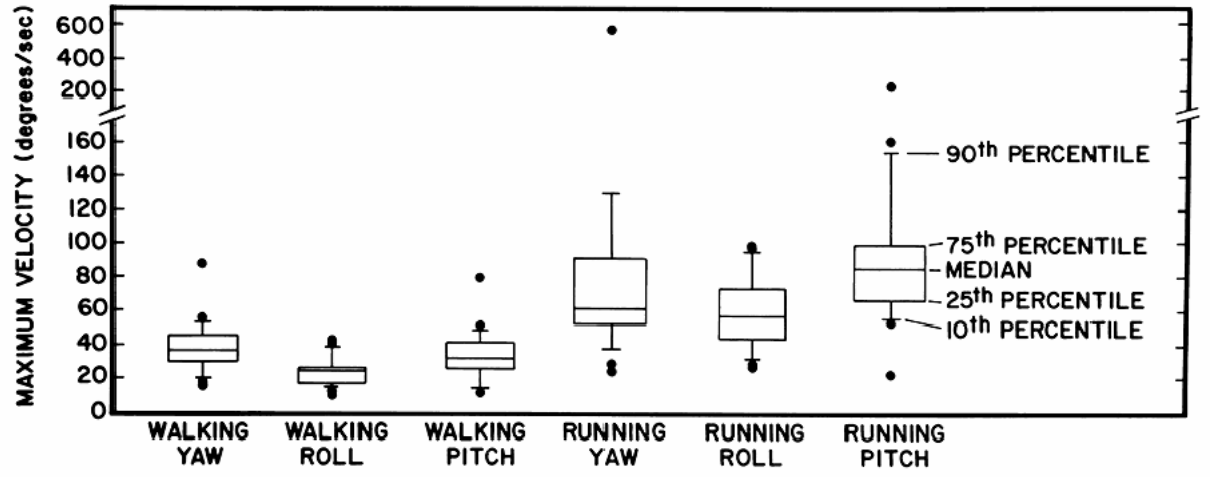

Figure I-8: Maximum velocities during locomotion.
Figure shows a summary of the ranges of maximum velocity of rotational head perturbations occurring during walking or running in place. Distribution of data from 20 normal subjects is displayed as Tukey box graphs, which show selected percentiles of the data. All values beyond the 10th and 90th percentiles are graphed individually as points (Leigh RJ, 1999).

The VOR performance measurement shows saturation thresholds. The gains start to decrease if the rotational head velocity exceeds approximately 350 deg.sec^{-1}. Such movements with vigorous head rotation can be reached during voluntary active head-shaking movements. For amplitudes up to 80°, speeds equal to 700 deg.sec^{-1} in vertical plane and equal to 1100 deg.sec^{-1} in horizontal plane can be accomplished (Grossman, Leigh, Abel, Lanska, & Thurston, 1988;Grossman, Leigh, Bruce, Huebner, & Lanska, 1989).

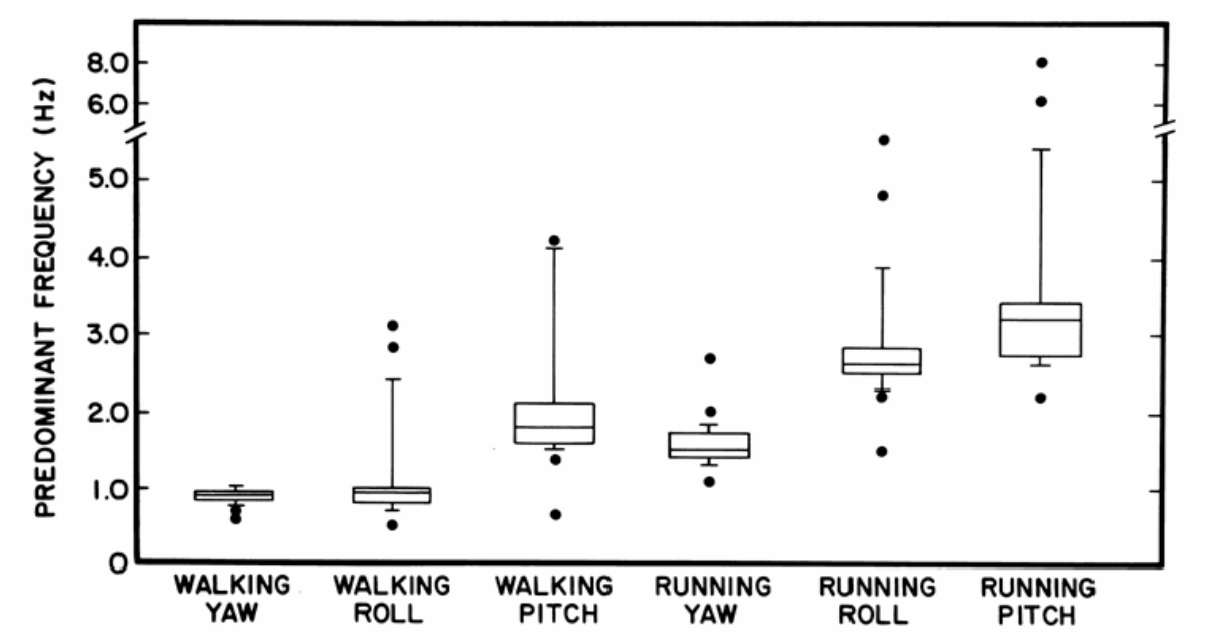

Figure I-9: Predominant frequencies during locomotion.
Figure depicts a summary of the ranges of predominant frequencies of rotational head perturbations occurring during walking or running in place. Distribution of data from 20 normal subjects is displayed as Tukey box graphs, which show selected percentiles of the data. All values beyond the 10th and 90th percentiles are graphed individually as points (Leigh RJ, 1999).

As mentioned above, other reflexes may influence some characteristics of the locomotion. However, it has been suggested that the vestibular system works in a "top-down" fashion, with the brain paying particular attention to the orientation of the head in space rather than to the orientation of the trunk to which the head is "rigidly" attached, and, additionally, with the head serving as a "gaze-anchored" reference system (Leigh & Brandt, 1993). The reaction of the oligosynaptic elementary VOR arc is quick enough and the action of the eyes is sufficient in amplitude for both to reduce maximally the foveal slip. The r-VOR has a *latency* of action (i.e., a time from start of the head turn to the initiation of compensatory eye rotation) that has been reported to be in the range of 5 to 15 msec. The otolith response begins about 25 to 90 ms after the onset of head movement. The ratio between the amplitudes of head and eye displacement during the VOR is near one (Crane & Demer, 1998;Aw, Haslwanter, Halmagyi, Curthoys, Yavor, & Todd, 1996;Leigh RJ, 1999).

Additionally, the VOR is involved in addressing other common perturbations, e.g. head movements caused by transmitted cardiac pulsations (Leigh & Brandt, 1993).

I.2.4.3 Oculomotor Symbiosis

Even though no other sensory mechanism involved in the generation of eye movements compensating for head movements is as prompt in its action as the VOR (e.g., the latency of visual-mediated eye movements is >75 msec), other parts of the oculomotor system overlap in vision-stabilizing function with it should the conditions be changing quickly (see **Table I-F**) (Leigh & Brandt, 1993). One of the typical complementary functions of the oculomotor system is the VOR and OKN system symbiosis. A good example is a sustained rotation of the subject in a large circle, e.g., running on the oval. Because of the mechanical properties of the semicircular canals, the r-VOR by itself can only hold the eyes steady during the first few seconds of turning (the hair of the hair cells slowly return toward its initial position during a sustained rotation). Eventually, the seen world increasingly slips across the retina. That acts as the stimulus to the optokinetic system. Similarly, at the end of a rotation, new change of hair cell bending, as a reaction to deceleration, must occur. The ensuing inappropriate postrotatory vestibular nystagmus is fortunately silenced by a discharging behavior of the OKN called the *optokinetic after-nystagmus (OKAN)*. Consequently, vestibular compensation is supplanted by an optokinetic visual following during a sustained self-rotation.

Head movement		**Reflexes and systems**	**Manifestations**	**Anatomy**
Quick acceleration, frequency of 0.5-5 Hz	Rotational	r-VOR	Quick compensatory eye movements	SCC
	Translational	t-VOR		Otoliths
Slow acceleration with frequency below 0.5 Hz		OKN system	OKN	Striatal, MT a MST cortex
No movement	Frequency of target 0.3-0.5 Hz	Smooth pursuit	Smooth pursuit of the eyes	P-T cortex
	Sustained tilt of the head	Ocular counterrolling	Static torsion of eyes	Otoliths

Table I-F: Simplified map of oculomotor system according to head and target movement. r-VOR – rotational vestibulo-ocular reflex, t-VOR - translational vestibulo-ocular reflex, OKN – optokinetic eye movements, SCC – semicircular canals, P-T – parieto-temporal, MT – middle temporal visual area, MST - medial superior temporal visual area.

I.2.4.4 The VOR Adaptation

The VOR is continually adjusted. It can compensate for the effects of a disease and trauma and the changes that occur with growth and aging. The *VOR adaptation* that corrects the action of vestibulo-ocular reflex to reduce retinal slip is quite potent allowing the system

to change not only the magnitude of eye movements but even its direction [for review about VOR adaptation, see (Leigh RJ, 1999)].

I.2.4.4.1 The VOR Habituation

The VOR may show ability to habituate (i.e., reduction in reaction amplitude etc.). Habituation is most evident after repeated constant-velocity rotations or low-frequency continuous oscillations (stimuli outside the frequency range of most natural head rotations). The functional significance of the vestibular habituation is uncertain, although it may contribute to eliminating the spontaneous nystagmus that follows a unilateral labyrinthine lesion.

I.2.4.4.2 Short-Term VOR Adaptation

The presence of a persistent, unchanging vestibular stimulus engages adaptive mechanisms. Such a stimulus almost never occurs in natural circumstances except when there is a lesion creating an imbalance in vestibular tonus between the two sides. In testing conditions with a constant-velocity rotation, after the original nystagmus dies out, a reversal phase of nystagmus may develop with slow phases in the opposite direction (i.e., the same direction as the head rotation). This phenomenon probably reflects an adaptive mechanism, residing in both the brain stem and the peripheral vestibular apparatus, which has been activated by a persistent vestibular stimulus. This adaptive mechanism has a time constant of action of about 80 sec, so that its effect is completed in minutes.

I.2.4.4.3 Visually Induced VOR Adaptation

As explained above, visually guided eye movements are not quick enough to prevent the slippage of the picture on the retina. In other words, the VOR short latencies exclude the reflex to be quickly adapted by visual inputs. Fortunately, it seems that the system works in open loop manner, and imperfections of the VOR are continuously monitored by the brain, which centrally adjusts the VOR effectiveness. However, longer-term adaptive capabilities based upon visual error signals during head motion must be used.

A visually induced adaptation of the VOR best demonstrates the plasticity of the oculomotor system. It is so elastic, that wearing head-fixed mirrors that cause to move the environment in the same direction like the head moves, changes the VOR reactions in bare minutes. Wearing such device for 3 to 4 weeks actually reverses the VOR.

A plasticity of the VOR shows variety of probable adaptational possibilities. For instance, training the oculomotor response to a vertically moving target while head is moved horizontally adapts the system in *cross-axis* manner, so, afterwards, an eye movement recording during the horizontal head movements shows a vertical component. The system can adapt even after imagination of a visual stimulus, although at about half the rate it occurs when visual stimuli are used. Some adaptations are so instant that probably the brain has mechanisms to enlist different learned vestibular responses depending upon the circumstances in which they must occur.

I.2.4.4.4 Adaptation to Vestibular Asymmetry

A unilateral labyrinthine lesion generates a static and dynamic vestibular imbalance leading to typical manifestations and adaptational processes.

Manifestations of a *static vestibular imbalance* consist of a head tilt and turn together with an ocular torsion of the otholith origin, and a spontaneous nystagmus with slow phases directed towards the side of the lesion. Subject perceives the phenomenon as mostly a rotational vertigo. However, through the brain recalibration of the whole system, recovery of the static balance from a unilateral labyrinthine loss in humans may never be complete; in darkness, some patients show spontaneous nystagmus years after their lesion. Experimental results show that such "resurgence" does not depend on a vision.

A *dynamic vestibular imbalance* shows decrease in corrective eye movements evoked by head movements. In order to correct reaction of a dynamic vestibular imbalance, the system could use information from the remaining intact canals. Nevertheless, dynamic vestibular deficits that follow a complete unilateral labyrinthine lesion (vestibular deafferentation - uVD) are clear and permanent, and experimental results show quite ineffective recovery of human dynamic VOR function (Curthoys, 2000). There are evidences that adaptation to the dynamic imbalance may employ early saccades in the direction in which slow phases are inadequate to keep the stable vision, especially in conditions when movement towards this direction is voluntary, thus predicted. This is found particularly at high speeds and accelerations (Halmagyi, Black et al., 2003;Segal & Katsarkas, 1988).

Hence, in case of the uVD, a stable vision depends mostly on the vestibulo-visual experience in a dynamic vestibular imbalance setting (see also "V.5.1 Multisensory Co-operation in Adaptational Strategies"). A comprehensive review of such compensation and substitution of a dynamic vestibular imbalance was published by Ian Curthoys (Curthoys, 2000).

I.2.4.4.5 Neural Substrate of the VOR Adaptation

Unfortunately, the anatomical background of the VOR adaptation and learning is not quite clear. Vestibular malfunction recruits a readjustment of the VOR reaction but also changes the oculomotor behavior as a whole. It is obvious that the cerebellum, and especially the *floccular* region, is crucial for the elementary VOR changes. Even if Ito's hypothesis of integration of the error signal at the level of flocculus and its reaction on the vestibular nuclei does not account for all experimental data, it has many interesting features and must be discussed (Ito, 1972;Ito, 1982). The flocculus receives vestibular, visual, and ocular motor signals (bilateral, *mossy fiber* inputs, primarily from the vestibular nuclei and the *nucleus prepositus hypoglossi (NPH)*, the *pontine nuclei* and the *nucleus reticularis tegmenti pontis*, *climbing fibers* from the contralateral inferior *olivary nucleus*). The flocculus projects to the ipsilateral vestibular nuclei (y-group, and the basal interstitial nucleus of the cerebellum, important connections to the floccular target neurons (FTN) of VN). The VOR learning could happen on account of modifiable synapses between the *parallel fibers* and the *Purkinje cells*. Ito has proposed that this learning is due to a *long-term depression (LTD)* of synaptic transmission from parallel fibers to the Purkinje cell. An alternative explanation is that the flocculus, rather than being the sole site of the VOR learning, serves other functions in the VOR adaptation. The flocculus could provide an error correction signal to certain neurons in the vestibular nucleus called the flocculus target neurons (FTN). Those in turn would serve as one site of motor learning for the VOR adaptation. In contrary to above hypothesis, computer models of the VOR and vestibular compensation show that the *vestibular nucleus neurons on the contralesional (intact) side* are the cells whose gain changes the most (Carthwright, Curthoys et al., 1999).

I.2.4.5 Quantitative Aspects of the VOR

Only basics of the VOR metrics are presented in this chapter to complete the whole topic of the VOR question. Due to novel approach in VOR measurement presented in this study, the topic will be expanded in the chapter "III Material and Methods".

To quantitatively describe function of the VOR the measurement of output with known input are compared. The compared measures are:

1. Amplitudes
2. Temporal synchrony

The ratio of amplitudes of displacement or velocities of the output and input is called the *gain* (amplitude or velocity gain). The temporal synchrony between the output and input can be

described by *phase* and *time constant*. The VOR response can be treated as a linear control system. There are, however, important nonlinearities in the VOR, especially at high velocities and high accelerations.

Using sine-wave stimuli for the frequencies of head rotation that correspond to natural head rotations (0.5 to 5.0 cycles/sec), gain is about 0.75 (Leigh & Brandt, 1993). The phase of eye and head movements may be compared during sinusoidal movement, and the difference (or *phase shift*) expressed in degrees. The phase shift for above head rotations in healthy subjects is close to 180°: equal-sized eye movements and head movements occur synchronously in opposite directions. By convention, the gain of the VOR that perfectly compensates for head rotations is assigned a value of 1.0, and the phase that perfectly compensates for head rotations is assigned a value of 0°.

The gain of the VOR is affected by the proximity of the visual scene being viewed during rotation or the imagined location of the target of interest. During viewing of a near target the brain compensates not only for the rotation of the head but also for the lateral or vertical displacement (translation) of the eyes—the VOR gain increases. Imagined targets affect gain in the same manner like targets visible. VOR gain in t-VOR shows lower gains in humans; there are many other aspects to consider e.g. target distance and r-VOR contribution that may influence t-VOR gain.

For a sustained, constant-velocity rotation in darkness, the vestibular eye movements (slow phases of nystagmus) progressively decline in velocity, and after about 30 sec, the eye movements cease. The time course of the decline of a slow-phase velocity is similar to a decaying exponential curve that can be defined by a time constant. After one time constant, eye velocity declines to 37% of its initial value; after three time constants, eye movements nearly stop. This central phenomenon, by which the raw vestibular signal is prolonged or perseverated, is accomplished by the velocity-storage mechanism. The vestibular commissure and the cerebellar nodulus seem to be important for the velocity storage. In velocity step rotations, time constant ranges between 10 and 15 sec. As explained above (see chapter “I.2.4 Physiology and Function of the Vestibulo-Ocular Reflex”), the torsional VOR, in response to roll head movements, has lower mean gain value (0.5 for sinusoidal rotations) and short time constant (4 to 5 sec) than the horizontal or vertical VOR. The latter suggests that there is little velocity storage for the roll VOR [for review, see (Leigh RJ, 1999)].

I.2.4.6 Laboratory Evaluation of the VOR Function

The VOR function can be tested best through recording the reaction of the VOR after delivering the stimulus to the vestibular organs. This is usually performed by recording the eye movements after stimulating the vestibular organ either by rotational, caloric or galvanic stimuli.

I.2.4.6.1 Recording of the Eye Movements

There are a number of different techniques for recording eye movements. Each method has its own advantages and limitations. It is important to select the appropriate technique for the particular task, stimulus, and type of eye movement evoked. No single technique is entirely suitable for every occasion and it is important that an appropriate technique is selected. Most common systems used in VOR study is *Electronystagmography (ENG,* alias *Electrooculography, EOG)*, V*ideooculography (VOG)* and *Search-coil Technique (SCS).*

Electronystagmography (ENG) uses the electrodes placed on the skin around the eye to scan for the changes in the electrostatic field during the eye reposition. Examinations by ENG are limited by significant recording artifacts (Chioran & Yee, 1991). Even so, ENG continues to be a dominating and popular clinical method (Schmid-Priscoveanu, Bohmer et al., 2001). ENG unit is usually a robust system with a rotating chair (permitting large scale sinusoidal or asymmetrical stimulations for VOR testing), screen (for stimulation of the OKN, saccadic eye movements and smooth eye movements), caloric test device, and interface for digital recording of eye movements.

Videooculography (VOG) is a modern portable system designed for recording eye movements in two or even all three dimensions. The system typically consists of a stimulating and recording unit. The recording unit usually includes sensory glasses-like device with a built-in CCD camera capable of detecting the movements of the corneal center or corneal reflection, all without any direct touch. Generated signal is used to determine the actual position of the bulb. Together with the recording of the head movement or during the head-fixed recordings, the direction of the gaze can be computed. The movement of the bulb is evoked by precisely defined stimulating paradigms, projected on the screen, or by combining the VOG with rotational chair. In spite of its limitations(van der Geest & Frens, 2002;Schmid-Priscoveanu, Bohmer, Obzina, & Straumann, 2001) VOG is an inexpensive and highly available alternative to other objective methods for recording of eye movements.

Search-coil System (SCS) consists of two systems of coils. The first one, usually mounted to the sides of a big cubic frame, generates two or three orthogonal magnetic fields. During testing, the subject's head is positioned in the center of this coil frame. The second, sensory coil is built into a thicker version of a standard contact lens, positioned on the subject's eyeball. Low-intensity AC voltages induced in the sensory coil are separated to the vertical, horizontal, and torsional eye movements. To date, there are no published occurrences of any permanent eye injury, even when placed on the eyeball for periods longer than stated by the manufacturer's specifications (Irving, Zacher et al., 2003;Murphy, Duncan et al., 2001). Eye-movements measurement using the SCS (Collewijn, van der et al., 1975;Robinson, 1963) (and many others) represents a method used frequently in clinical examinations and research projects for its superior linearity, low noise, high resolution, and possibility to observe rapid changes in eye position (>1 kHz) (van der Geest & Frens, 2002). Modern materials used in contact lens manufacturing position this method into the center of interest. SCS has become a "golden standard" method for measuring the exact eye positions.

I.2.4.6.2 Stimulation Paradigms and Usual Responses

In quantifying the performance of the VOR, the goals of testing are to determine dynamic imbalance (VOR gain, phase) and static imbalance. [for review, see (Demer, Crane et al., 2001;Brandt, 1998;Leigh RJ, 1999)].

To detect the real state of vestibular endorgans and their peripheral connections, *caloric testing* is useful. The caloric response is due to two separate effects of the thermal stimulus: convection currents induced in the endolymph, and a direct effect of the temperature change on the discharge rate of the vestibular nerve. The convection currents are more important. During testing, water is infused into the external auditory meatus traditionally at temperatures of 30° and 44°C. Artificial static vestibular imbalance is evoked. According to the stimulation (warm water) or inhibition (cold water) direction of the nystagmus is elicited. When caloric stimuli cause a greater ocular response in one direction there is a directional preponderance of the vestibular system. If the asymmetry of leftward and rightward slow phases exceeds 30%, then the directional preponderance is likely to be significant. Caloric stimulation is considered a low-frequency stimulus(Halmagyi, Curthoys et al., 1990;Leigh & Brandt, 1993).

Similar to caloric testing but not widely used, due to problems in interpretation of the results, is *galvanic stimulation* of vestibular endorgans. *Vestibular galvanic stimulation (GVS)* provides non-physiological stimulation, and although it is different than natural head

accelerations, it is very selective and thus an attractive tool for experimental testing of vestibular function (Day, 1999;Fitzpatrick, Wardman et al., 1999;Jahn, Naessl et al., 2003). During stimulation, two electrodes are placed over both mastoid processes (for binaural stimulation) or one electrode is placed over the mastoid and the second, indifferent electrode, at the posterior neck over the C7 spinous process (for monaural stimulation). Rectangular, unipolar electric direct current pulses of 10 sec. duration with amplitude of either 1 mA or 3 mA are delivered. GVS stimulates the irregular afferents of vestibular nerve rather than the hair cells (it acts at the spike trigger site of primary vestibular afferents, which extends 10±50 mm from the synapse to the first level of myelinization and is thought to involve afferents from all vestibular endorgans) (Goldberg, 2000;Jahn, Naessl, Schneider, Strupp, Brandt, & Dieterich, 2003). Afterwards, eye movements can be recorded (Jahn, Naessl, Schneider, Strupp, Brandt, & Dieterich, 2003) or the body movements analyzed (Fitzpatrick, Wardman, & Taylor, 1999).

A **static vestibular imbalance** is pathological status, which manifests by a spontaneous nystagmus, and is best detected by recording eye movements in the absence of fixation. Such nystagmus may follow *Alexander's law* (nystagmus due to a vestibular lesion is more intense when the patient looks in the direction of the quick phases) and according to that can be classified as:

- first degree (present only when looking in the direction of quick phases),
- second degree (also present in central position), and
- third degree (present in all directions of gaze).

The effects of different gaze positions upon vestibular nystagmus probably relate to interactions between a vestibular imbalance and the gaze-holding network *(neural integrator)*.

Dynamic imbalance is usually tested by *rotational tests* (Baloh & Demer, 1991;Demer, 1992;Allum, Yamane et al., 1988). Typical tests consist of sinusoidal rotations of the body (and head) with frequency up to 2 Hz in darkness with eyes open. Such rotation is a stimulus for nystagmic jerks; the VOR gain is then computed as ratio of peak velocity of the slow nystagmic component *(slow phase velocity – SPV)* to peak velocity of the stimulus. From temporal differences of the sine waves the phase shift is calculated. The VOR time constant is estimated after a sudden stop subsequent to a constant velocity rotation (see above, chapter "I.2.4.5 Quantitative Aspects of the VOR"). Unfortunately, none of the above stimuli used to test a dynamic imbalance obey quantitative principles of movements during locomotion and other common daily activities (see chapters "I.2.2.1 Semicircular Canals", "I.2.4.5 Quantitative Aspects of the VOR", and "I.2.4.2 Physiology of the VOR During

Locomotion"). It was recently demonstrated by Wiest and colleagues (Wiest, Demer et al., 2001) that usual testing paradigms described in this chapter, which do not comply with typical head perturbations, may not describe real function of the vestibular system. In their study, patients with bilaterally absent caloric vestibular response had near-zero VOR gain, in response to rotational sinusoidal stimulus showed essentially normal gain at 0.8Hz at a peak velocity 30 deg.sec^{-1}. Results were compared with recordings of the same patients during first 100 ms after onset of whole body yaw (horizontal) rotations at peak accelerations of 2800 deg.sec^{-1}. Patients showed profoundly attenuated responses with near-zero VOR gain. To clearly describe the problem, I offer an alternative look at this question: previous chapter sets gain response to the sinusoidal rotations in normal subjects to approximately 0.75. Such performance during common locomotion would lead to a significant retinal slip (appropriate to approx. 17 deg.sec^{-1}) which would impair visual acuity greatly. Tests of visual acuity and quantitative aspects during locomotion disclosed very accurate compensatory movements with gains from 0.9 to 1.1 in both yaw and pitch planes of movement (Grossman, Leigh, Bruce, Huebner, & Lanska, 1989). The gain can be relatively stable even when harmonic frequencies of head rotation range up to 15 Hz.

I.2.4.6.2.1 Head Impulses

To address above concerns, an arguably more reliable method for testing the dynamic imbalance in the VOR that uses properties of common locomotion (acceleration, speed, amplitude, frequency spectrum, randomness) was invented. This technique that incorporates sudden head thrusts was first described by Halmagyi and colleagues in 1990 (Halmagyi, Curthoys, Cremer, Henderson, Todd, Staples, & D'Cruz, 1990) and was named „***Head Impulses***"*(HIT's)*. Physiological background was derived from the SCC ampulofugal and amupulopethal stimulation /inhibition asymmetry which obey second Ewald's law (see chapter "I.2.2 Mechanical Properties of the Sensory Organs"). During head impulse, a passive, unpredictable, rotational, low-amplitude, high-acceleration head thrust is manually delivered in planes of VOR function (yaw, pitch, roll) (Aw, Halmagyi et al., 1994;Aw, Haslwanter, Halmagyi, Curthoys, Yavor, & Todd, 1996;Aw, Halmagyi et al., 1996;Halmagyi, Curthoys, Cremer, Henderson, Todd, Staples, & D'Cruz, 1990) or in the semicircular canal planes (Cremer, Halmagyi, Aw, Curthoys, McGarvie, Todd, Black, & Hannigan, 1998) while fixating the gaze straight ahead. The velocity of such impulse is about 100 deg.sec^{-1}, the eccentricity of rotation does not exceed 20°, and the acceleration goes above 2000 deg.sec^{-2}. Detected responses after selective and global unilateral vestibular deaferentations show large

and apparently permanent decrease in ampullofugal (towards the affected site) rVOR gains (approx. to 0.2 velocity gain) even in patients being otherwise free of any other vestibular symptoms, and with normal ampullopethal responses (Halmagyi, Curthoys, Cremer, Henderson, Todd, Staples, & D'Cruz, 1990;Aw, Halmagyi, Haslwanter, Curthoys, Yavor, & Todd, 1996). If the impulses are delivered in vertical planes, a unilateral affection of any side decreases the responses to 0.5 velocity gain (symmetrically for both downward and upward thrusts), a bilateral vestibular deafferentation shows no response to any of the head impulses (Aw, Halmagyi, Curthoys, Todd, & Yavor, 1994). It is apparent that the head impulses disclose lack of any effective vestibular compensation after a vestibular affection (e.g. the unilateral deaferentation) (compare with "I.2.4.4.4 Adaptation to Vestibular Asymmetry").

Pathophysiologically, attenuated eye responses during the ipsilesional (ampullofugal) rVOR might be probably due to lower sensitivity to stimulation, or could be caused by saturation of neural activity. First was evidenced during eye measurements of patients several months after deaferentation. Responses showed linear velocity increase as a function of head velocity with a velocity gain, which was constant at about 0.2 (Halmagyi, Curthoys, Cremer, Henderson, Todd, Staples, & D'Cruz, 1990). Latter, in contrary, was shown in eye velocity saturations of patients examined early after deaferentation. Similarly, saturation values at about 400deg.sec^{-2} for eye accelerations were also recorded (Aw, Halmagyi, Haslwanter, Curthoys, Yavor, & Todd, 1996;Halmagyi, Curthoys, Cremer, Henderson, Todd, Staples, & D'Cruz, 1990).

I.3 Ageing, Brain and the VOR

Age-related alterations are observed at every level of the central nervous system, from neuronal organelles to the cerebrum as a whole, and are diverse in their appearance, timing and etiology. Some of the changes are global, universal and inevitable; others are regional, specific, and may be preventable. Some seem to emerge as matter of mere passage of time, whereas others can stem from age-related disease processes and cumulative exposure to toxins and pathogens.

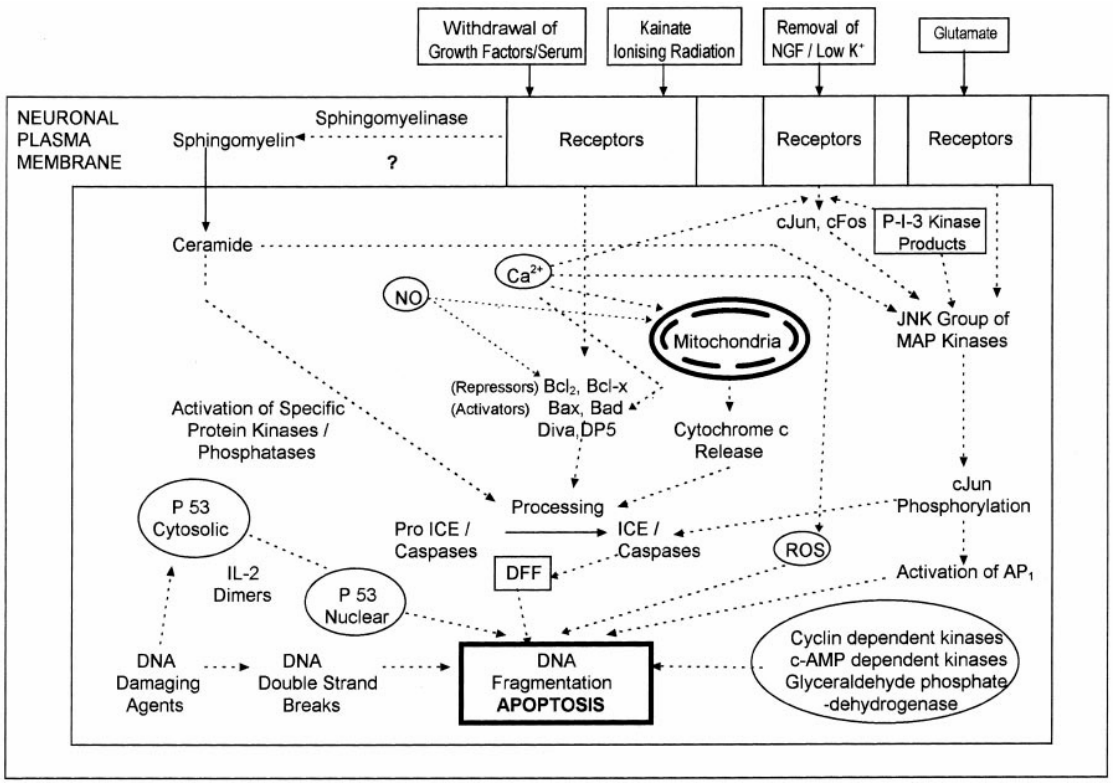

Figure I-10: Putative pathways for apoptosis in the nervous system.
NGF, nerve growth factor; cJun, cFos; transcriptional protein factors; JNK group of MAP kinases, c-Jun N-terminal kinase group of mitogen-activated protein kinases; BCL, BA, protooncogene proteins; DIVA, DP_5, apoptosis regulators;c-AMP, cyclic AMP; DFF, DNA fragmentation factor; IL-2, interleukin-2; P-I-3 Kinase, phosphatidylinositol 3-kinase (Sastry & Rao, 2000).

I.3.1 Apoptotic Changes in the Brain

Generally, there is a significant neuronal loss and accordant cellular changes in the brain that occur with age. This was evidenced in the cerebral cortex (Haug, Knebel et al., 1981;Flood & Coleman, 1987;Simic, Bexheti et al., 2004) as well as in the brain stem (Alvarez, Diaz et al., 2000;Lopez, Honrubia et al., 1997;Tang, Lopez et al., 2001) or the cerebellum(Chen & Hillman, 1999;Fattoretti, Bertoni-Freddari et al., 1998;Hadj-Sahraoui, Frederic et al., 1997;Hall, Miller et al., 1975;Larsen, Skalicky et al., 2000). Structural and neurochemical properties of neurons must change with age. As the brain progresses into senium, an increased production of free radicals and an accumulation of *nuclear (n)* and *mitochondrial (mt) DNA* damage becomes an important aspect. This is accompanied by an age-related decline in the amount of nDNA repair (Rutten, Korr et al., 2003). The response to nDNA damage in eukaryotic cells can lead to apoptosis. Neuronal apoptosis is an evolutionarily conserved form of cell death that occurs through an orderly series of cellular events, resulting in the activation of *caspases* that triggers a *proteolytic cascade* leading to the degradation of the cell's nuclear and cytoplasmic proteins (Matsui & Cotanche, 2004). In detail, intracellular accumulation of nDNA leads to oligomerization of *procaspase-9*, which results in the formation of a

multimeric complex called the *apoptosome*. This brings *procaspase-9* molecules into close proximity with each other, allowing enzymatic self-activation. Caspase-9 *(initiator)* is then able to cleave and activate the downstream effector caspases-3, -6, and -7*(executioner)* (Hajra & Liu, 2004). Even though this *intrinsic pathway* seems to be most common in natural circumstances in the brain, surprisingly, cells of the vestibular pathways, (e.g., Purkinje cells in the cerebellum or the large neurons in the lateral vestibular nucleus) did not show an age-related decline of the rate of spontaneous nDNA repair which lead to age related accumulation of nDNA (Rutten, Korr, Steinbusch, & Schmitz, 2003). This finding suggests different *intrinsic pathway* initiated e.g. by mitochondrial damage (which probably results in the leakage of *cytochrome c* into the cytoplasm that triggers the caspase cascade) or *extrinsic pathways* mediated by specific ligands. The reasons for the difference, as well as, the neurochemical properties are not clear yet. Possible apoptotic pathways in neurons are summarized in **Figure I-10**. In contrary to the central vestibular neurons, apoptotic pathways are better understood in the vestibular hair cells (Matsui & Cotanche, 2004). Models of aminoglycoside treatment show mitochondrial release of cytochrome c into the cytoplasm. Aminoglycoside antibiotics initiate the oxidative stress in the cell which leads to the leakage. Antioxidant gene therapy shows protective results even for overexposing to hearing thresholds in the auditory hair cells. Intracellular increase of Ca^{2+} second messenger linked with activation of hair cell death was observed. There may be a link between the detected rise in Ca^{2}+, and the release of cytochrome c, but further studies are needed. Mechanical damage to a single hair cell causes a wave of intracellular Ca^{2+} to spread from the damaged hair cell to the surrounding supporting cells. It is likely that Ca^{2+} pathways (followed by c-Jun-N-terminal kinases) either trigger the apoptotic signaling pathway or support cell proliferation. In aminogycoside models, the role of any extrinsic pathways was not proven (Matsui & Cotanche, 2004).

The evidence of histological changes in all anatomic structures involved in the VOR clearly shows that even different probable apoptotic pathways in comparison with other parts of brain do not exclude the vestibular system from age-related neuronal loss.

I.3.2 Degenerative Patterns in the Vestibular System

The decrease in the **hair cells** population can be supposed. It is in generally agreed that age-related hearing loss, commonly experienced as *presbyacusis*, is linked to the acoustic hair cell deficit (Seidman, 2000). Subsequently, age-related vestibular hair cell loss must be

also expected. Quantitative analyses of the vestibular hair cell populations showed statistically significant reduction in individuals over 70 years of age. However, this reduction often show a large variability among older individuals from normal hair cell population up to 60% loss; as compared with groups of children and young adults, clear gradient progression of lower density of hair cells for subjects more than 30 years old is found with average of approximately 6% per decade. Extracellular changes, like the incidence and densities of intraepithelial inclusion bodies also increases in correlation with hair cell loss. Some results suggest higher loss in the striola regions of the maculae in comparison with peripheral regions. Related cristae ampullares show a more pronounced age-related reduction of hair cell populations than maculae (**Figure V-3** (Richter, 1980;Rosenhall, 1973)).

Even more evident reduction in vestibular structures is seen in number of **nerve fibers** of the preganglionic portion of the vestibular nerve, which significantly and gradually decreases with age. Records exist showing an averages 37% loss in subjects over 75 years of age compared with subjects younger than 35, with slight interindividual variation, and with decrease especially in proportion of thick myelinated fibers. Hence, slow deviation of the caliber spectrum towards the thinner side is seen in old age groups. These changes are most pronounced in the ampullary nerve branches. It is most likely that the thick fibers disappear first because of the change in a caliber pattern as the result of a general involution of all nerve fibers in old age. This is supported by the evidence of an age-related decrease in the transverse areas of myelinated axons, although the numbers of the axons does not change. In the case of unmyelinated axons, both the transverse areas and the numbers do not change. The spectrum of macular fibers is shifted to the thin calibers already in young (**Figure V-1** (Bergstrom, 1973;Bergstrom, 1973;Bergstrom, 1973;Nagai, Goto, Goto, Kaneko, & Suzaki, 1999)) subjects

At around the age of 60, a significant drop in the average number of the **vestibular ganglion cells** has been reported (Richter, 1980). Another more recent study set the highest rate of decline between 30 and 60 years of age with the highest rate of decline of about 5% per year at around 44 years of age (**Figure V-4** (Park, Tang et al., 2001)).

The number of **neurons in the vestibular nuclei** shows a highly significant decrease with age. The neuronal loss is approximately 3%-5% per decade between 40 and 90 years of age with the highest loss in the SVN and lowest in the MVN. Relatively similar age-related decline in volume, neuronal density is seen together with an increase in neuronal degenerative changes. The greatest age-dependent loss occurs in small and medium neurons. This is partly due to a hypertrophy of the remaining neurons (Lopez, Honrubia, & Baloh, 1997;Tang,

Lopez, & Baloh, 2001;Alvarez, Diaz, Suarez, Fernandez, Gonzalez, Navarro, & Tolivia, 2000).

The role of the cerebellar *Purkinje cells (PC)* in the VOR function, memory and adaptation is unquestionable (Ito, 1984;Ito, 1972;Ito, 1982). There is reported gradient cerebellar weight and volume loss through all decades (greater in man then woman), and Purkinje cell loss of 25 % over the age span 0 to 100 years with sudden decline after 60 years of age (with wide interindividual variation) (**Figure V-2** (Hall, Miller, & Corellis, 1975)). Aged Purkinje cells show loss of dendritic synapses, shrinkage of mitochondrial volume, and changed intracellular structural parameters, as well as smaller PC somata. Protective influence of long-term physical exercise to age-related PC loss has also been also proven (Chen & Hillman, 1999;Fattoretti, Bertoni-Freddari, Caselli, Paoloni, & Meier-Ruge, 1998;Hadj-Sahraoui, Frederic, Zanjani, Herrup, Delhaye-Bouchaud, & Mariani, 1997;Larsen, Skalicky, & Viidik, 2000). Hall and associates (Hall, Miller, & Corellis, 1975) also assessed systematically postmortem specimens for small and large vessel disease, and even after exclusion of all cause with vascular disease, they found a clear cut age-related loss of the Purkinje cells within the cerebellum. This proved an unbiased truly age-dependent cell decrease in vestibular system.

I.3.3 Age-Related VOR Performance

Majority of the previous studies pertaining to the age-related changes of VOR function were limited to whole-body sinusoidal rotations in horizontal plane. The results are varying greatly, but a large amount of studies indicate decreased gain with increasing age. Unfortunately, mostly low frequencies have been studied (approx. from 0.005 to 0.8 Hz). In this range, the gain trend has been more consistent at lower frequencies than in higher ones. Parallel changes were described in phase shift increase (Wall, III, Black et al., 1984;Peterka, Black et al., 1990;Paige, 1992). Age differences have been more pronounced in high peak head velocities (300 deg.sec^{-1}) (Paige, 1992). The VOR average responses to caloric stimuli show minor decrease for subjects of up to about 40 years, and then increase at a low rate for older subjects. Slight increase of labyrinthine asymmetry in subjects after 60 years of age was also described (Peterka, Black, & Schoenhoff, 1990). Peterka et al. (Peterka, Black et al., 1990) applied rotational stimuli used however on a pseudorandom pattern. The pseudorandom stimulus consisted of summation of 8 discrete sinusoidal frequencies (from 0.01 to about 1.5 Hz) with nominal amplitudes of 7.8° or 15.6°. The highest instantaneous stimulus velocity

delivered was about 100 deg.sec^{-1}. Results suggested decrease in the VOR gain from youth till the age of 50 and then a very small increase slope for the older subject. The VOR time constant decreases respectively with the break point at the age of 30. Paige (Paige, 1992;Paige, 1994) used sinusoidal rotation at 7 frequencies from 0.025 to 4 Hz, and peak velocities between 100 and 300 deg.sec^{-1}. Lower gain in elderly was associated only at 0.025 Hz but age difference became very significant at high velocity (300deg.sec^{-1} tested at 0.25 Hz). Kim and Sharpe (Kim & Sharpe, 2001) delivered sinusoidal rotations of 20° amplitude and with frequencies between 0.25 and 2.0 Hz in horizontal and vertical planes. They found no difference with increasing age except for a downward movement at 0.25 Hz. One earlier study by Yagi and colleagues (Yagi, Sekine et al., 1983) described a strong influence of the horizontal rotational VOR gain by age. However, the highest gains were seen in pediatric age groups and lowest gains in the 30s, followed by a gradual increase to the 70's.

In a recent study by Tian and colleagues (Tian, Shubayev et al., 2001), more natural, transient, mechanically delivered, rotational testing at high acceleration was used to disclose an age-related deterioration of the VOR function. Twelve older subjects were tested and compared to equivalent group of young subjects. All were rotated in yaw plane at two peak stimulus accelerations of 1000 deg.sec^{-1} and 2800 deg.sec^{-1}. Initial VOR gain (recorded in interval 35-45 ms from onset of rotation) among older subjects was only about half of that of the younger ones. About 75ms after rotation onset gain increased to become comparable. Mean latency of the VOR response in older subjects was about 4ms more prolonged in both accelerations.

Quite recently, age-related changes in the VOR have been tested using non-rotational stimuli. GVS were used by Jahn and co-workers (Jahn, Naessl, Schneider, Strupp, Brandt, & Dieterich, 2003) in a large, age-varied subject group. Reactions in torsional eye movements were recorded. Although the subjects showed large interindividual differences typical for the GVS especially in older subjects, binaural 3mA stimulations caused a significant increase in responses with increasing age from the third to the sixth decade, but decrease for more advanced ages. This was acknowledged for both the torsional nystagmus SPV and the amplitude of ocular counterrolling. Responses in torsional eye movements in this study showed an inverse U-shaped curve indicating age dependency. Since the GVS stimulates the vestibular nerve rather than the hair cells (Goldberg, 2000), Jahn and colleagues speculated that this U-shaped curve of function was due to an increased sensitivity of the central vestibular structures, which could maintain normal function despite reduced peripheral input caused by gradual decrease in number of hair cells [see (Richter, 1980;Rosenhall, 1973), and

Figure V-3, Figure V-9]. It is accepted, that central neuron decline begins at midlife, increasing in rate at an older age [see (Lopez, Honrubia, & Baloh, 1997;Tang, Lopez, & Baloh, 2001;Alvarez, Diaz, Suarez, Fernandez, Gonzalez, Navarro, & Tolivia, 2000), and **Figure V-4**], which could subsequently lead to a breakdown of the GVS response in the late-age elderly (see **Figure V-8**). Although irregular afferents stimulated mainly by the GVS do not play a crucial role in the VOR function, their observation suggests that higher binaural currents of 3mA are large enough to stimulate regular afferents who have higher thresholds to stimulation (and do not decrease with age so apparently). Similar U-shaped responses associated with age were shown in other studies that applied the GVS stimulation on other vestibular dependent reflexes (Welgampola & Colebatch, 2001;Welgampola & Colebatch, 2002) The compensatory increase of the cervico-ocular reflex with age seen in healthy humans appears consistent with the above findings. In this study by Kelders at al (Kelders, Kleinrensink et al., 2003), no breakpoint age was found but the COR had an augmented gain of response especially at ages above 60.

II Hypothesis

Should one assume that the VOR performance is related to a normal function of peripheral receptors and applicable peripheral anatomical structures, a gradual age-related impairment of quantitative parameters of the VOR could be expected. In the circumstances where central adaptive control mechanisms are functioning properly, the system can behave normally even in the situation of decreased peripheral activity. According to the literature review, we can speculate that most central compensatory mechanisms show some capacity to facilitate inputs from the peripheral vestibular structures. Probable critical threshold age can be suggested, after which these central mechanisms are not able to serve any more, resulting in a distinct decline in the VOR output.

In my study, I set to describe the VOR performance at different ages in circumstances that closely simulate perturbations of common locomotion. These perturbations will be reproduced by the head impulse test (HIT), while response of the VOR will be evaluated with the SCS eye movements recording. In agreement with previously published literature, I presume a gradient decline in the VOR performance associated with age, with a probable border age period after which the central mechanisms will no longer be able to adapt to anatomical changes any further. This will consequently lead into a progression of the VOR decline.

III Material and Methods

III.1 Subjects

38 normal human subjects (mean age 46,7 ± 18,09 SD, range 58, max 81, min 23, 22 males, 16 females) divided into 3 groups according to age were studied (twelve in young group: age up to 30; thirteen in middle age group: age 30-60; thirteen in old subjects: age over 60; for subjects' age distribution see histogram and scatterplot in **Figure III-1** and **Figure III-2**). All subjects were presenting with no history of any disease or injury that could indicate any vestibular disorder. All had no evidence for a neurological, ENT, or ophthalmologic disorder. The subjects with presbyopia and myopia of low degree were not excluded. All subjects gave their informed consent after explanation of the experimental procedure in accordance with the Declaration of Helsinki.

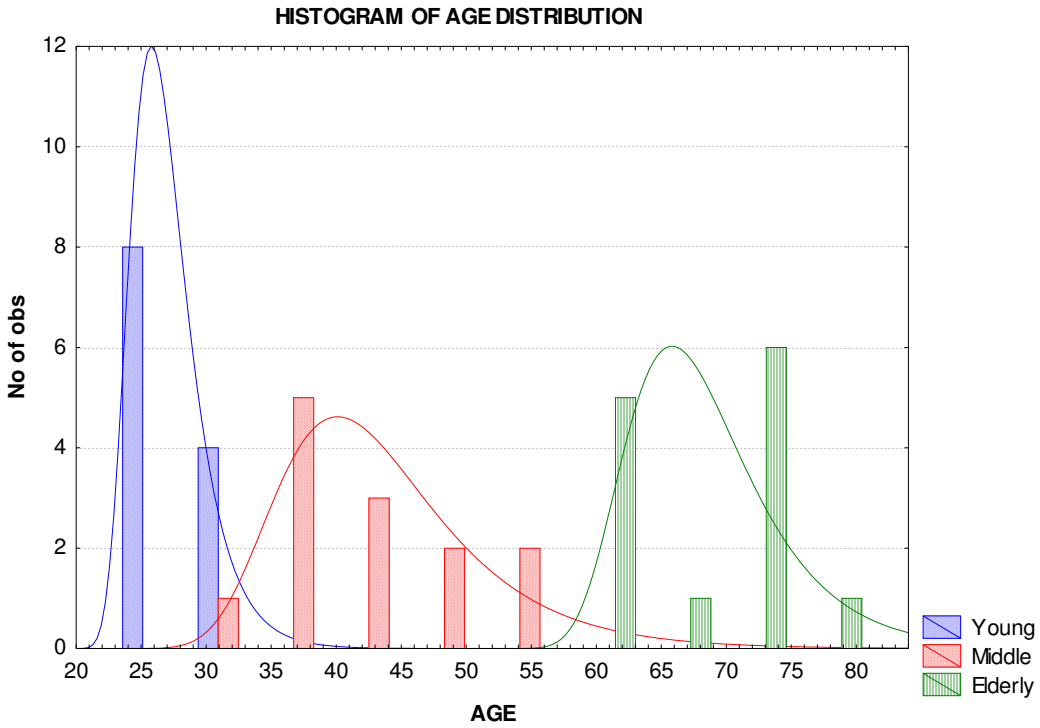

Figure III-1: Histogram of age distribution.
Histogram shows the smallest age dispersion of subjects in young group and quite equal age distribution between middle and elderly groups.

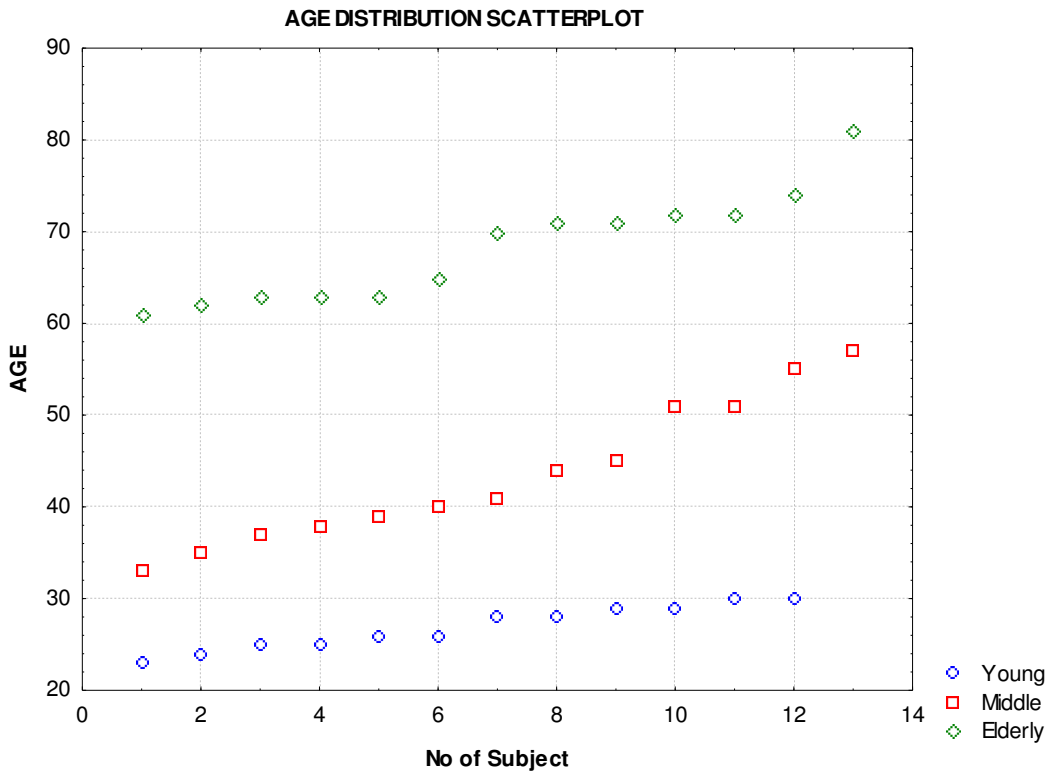

Figure III-2: Scatterplot of age distribution.
Plot shows gradient distribution of subjects in age in all three age groups. The skewness of the distribution is smallest in the young age group, illustrating a small age differences in this group. In the elderly group an apparent age step is seen between age 65 and 70, similarly a step between ages 45 and 50 is seen in the middle group. One evident outlier in the elderly group is of age above 80.

III.2 Procedure

III.2.1 Search Coil Recording

Angular displacement of the head and eye in yaw, pitch and roll were recorded using the search-coil technique.

The magnetic field search coil technique (introduced for the first time by Robinson, modified by Collewijn and others (Collewijn, van der, & Jansen, 1975;Remmel, 1984;Robinson, 1963)), is based on a phase-locked amplitude detection of the voltage induced in a search coil in the external AC magnetic field. The angular orientation or displacement of the search coil in three-dimensional space is detected by using two or three external magnetic fields, which are arranged in space quadrature. Demodulation of the induced signals with respect to the magnetic field directions is obtained on the basis of phase or frequency coding by driving the external magnetic fields in phase quadrature or at different frequencies (Remmel, 1984). In order to obtain reproducible results, the search coil measurements have to be restricted to the uniform part of the external magnetic field.

Data in this study were recorded using electromagnetic eye-movement monitor, invented by Ronald Remmel (Remmel Labs, Ashland, MA, USA (Remmel, 1984)) (see **Figure III-3** and video Remmel.mov on enclosed CD). Available system offers low noise and appropriate stability (2006).

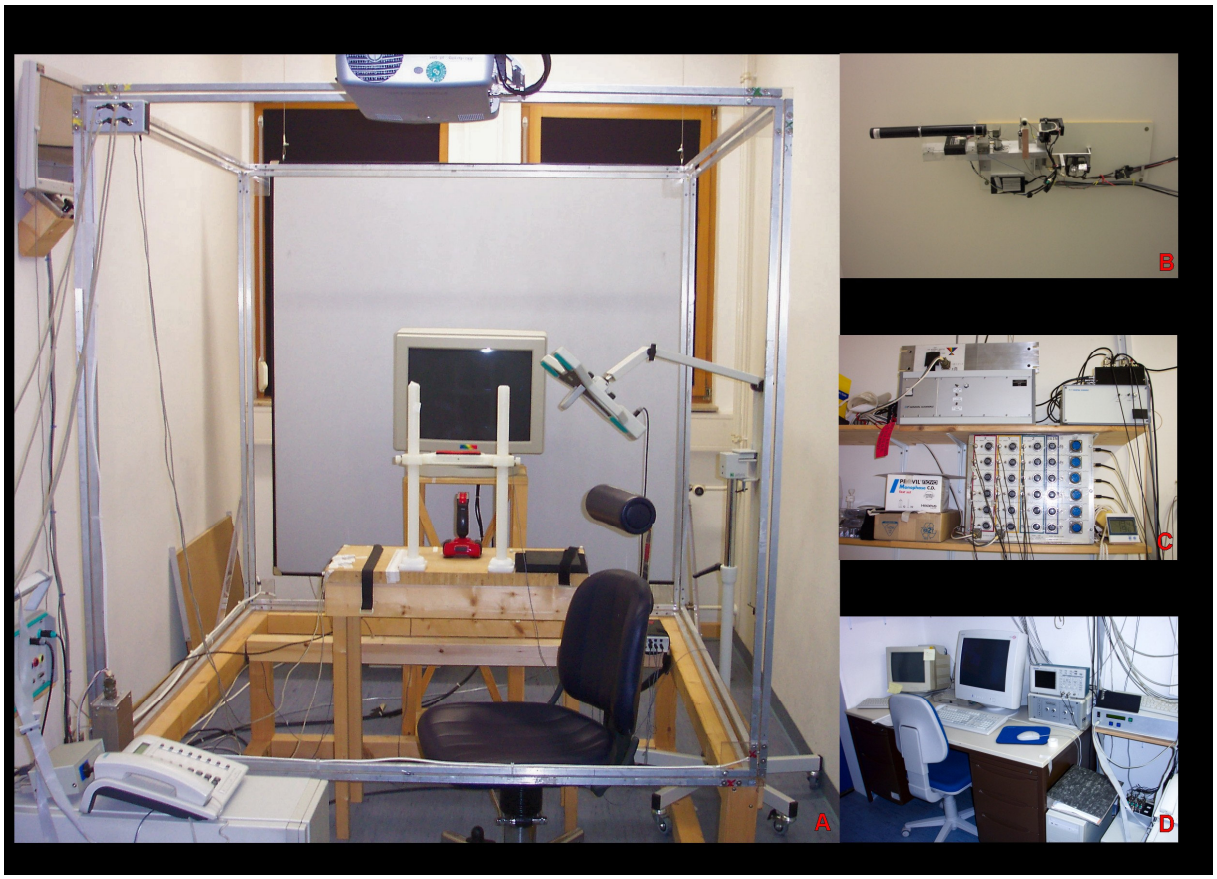

Figure III-3: Setting of Remmel electromagnetic eye-movement monitor system.
Presented setting was used during all recordings in Sensomotorikforschung laboratory at the Department of Neurology, Klinikum Grosshadern, Ludwig-Maximilians-University Munich, Germany.
Part (A) shows cubic aluminum frame that produced three orthogonal alternating magnetic fields. In the middle is seating and head rest for the examined subjects. On the left we can see LCD display, that was used to show traces of head rotations in pitch, yaw and roll during testing, this served as a feedback for operator about correctly performed HIT's.
Part (B) demonstrates stimulating laser (General Scanning G120D, Watertown, Mass., USA) controlled horizontally and vertically by a mirror galvanometer. In this research was laser used mostly for calibration purposes and for displaying the fixation dot during HIT delivery.
Part (C) displays Remmel interface for dual search coil lens for setting the offsets and gains.
Part (D) shows recording and stimulation hardware (IBM PC compatible, Intel® Pentium III based computers running under the real time operating system QNX). All HIT's were recorded in one session; data were separated and analyzed off-line.

In the study setup, subjects were seated in the center of a field coil system consisting of a cubic aluminum frame (side length 140 cm) that produced three orthogonal alternating magnetic fields in the X, Y and Z directions at 48, 60 and 80 KHz, respectively, which are generated by Helmholtz field coils. Dual eye search coil (Skalar, Delft, the Netherlands),

constructed of a contact lens containing a fine coil of wire, with leads coming out on the side, was placed in the subject's left eye after anesthetization of the conjunctiva /cornea with Oxybuprocain-HCl (see **Figure III-4**). Magnetic fields induced voltages into the eye coil, which vary with eye rotation. These voltages were demodulated to give three analog signals for the eye rotation in the X, Y and Z directions. Ocular rotation of the left eye around the horizontal (z- axis), vertical (y-axis) and the torsional (x-axis) was recorded. A second coil, that records head movements, was fixed at the center of the forehead (glabella). This part of the head was chosen due to firm connection with the bony bottom that reduces unwanted slips coil during HIT. Additionally, a coil was fixed bitemporally and vertically with an adhesive tape. We took a special care to ensure that this coil did not move during measurements. Erroneous data caused by an unwanted head coil movement complicated recordings and data analysis in previous investigations (S.T.Aw personal communication), and were also experienced during early data acquisition in our study. To minimize the effect of slippage of the scleral search coil, also observed often (Straumann, Zee et al., 2000;Van Rijn, Van der et al., 1994;Van Rijn, Van der, & Collewijn, 1994), position of the coil was frequently visually controlled during recording. In addition, eye position at gaze straight ahead, to which the eye and head returned after HIT, served as a control. For initial alignment and calibration, the head was secured in a head holder with chin rest and positioned such that Red's line was tilted max 10° nose-up above the earth horizontal as measured with hand-held goniometer. The height and position of the subject's eye was adjusted to ensure that it was in the centre of the coil field and 140 cm from the screen. At the center of a screen, subjects fixated on a red laser dot – visual target (size 0,1 deg), which was controlled horizontally and vertically by a mirror galvanometer (General Scanning G120D, Watertown, Mass., USA), capable to provide short-step responses within less than 2 ms. Except for the target acquisition phase, the tests were done in the darkness.

The head impulses were manually delivered, passive, unpredictable in timing and direction, low in amplitude (10-20°), high in acceleration (>1000°/s^2), head rotations in the directions of the vestibulo-ocular reflex (VOR) (yaw, pitch, roll), with subjects sitting in the upright position and fixating stationary target. Operator stood behind the subject, held the subjects head and delivered the impulses. A minimum of ten impulses in each direction was done (see video Hits.mov on enclosed CD):

1. Right and left in yaw,
2. Up and down in pitch,
3. Counterclockwise (CCW) and clockwise (CW) in roll.

We referred to the three components of the head and eye rotations as the torsional, vertical, and horizontal components expressed with respect to the subject. CCW means that the upper pole of the head of eye is rotated toward the left and CW means it is rotated toward the right. To keep the magnetic field homogenous, no metal was allowed in the aluminum coil frame during recording. 3D-search coil data were digitized with a 12 bit analogue-digital converter at a sampling rate of 1 kHz (National Instruments DAQ board PCI-MIO-16E-1, National Instruments Corp., Austin, TX, USA). Data were recorded by the UNIX - based multiple process system for real-time data acquisition and control - the REX system (by Hays AV, Richmond BJ, & Optican LM, Laboratory of Sensorimotor Research, National Eye Institute, NIH, Bethesda, MD, USA, (Hays, Richmond et al., 1982)). All HIT's were recorded in one session; data were separated and analyzed off-line. Recording and stimulation hardware consists of two IBM PC compatible, Intel® PentiumIII-based computers, running under the real time operating system QNX and REX recording system. Recording hardware projected three traces of head rotations in pitch, yaw and roll on a dimmed LCD display during testing. Display was out of sight for the subject but served as a feedback for operator about correctly performed HIT (correct waveform and maximal speeds).

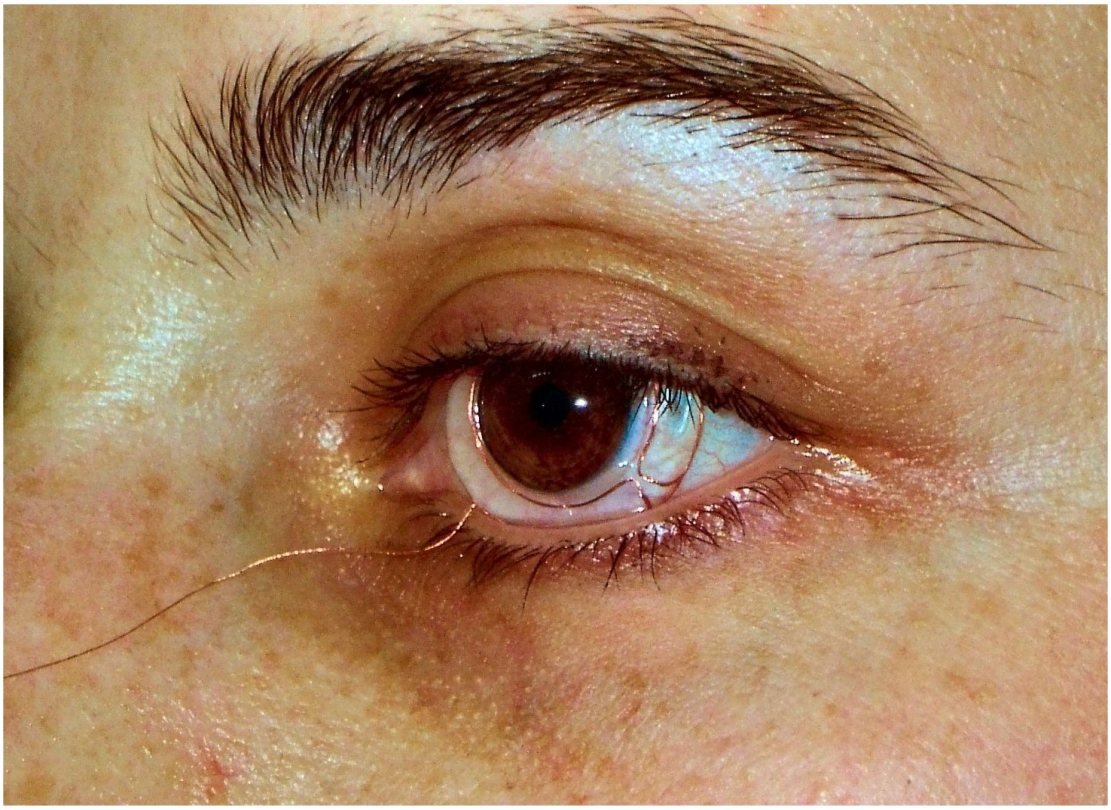

Figure III-4: Dual eye search coil placed in the eye.
Coil is constructed of a contact lens containing a fine coil of wire, with leads coming out on the side, was placed in the subject's left eye after anesthetization of the conjunctiva with Oxybuprocain-HCl.

III.2.2 Calibration

Immediately before each eye movement recording, the coil was moved manually within the coil frame to determine the magnitude and relative orientation of the three magnetic fields and the gain of the directional coil. The linear relation between the normal vectors $\underline{c}_d/\underline{c}_t$ of the effective plane of the directional/torsional coils and the induced voltages $\underline{u}_d/\underline{u}_t$ was expressed as

$$\underline{u}_d = g_d \cdot H^T \cdot \underline{c}_d + \underline{o}_d \tag{11}$$

$$\underline{u}_t = g_d \cdot H^T \cdot \underline{c}_t + \underline{o}_t \tag{12}$$

where the vectors o_d/o_t denote the offsets due to induction in the non-moving parts of the lead wire of the coil (e.g., connectors). The columns of the matrix H represent the three magnetic fields and the scalar factors g_d/g_t represent the total gain combining the inductance of the coil and the amplifier gain. In a first step, the coil was moved manually covering all possible directions between $-\pi$ and $+\pi$ of horizontal eccentricity and between $-\pi/2$ and $+\pi/2$ of vertical elevation. The measured voltages u_d/u_t were used to determine the field matrix H and the gain factor g_d by minimizing the distance between the endpoints of the coil-vectors c_d/ct and the surface of a sphere with radius 1 under the additional constraint that the angle between the directional and the torsional coil vector stayed constant. In a second step of the calibration, the subject was wearing the coil and fixating target positions within ±20° horizontal eccentricity and ±15° of vertical elevation. In each session intervals of stable eye positions of 300 ms were collected from the late fixation periods (within a period of 500 ms immediately before the target stepped). These data were used to determine the offsets o_d/o_t and the gain factor g_t by the same minimization procedure, again assuming that the angle between the directional and the torsional coil stayed constant and did not depend on accurate fixation of the target. In a third step, the subject repeatedly fixated a target at straight ahead. From these data, the relative rotation of the coil on the eye was computed. The resulting eye positions were expressed as rotation vectors (Haustein, 1989). This method provided a reliable calibration within the examined range of horizontal eccentricities (max ±25°).

III.3 Data Analysis

Data were analyzed off-line in Matlab® (Mathworks, Natick, MA, USA). The calibrated data were low-pass filtered using a digital Gaussian filter with a bandwidth of 33 Hz. Saccade and fast phase were automatically detected and removed from the data using a combined velocity-acceleration criterion in interactive software so that detection errors could be corrected manually.

The orientation of the eye in the head was calculated from the gaze and head positions (Haslwanter, 1995). Head and gaze velocity was determined in space-fixed coordinates, the eye velocity in head-fixed coordinates from the head, gaze and eye positions. The time traces of head, gaze and eye positions were smoothed and differentiated with the use of the formula by Savitzky and Golay (Savitzky & Golay, 1964):

$$f_i = \sum_{k=0}^{k=n} b_{nk} i^k = b_{n0} + b_{n1} i + b_{n2} i^2 + \cdots + b_{nn} i^n \tag{13}$$

The formula uses a set of *2m +1* consecutive values in the determination of the least-mean fit through these values of a polynomial of degree *n (n<2m+1).* The derivatives of the polynomial are:

$$\frac{df_i}{di} = b_{n1} + 2b_{n2} i + 3b_{b3} i^2 + \cdots + n b_{nn} i^{n-1} \tag{14}$$

Angular head, gaze, or eye velocity $\vec{\omega}$ was determined from its corresponding rotation vector $\vec{r}$ by the following equation (Hepp, 1990):

$$\vec{\omega} = \frac{\left(\frac{d}{dt}\vec{r} + \vec{r} \times \frac{d}{dt}\vec{r} \right)}{(1 + \vec{r}^{\,2})} \tag{15}$$

where × denotes the vector cross product. Similarly, the velocity was differentiated to obtain acceleration. Data were analyzed spatially by projecting them onto the three coordinate planes.

Head impulses were automatically detected from the data according to a combination of several criteria: Peak angular head velocity had to be reached within the first 150 milliseconds after onset of head impulse and had to exceed 70 deg.sec^{-1}, head acceleration had to exceed 1,000 deg.sec^{-1}, head velocity 50 milliseconds before onset of the impulse did not exceed 20 deg.sec^{-1}, the relevant component of head velocity did not change sign during the impulse, the maximum difference between eye and head velocity before onset of the head impulse did not exceed 20 deg.sec^{-1}, and the direction of the rotation axis of the head at maximal velocity had

to lie within ±45° of the intended direction. Head impulses with a maximum head velocity outside 1.5-fold the interquartile range were rejected as outliers. The onset of the head impulse was defined as the time when head velocity exceeded 20 deg.sec^{-1}. Because of this procedure, at least six valid head impulses per stimulation plane and subject remained for subsequent analysis. The additional slow-phase drift of the patients was computed as the median eye velocity vector of all data points when the head was stable in space. This eye velocity offset was subtracted from the eye velocity data before computing the gain values. We minimalized the contribution of other reflexes (VCR, COR, visually guided reflexes), by restricting our analysis to an interval of 80 ms from the onset of the head impulse.

III.3.1 Vector Analysis of Three-dimensional Input-Output Kinematics of the VOR

A three dimensional vector is a quantity that possesses both magnitude and direction and can be represented in terms of its components parallel to the axes of a Cartesian coordinate system. These component or projections are the torsional, vertical, and horizontal. Whereas in one-dimensional vector analysis only one of the three components of the vector is used, all three components of the vector are used in the three-dimensional vector analysis. This distinction is important when the compensatory eye rotation axis is misaligned with head rotation axis. Omitting two of three vectors in this case will lead to biased information about VOR performance [for review, see (Aw, Haslwanter, Halmagyi, Curthoys, Yavor, & Todd, 1996)]. To quantitatively describe function of VOR we can compare the measurement of output with known input (see chapter "1.2.4.5 Quantitative Aspects of the VOR"). Therefore, the magnitude of three-dimensional input-output kinematics of the VOR, expressed as G *(velocity gain)*, is defined as the ratio of the eye velocity magnitude in head-fixed coordinates to the head velocity magnitude in space fixed coordinates and is given by:

$$G = \left| \frac{\vec{\omega}_e}{\vec{\omega}_h} \right| = \frac{\sqrt{\omega_{e,x}^2 + \omega_{e,y}^2 + \omega_{e,z}^2}}{\sqrt{\omega_{h,x}^2 + \omega_{h,y}^2 + \omega_{h,z}^2}} \tag{16}$$

where the vectors are as follows: eye velocity:

$$\vec{\omega} = \begin{pmatrix} \omega_{e,x} \\ \omega_{e,z} \\ \omega_{e,z} \end{pmatrix} \tag{17}$$

and head velocity:

$$\vec{\omega} = \begin{pmatrix} \omega_{h,x} \\ \omega_{h,z} \\ \omega_{h,z} \end{pmatrix} \tag{18}$$

As explained above, three-dimensional analysis gives us the possibility to analyze total VOR performance. We can measure not only the velocity of eye response in three-dimensional coordinates but also the difference in temporal space alignment. *Misalignment angle (δ)* then can be defined as the instantaneous angle by which the eye rotation axis deviates from perfect alignment with head rotation axis in three dimensions. By convention, when the eye rotation axis aligns perfectly with head rotation axis and when the eye velocity is in the direction opposite to head velocity, $\delta=0$. To correctly calculate the angle common reference system must be picked, e.g., the head fixed coordinate system. Therefore, it is necessary to transform the direction of head velocity referenced to space-fixed coordinates ($\vec{\omega}_h^{space}$) to the same head-fixed coordinates as eye velocity ($\vec{\omega}_h^{head}$) [for exact explanation and equations, see (Tweed, Sievering et al., 1994)]. δ is then calculated as the instantaneous angle in three dimensions between the inverse of the eye velocity axis and the head velocity axis by the use of the scalar product o two vectors, where δ measures the smaller angle between the two vectors when their initial points coincide. The inverse of eye velocity ensures that $\delta=0$ when the eye velocity axis aligns perfectly with the head velocity axis and eye velocity is directed opposite to head velocity:

$$\delta = \cos^{-1}\left(\frac{-\vec{\omega}_e^{head} \cdot \vec{\omega}_h^{head}}{\left|\vec{\omega}_e^{head}\right| \left|\vec{\omega}_h^{head}\right|} \right) \tag{19}$$

If above values are acquired, the real ratio of head and eye velocities, the total VOR gain *(γ, γ-gain),* can be computed:

$$\gamma = G * \cos(\delta) \tag{20}$$

were γ is defined as the ratio of the inverse projection of the eye velocity to the projection of the head velocity. γ obtained during roll, pitch, or yaw impulses is termed as the roll-torsional, pitch-vertical, or yaw-horizontal γ, respectively. The important parts of Matlab script, based on the equations presented above and used for data analyzing, are available in Attachment A (with permission of the developer, Dr.-Ing. Stefan Glasauer, Geschäftsführung Zentrum f. Sensomotorik, der LMU und der TU München). All default options and important notes in the script concerning the study are retained.

The median data (for G, δ, and γ-gain) for each subject and condition (HIT in yaw, pitch, roll) were computed for 4 time points (20, 40, 60, 80 ms after onset) with exception for roll movements due to early resetting quick phases that occur before 80 milliseconds after onset of head impulse—only three time points were considered (20, 40, 60 ms after onset).

A repeated measures analysis of variance (ANOVA; Statistica® 6.1; Statsoft, Tulsa, OK, USA) with two within-subject factors (stimulation plane: roll, pitch, yaw; direction: positive, negative) and three between-subject factor (young, middle, elderly) was performed. Post Hoc Bonferroni test was used to consider significance between subject groups. Multivariate approach (multivariate measures of association) was used to consider significant differences in results according to age as a continuous predictor.

The purpose of analysis of variance (ANOVA) is to test for significant differences between means by comparing (i.e., analyzing) variances. More specifically, by partitioning the total variation into different sources (associated with the different effects in the design), we are able to compare the variance due to the between-groups (or treatments) variability with that due to the within-group (treatment) variability. Under the null hypothesis (that there are no mean differences between groups or treatments in the population), the variance estimated from the within-group (treatment) variability should be about the same as the variance estimated from between-groups (treatments) variability.

The Bonferroni procedure involves tests of multiple a-priori hypotheses while controlling the experimenter-wise error rate; specifically, it can be shown that the type 1 error rate (alpha(exp)) for a set of comparisons will not exceed the sum of the error levels (alpha(ind)) for a set of m tests of significance; or alpha(exp) < m*alpha(ind). The Bonferroni procedure uses this inequality to adjust the significance levels for the individual post-hoc comparisons.

Multivariate measures of association provide information about the strength of the relationships between predictor and dependent variables independent of the dependent variable interrelationships. From four commonly used multivariate measures of association we used *Wilks' Lambda* which is perhaps the most easily interpretable (StatSoft, 2003).

Significance was set to $p<0.05$

III.4 Potential Errors and Artifacts

Any artifact that appeared in the recording systems and during data acquisition was to be cancelled out by using standardized approach. Any systemic error should not produce differences (we compare relative responses among age different groups under identical conditions). Two possible errors were considered.

III.4.1 Artifacts Due to Translation of Head and Eye Coil

Rotational head movements invariably produce translations, or linear displacements, of the orbits and the coils attached. Even if the axis of rotation is centered on one orbit, the other eye will still be translated during rotation of the head. The same problem can be considered for the head coil, which is placed in the middle of the forehead. However, static translations of 5 cm from the center of the magnetic fields along the left-right axis produced very small artifacts of ≤ 0.01 deg.cm^{-1} for horizontal signal and ≤ 0.02 deg.cm^{-1} for the vertical and the torsional signals. Translations of the coils are usually less then ±2 cm during head impulse.

III.4.2 Artifacts Due to Displacement in Axes of Rotation of Head and Eye

The eyes are not located at the center of rotation of the head; they lie about 10 cm in front of the axis of head rotation. The eyes are displaced laterally and either anteriorly. Consequently, an additional rotation of the globes is required above what is needed to compensate for the head rotation if the line of sight is to be held upon the target, and higher biased gain can be expected. Fortunately, this compensatory movement is function of target distance (videlicet function of vergence, see chapter “1.2.4.1 Remarkable Apects of the VOR Function”) and for distant targets then changes in gaze are simply the sum of the eye-in-orbit and head rotations (Leigh RJ, 1999).

IV Results

IV.1 Typical Responses

Figure IV-1 - **Figure IV-9** demonstrate examples of responses obtained from the subjects in all three groups. Raw tracings denote several aspects of the recordings:

- First 80 ms were recorded.
- Eye response is very prompt and exact in time and in amplitude (eye tracing almost copies the head movement)
- Responses expressed as γ-gain rise with time to reach γ-gain of approx. 1 at the time point of 40 ms in a subject from the young group.
- A subject from the elderly group has lower γ-gains.
- Misalignment angles at the beginning of the head impulse show a larger variability in response and larger angle values with decrease to nearly zero at the time point of 40 ms.
- Data from misalignment angles comply with γ-gains values.
- Some fast phases are present at the end of recording; in particular, early saccades in roll plane can be seen.
- Appearance of early quick phases does not differ among the age groups.

As seen from the tracings, in order to compare reactions it is reasonable to compute age related significance in planes separately. For a complete result, all effects or interactions were also considered. Although, there is a clear relationship between γ-gain, misalignment angle and velocity gain (see methods), to explain all age-dependent associations of the VOR in three dimensions, measurable aspects of VOR have to be compare independently. We considered the results as significant at the time points 20,40,60,80 ms in yaw and pitch plane but only 20,40,60 ms in roll plane due to early fast phases. All the key results are described in **Table IV-A**, **Table IV-B** and **Table IV-C**.

Velocity Gain		Effects of				Post Hoc Bonferroni		Wilks' test
		Age Group	Time	Direction vs. Time	Direction vs. Group	Middle vs. Elderly	Young vs. Elderly	
Planes of rotation p values	Horizontal	0,092060	0,000000	0,000006	0,906338	0,221144	0,131511	0,473917
	Vertical	0,000577	0,000002	0,002676	0,604399	0,000406	0,016841	0,007035
	Torsional	0,023632	0,313664	0,443773	0,237681	0,029989	0,098048	0,012798

Table IV-A: Velocity Gain results.
Table summarizes important results and statistically significant effects (marked in red) of Velocity Gain revealed by repeated measures ANOVA, Post Hoc Bonferoni test and Wilk's test in all planes of stimulation.

Gamma-Gain		Effects of				Post Hoc Bonferroni		Wilks' test
		Age Group	Time	Direction vs. Time	Direction vs. Group	Middle vs. Elderly	Young vs.Elderly	
Planes of rotation p values	Horizontal	0,034078	0,000000	0,000429	0,389303	0,103551	0,049875	0,017682
	Vertical	0,000090	0,000000	0,008835	0,926541	0,000063	0,005525	0,001415
	Torsional	0,000483	0,306274	0,282848	0,026412	0,000891	0,003261	0,019641

Table IV-B: Gamma-Gain results.
Table summarizes important results and statistically significant effects (marked in red) of Gamma-Gain revealed by repeated measures ANOVA, Post Hoc Bonferoni test and Wilk's test in all planes of stimulation.

Misalignment Angle		Effects of				Post Hoc Bonferroni	
		Age Group	Time	Direction vs. Time	Direction vs. Group	Middle vs. Elderly	Young vs.Elderly
Planes of rotation p values	Horizontal	0,009794	0,000529	0,097477	0,435004	0,018768	0,025123
	Vertical	0,113342	0,117158	0,020100	0,538633	0,141950	1,000000
	Torsional	0,018205	0,020480	0,637803	0,313151	0,016430	0,163233

Table IV-C: Misalignment Angle results.
Table summarizes important results and statistically significant effects (marked in red) of Misalignment Angle revealed by repeated measures ANOVA and Post Hoc Bonferoni test in all planes of stimulation.

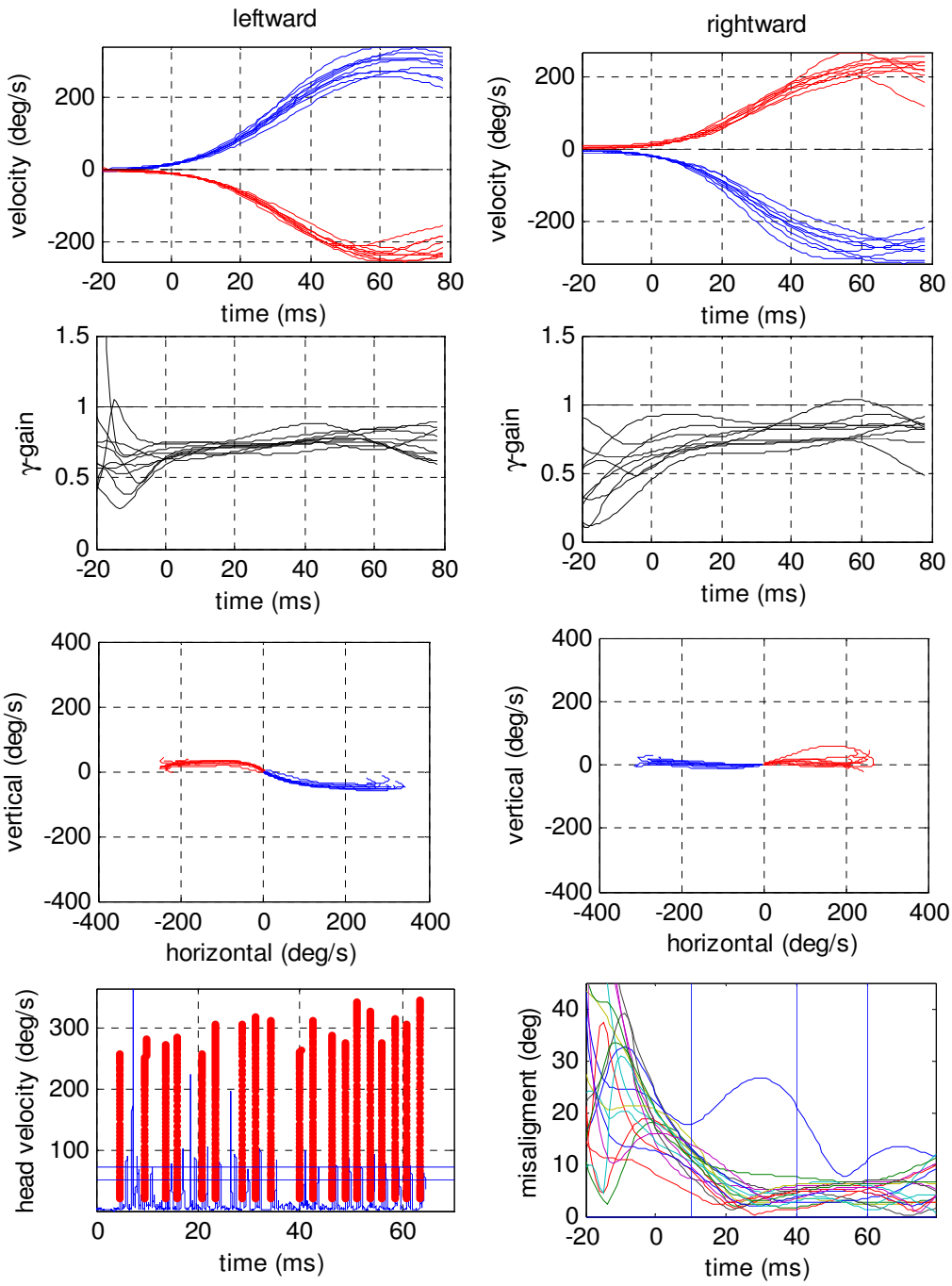

Figure IV-1: Example of raw horizontal data from young (28 y) subject.
The first row from top: all traces of horizontal eye and head velocity (blue: head velocity; red: eye velocity). Data points were taken from +20 to +80 ms for statistical analysis. The second row: γ-gains for horizontal head impulses. The third row: vertical vs. horizontal eye and head velocity. Last row: left illustration shows the original head velocity data in absolute values with marked head impulses which comply with selected criteria, right illustration show eye misalignment angles of all head impulses. The subject showed γ-gains (averaged over the median values of each time point) of 0.96±0.13 for leftward and 0.91 ±0.08 for rightward head impulses.

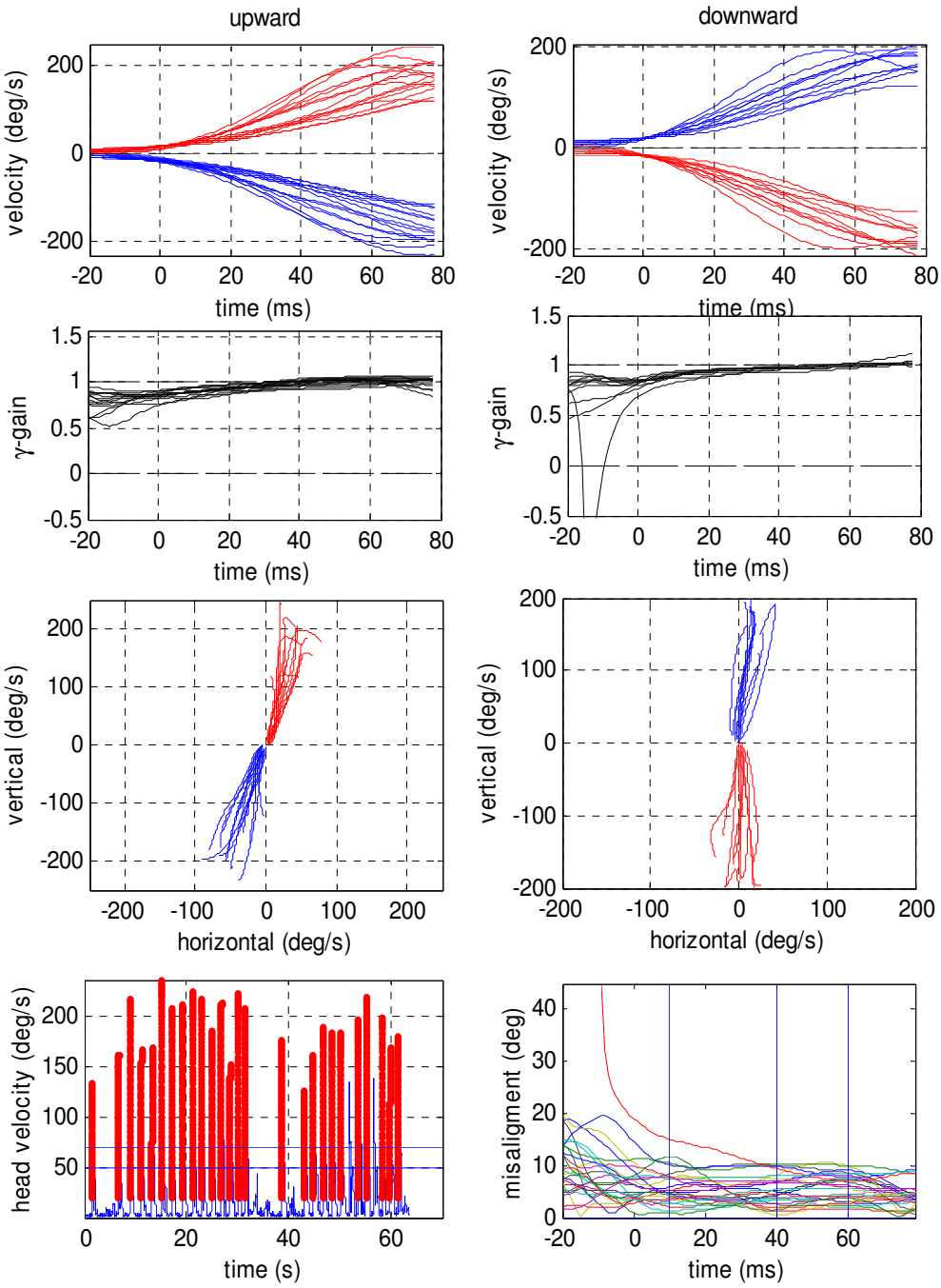

Figure IV-2: Example of raw vertical data from young (28 y) subject.
The first row from top: all traces of vertical eye and head velocity (blue: head velocity; red: eye velocity). Data points were taken from +20 to +80 ms for statistical analysis. The second row: γ-gains for vertical head impulses. The third row: vertical vs. horizontal eye and head velocity. Last row: left illustration shows the original head velocity data in absolute values with marked head impulses which comply with selected criteria, right illustration show eye misalignment angles of all head impulses. The subject showed γ-gains (averaged over the median values of each time point) of 1.06±0.11 for downward and 0.90 ±0.02 for upward head impulses.

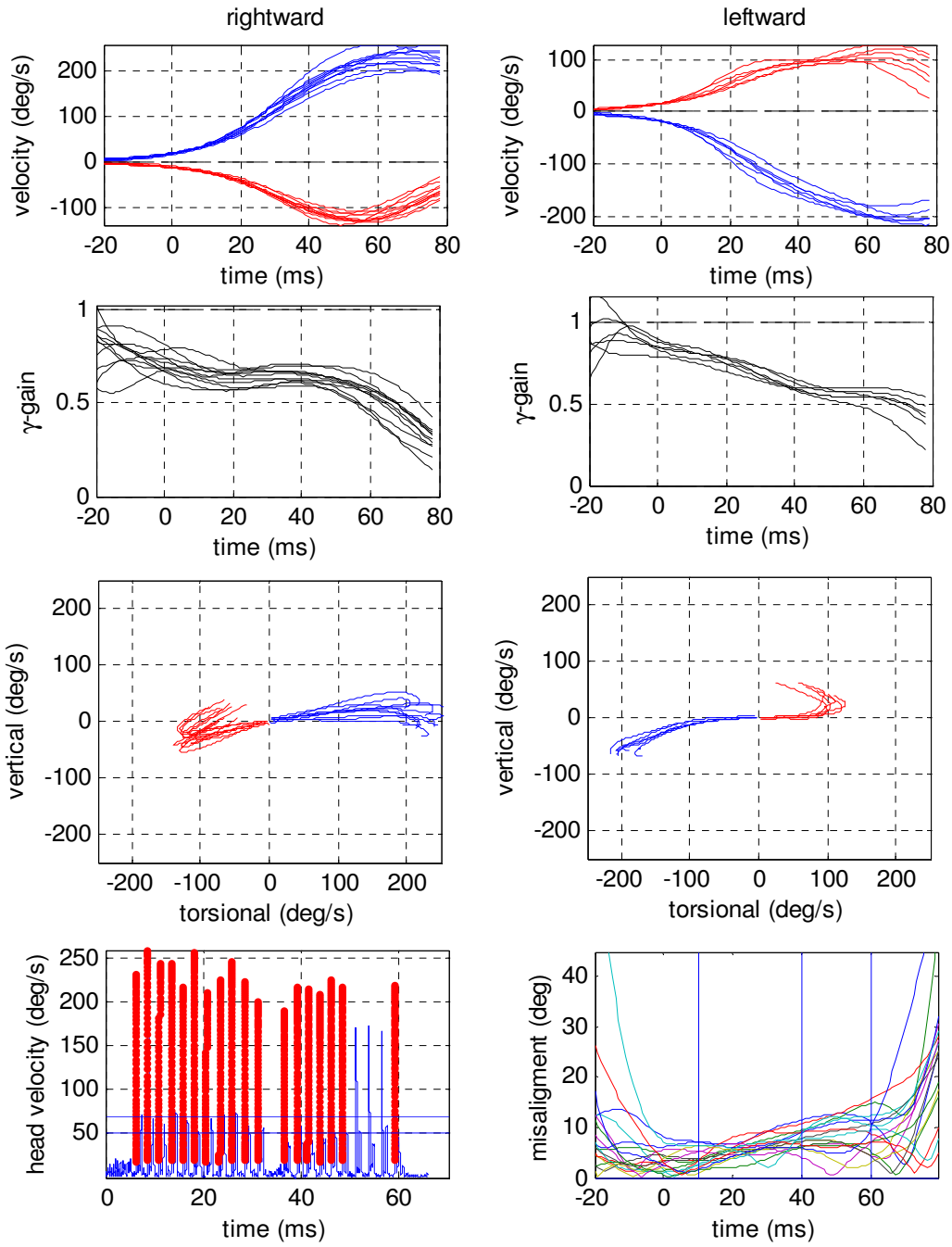

Figure IV-3: Example of raw torsional data from young (28 y) subject.
The first row from top: all traces of torsional eye and head velocity (blue: head velocity; red: eye velocity). Data points were taken from +20 to +60 ms for statistical analysis. The second row: γ-gains for torsional head impulses. The third row: vertical vs. torsional eye and head velocity. Last row: left illustration shows the original head velocity data in absolute values with marked head impulses which comply with selected criteria, right illustration show eye misalignment angles of all head impulses. The subject showed γ-gains (averaged over the median values of each time point) of 0.56±0.04 for leftward and 0.59 ±0.03 for rightward head impulses.

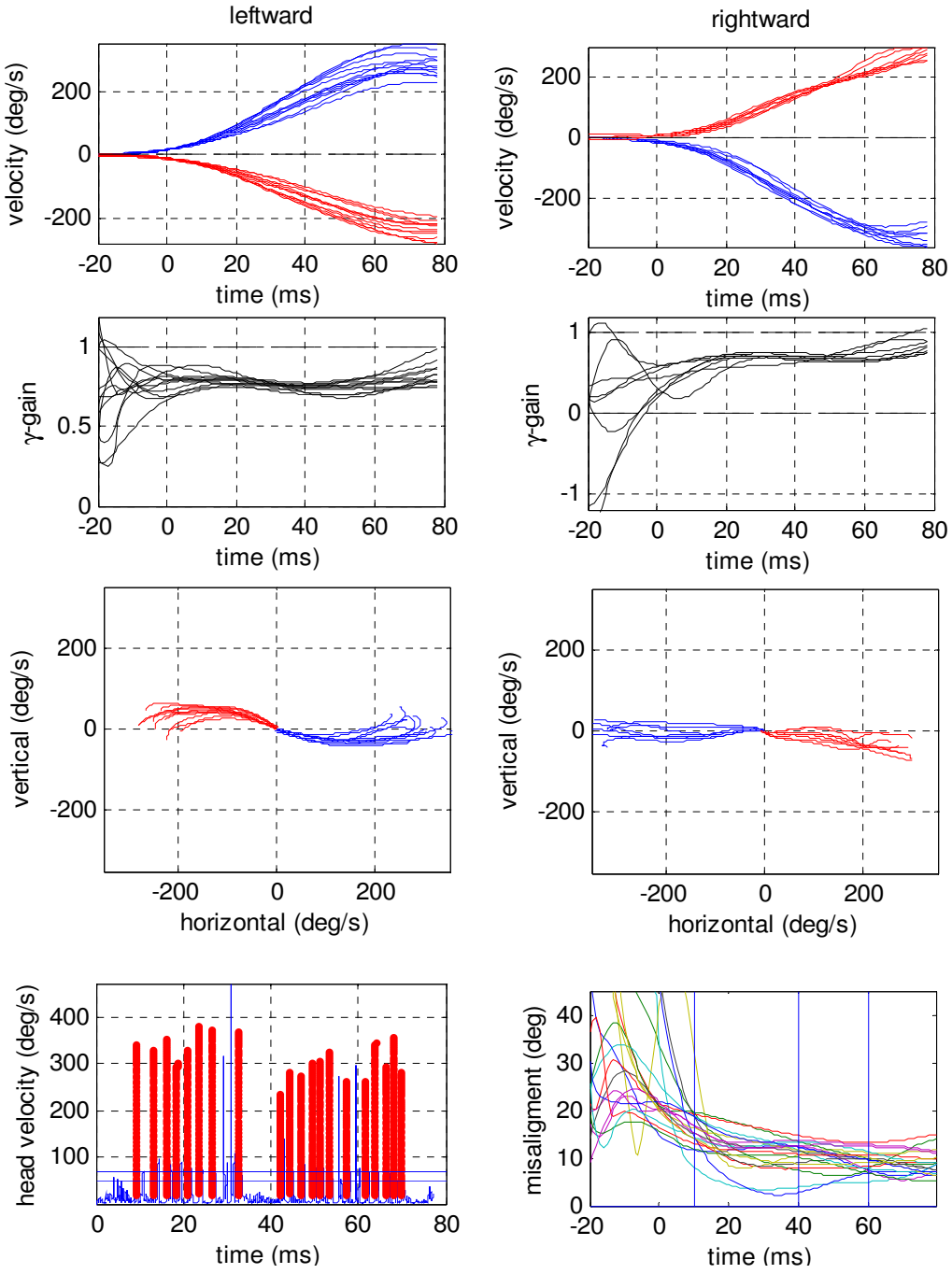

Figure IV-4: Example of raw horizontal data from middle aged (38 y) subject.
The first row from top: all traces of horizontal eye and head velocity (blue: head velocity; red: eye velocity). Data points were taken from +20 to +80 ms for statistical analysis. The second row: γ-gains for horizontal head impulses. The third row: vertical vs. horizontal eye and head velocity. Last row: left illustration shows the original head velocity data in absolute values with marked head impulses which comply with selected criteria, right illustration show eye misalignment angles of all head impulses. The subject showed γ-gains (averaged over the median values of each time point) of 0.74±0.02 for leftward and 0.80 ±0.05 for rightward head impulses.

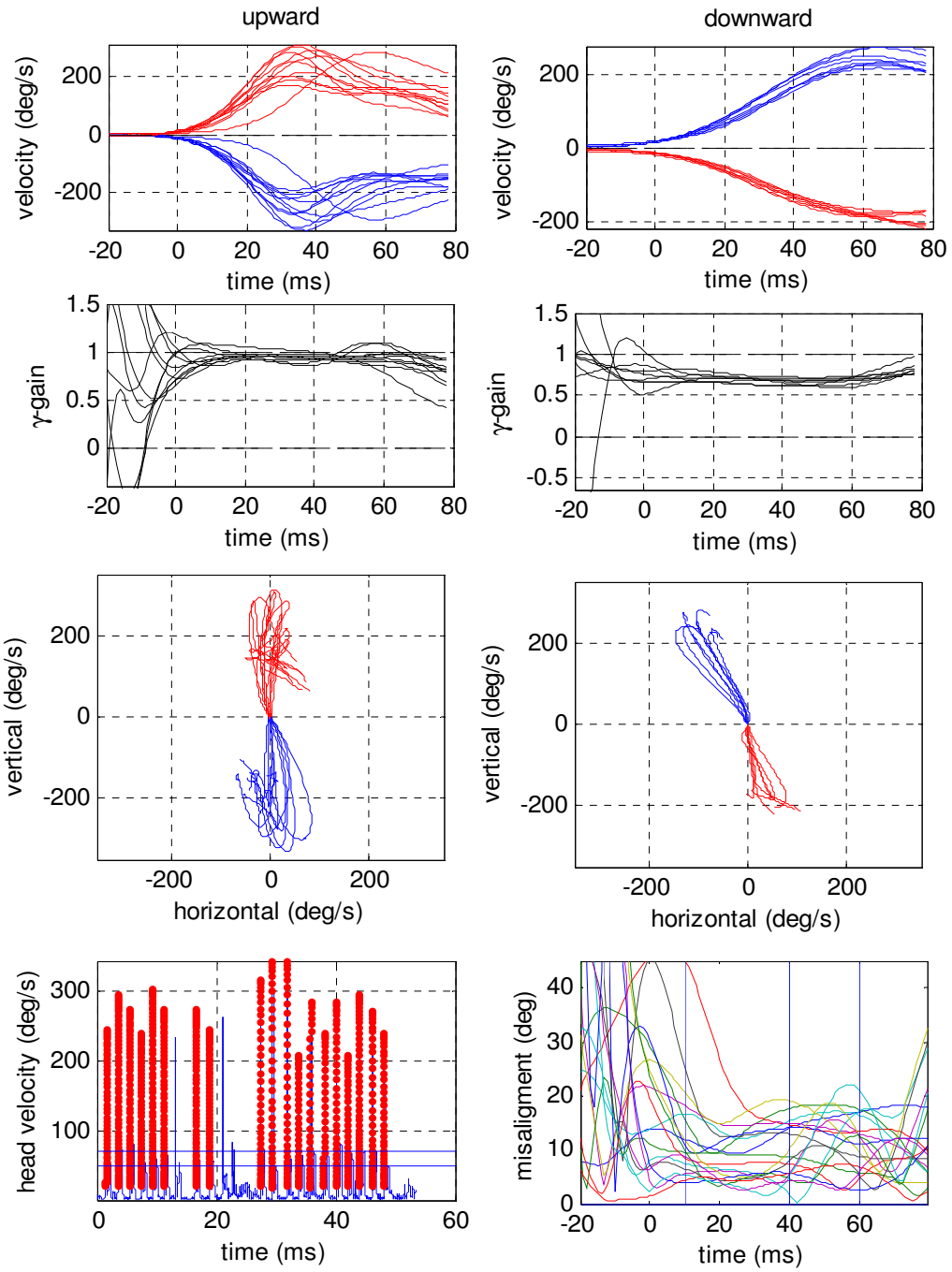

Figure IV-5: Example of raw vertical data from middle aged (38 y) subject.
The first row from top: all traces of vertical eye and head velocity (blue: head velocity; red: eye velocity). Data points were taken from +20 to +80 ms for statistical analysis. The second row: γ-gains for vertical head impulses. The third row: vertical vs. horizontal eye and head velocity. Last row: left illustration shows the original head velocity data in absolute values with marked head impulses which comply with selected criteria, right illustration show eye misalignment angles of all head impulses. The subject showed γ-gains (averaged over the median values of each time point) of 0.94±0.8 for downward and 0.88 ±0.04 for upward head impulses.

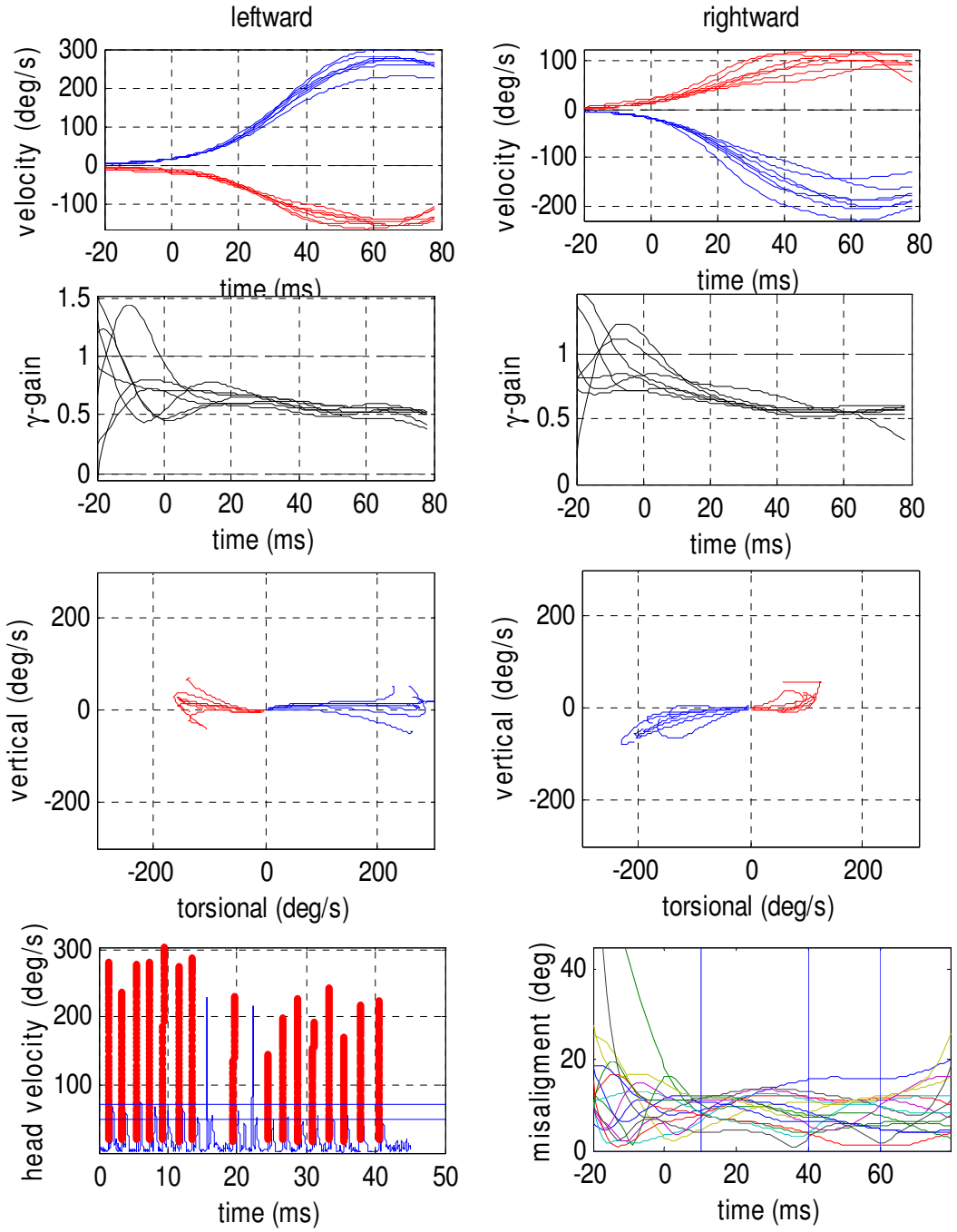

Figure IV-6: Example of raw torsional data from middle aged (38 y) subject.
The first row from top: all traces of torsional eye and head velocity (blue: head velocity; red: eye velocity). Data points were taken from +20 to +60 ms for statistical analysis. The second row: γ-gains for torsional head impulses. The third row: vertical vs. torsional eye and head velocity. Last row: left illustration shows the original head velocity data in absolute values with marked head impulses which comply with selected criteria, right illustration show eye misalignment angles of all head impulses. The subject showed γ-gains (averaged over the median values of each time point) of 0.62±0.06 for leftward and 0.64 ±0.11 for rightward head impulses.

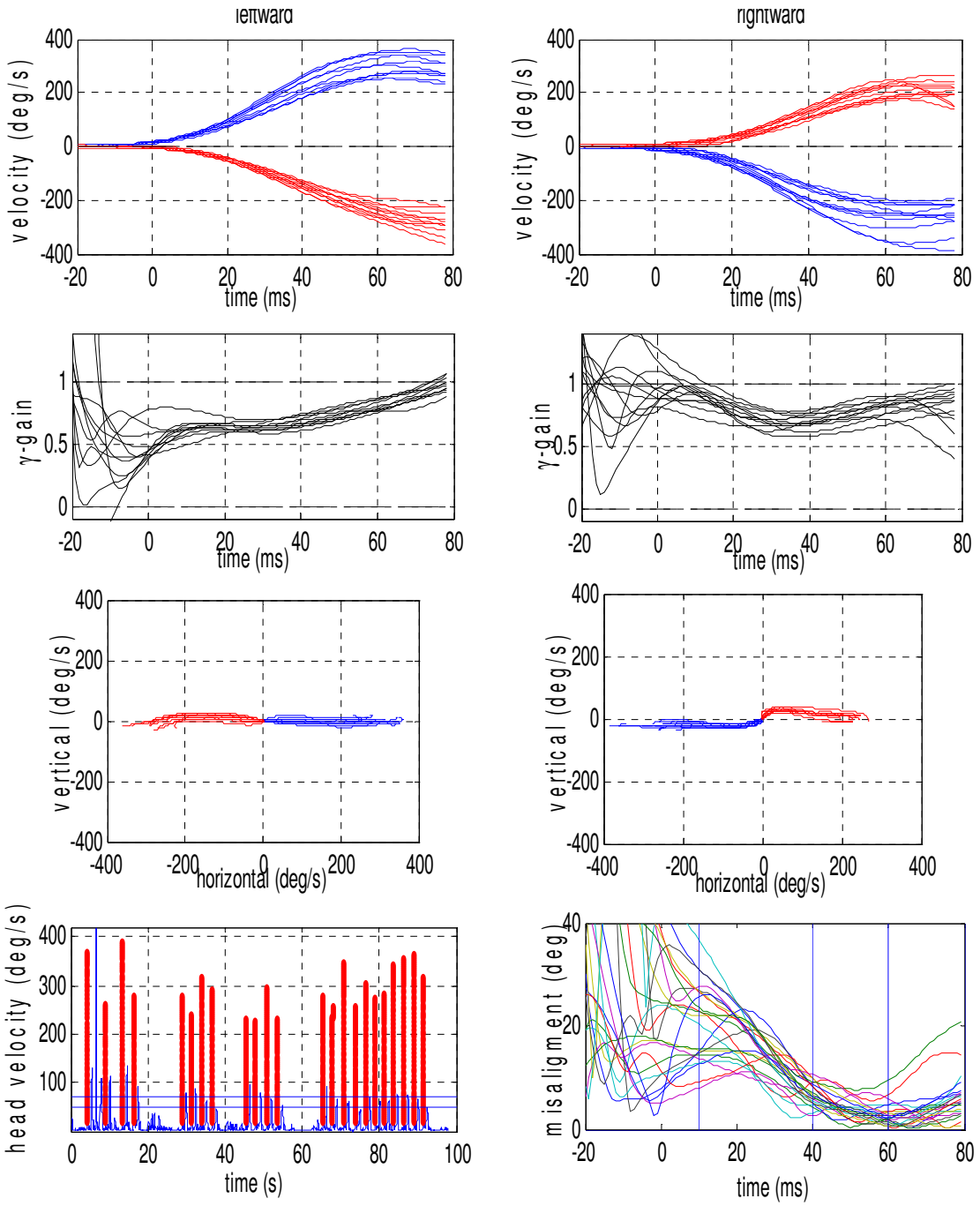

Figure IV-7: Example of raw horizontal data from elderly (63 y) subject.
The first row from top: all traces of horizontal eye and head velocity (blue: head velocity; red: eye velocity). Data points were taken from +20 to +80 ms for statistical analysis. The second row: γ-gains for horizontal head impulses. The third row: vertical vs. horizontal eye and head velocity. Last row: left illustration shows the original head velocity data in absolute values with marked head impulses which comply with selected criteria, right illustration show eye misalignment angles of all head impulses. The subject showed γ-gains (averaged over the median values of each time point) of 0.79±0.07 for leftward and 0.77 ±0.08 for rightward head impulses.

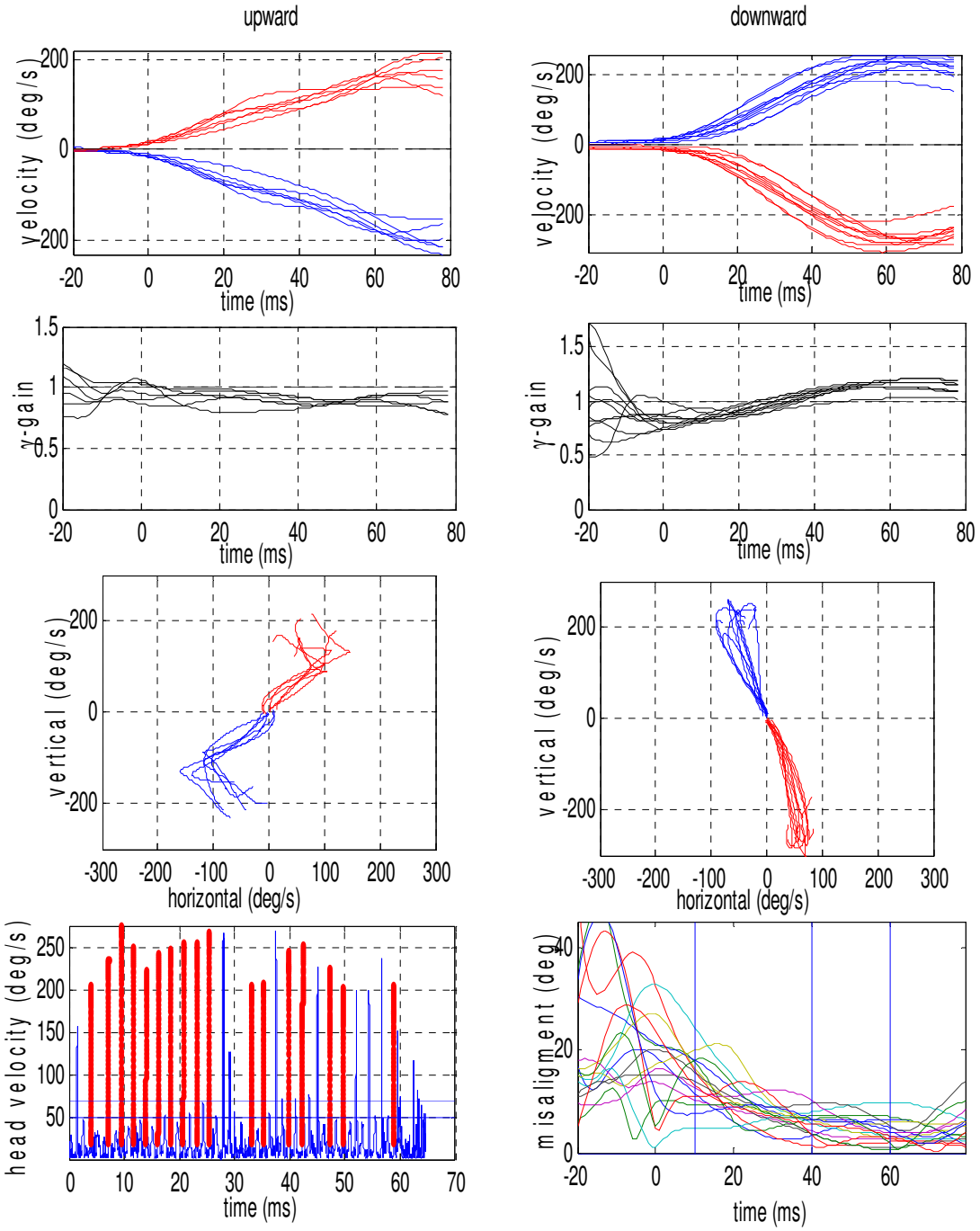

Figure IV-8: Example of raw vertical data from elderly (63 y) subject.
The first row from top: all traces of vertical eye and head velocity (blue: head velocity; red: eye velocity). Data points were taken from +20 to +80 ms for statistical analysis. The second row: γ-gains for vertical head impulses. The third row: vertical vs. horizontal eye and head velocity. Last row: left illustration shows the original head velocity data in absolute values with marked head impulses which comply with selected criteria, right illustration show eye misalignment angles of all head impulses. The subject showed γ-gains (averaged over the median values of each time point) of 0.91±0.07 for downward and 0.77 ±0.06 for upward head impulses.

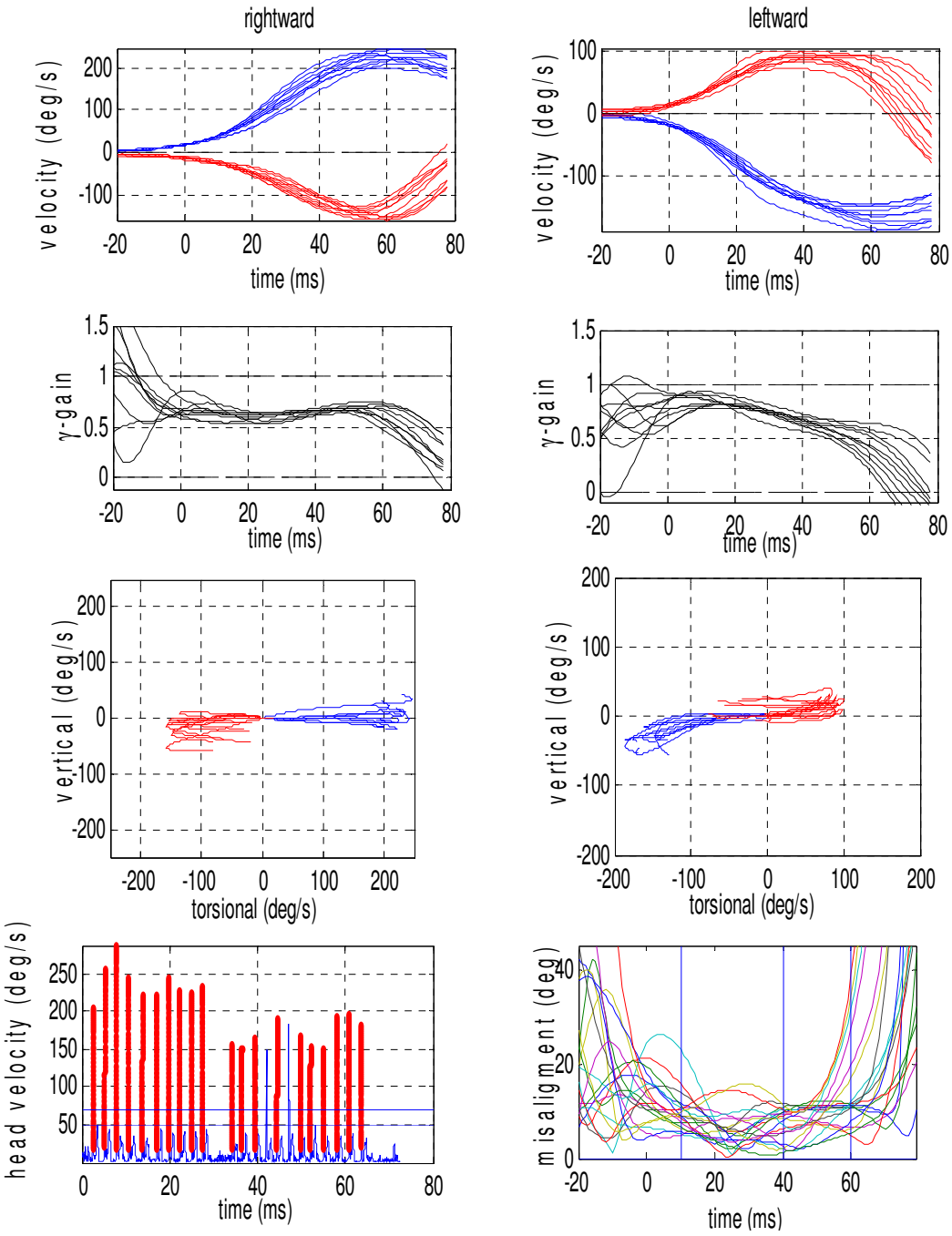

Figure IV-9: Example of raw torsional data from elderly (63 y) subject.
The first row from top: all traces of torsional eye and head velocity (blue: head velocity; red: eye velocity). Data points were taken from +20 to +60 ms for statistical analysis. The second row: γ-gains for torsional head impulses. The third row: vertical vs. torsional eye and head velocity. Last row: left illustration shows the original head velocity data in absolute values with marked head impulses which comply with selected criteria, right illustration show eye misalignment angles of all head impulses. The subject showed γ-gains (averaged over the median values of each time point) of 0.57±0.02 for leftward and 0.48 ±0.08 for rightward head impulses.

.

IV.2 Velocity Gain

Velocity gain is defined as the ratio of the eye velocity magnitude in head-fixed coordinates to the head velocity magnitude in space fixed coordinates, so it does not consider space differences between input (head movement) and output (eye response), but only how accurate is the vestibular system in amplitudes.

Important effects and dependencies of the velocity gains among groups are best depicted in **Figure IV-10**, **Figure IV-11** and **Figure IV-12**. The results are separated according to the plane of stimulation:

Yaw-horizontal plane

- The repeated measures ANOVA revealed **no statistically significant** age-related changes in velocity gain in yaw-plane [$F(2,30)=2.5$; $p=0.09$]. Even if the p-value is low, amplitude of response does not reach significant difference with respect to age.
- **Highly significant** effect of time [$F(3,90) = 10.4$; $p<0.0001$], and interaction of time and direction [$F(3,90) = 35.3$; $P <0.0001$] on velocity gain was found. Effect of time on velocity gain can be supposed from the raw tracings. Interaction of time and direction probably describes slight inconsistency in left-right comparison.

Pitch-vertical plane

- The repeated measures ANOVA revealed **statistically significant** age-related changes in velocity gain in yaw-plane [$F(2,26)=10$; $p<0.005$]. Significant age related changes apparently differ from the horizontal plane responses, where differences are not significant.
- **Highly significant** effect of time [$F(3,78) = 11.8$; $p<0.0001$] and interaction of time and direction [$F(3,78) = 5.1$; $p<0.005$] on velocity gain was found. This finding is similar to yaw plane results.
- Post Hoc Bonferroni Test revealed **highly significant** difference between the middle group and the elderly group ($p<0.0005$), significant difference between the young and elderly groups ($p<0.05$), but no difference between the young and middle groups ($p=0.253$). This result was expected.

Roll-torsional plane

- The repeated measures ANOVA revealed **statistically significant** age-related changes in the velocity gain in yaw-plane [$F(2,31)=4.2$; $p<0.05$].
- Interaction of direction and group reached **significance** [$F(2,31)=3.6$; $p<0.05$].

- Post Hoc Bonferroni Test revealed **significant** difference between the middle group and the elderly group ($p<0.05$) but not between the young and the middle ($p\sim1.000$) or the young and the elderly ($p=0.0980$).

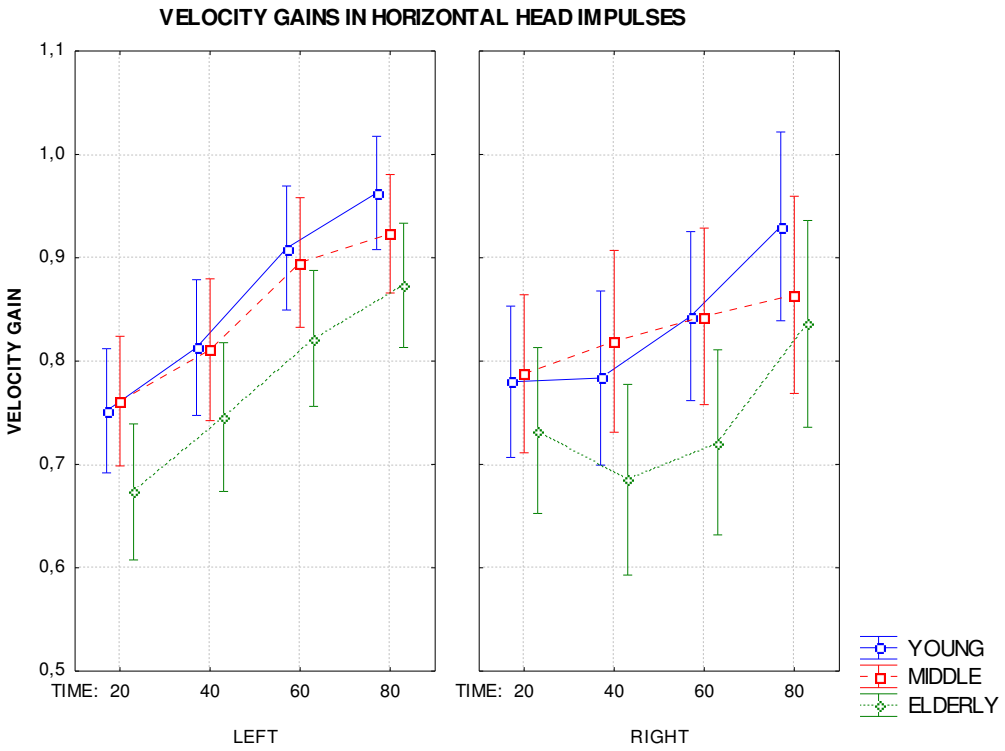

Figure IV-10: Velocity gains for horizontal head impulses.
ANOVA plots for time points from 20 ms to 80 ms. Vertical bars denote 0,95 confidence intervals.

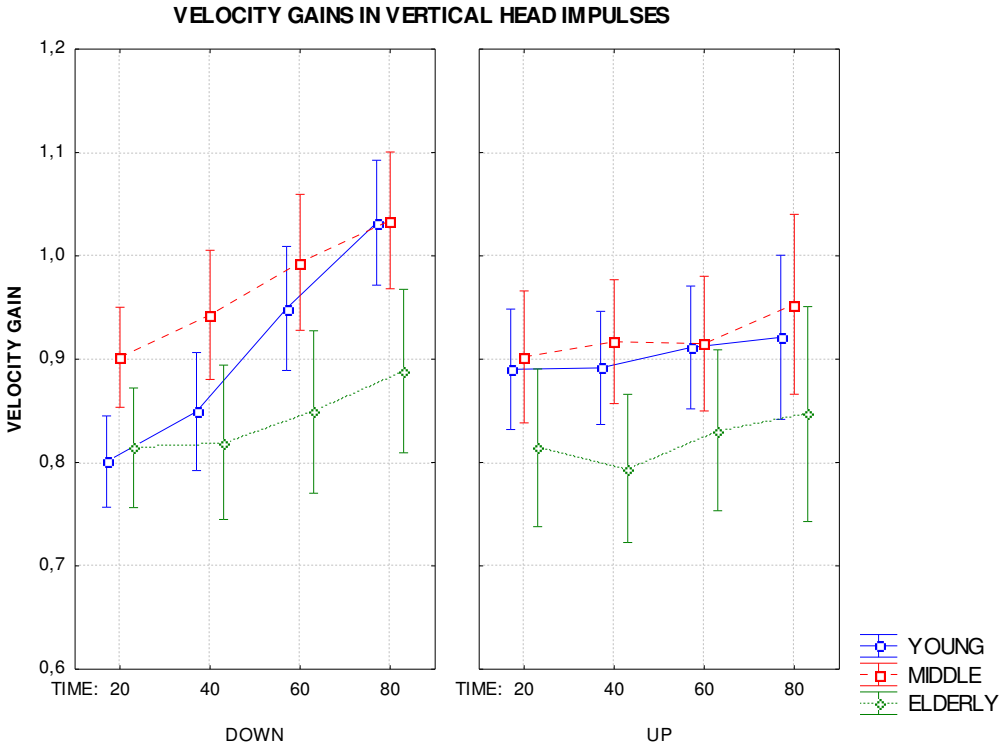

Figure IV-11: Velocity gains for vertical head impulses.
ANOVA plots for time points from 20 ms to 80 ms. Vertical bars denote 0,95 confidence intervals.

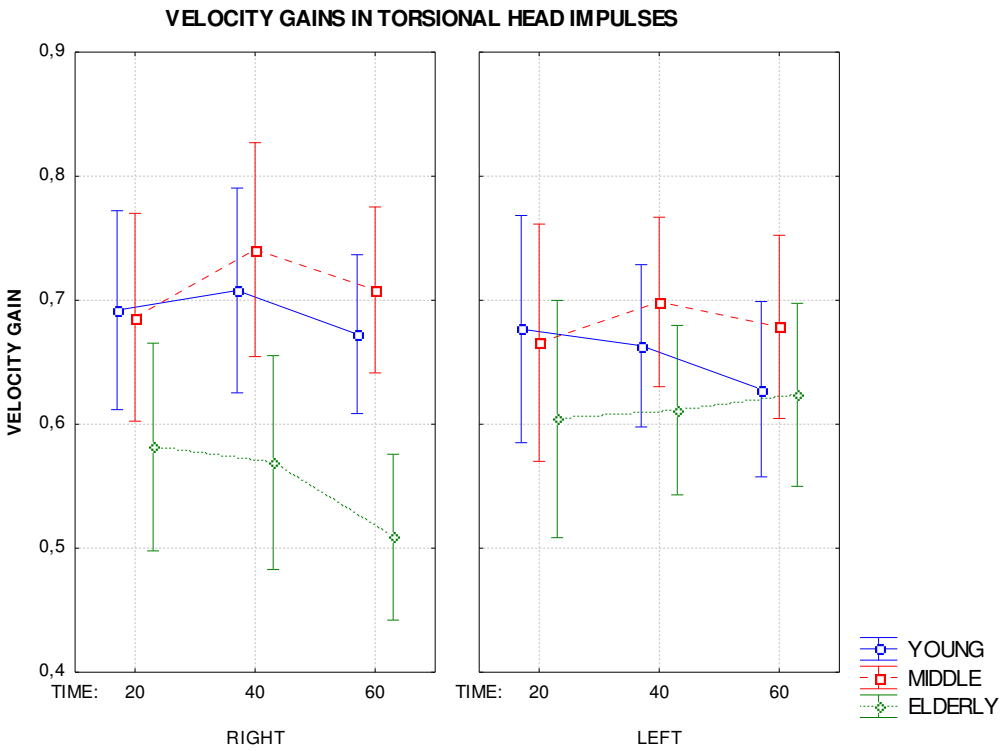

Figure IV-12: Velocity gains for torsional head impulses.
ANOVA plots for time points from 20 ms to 60 ms. Vertical bars denote 0,95 confidence intervals.

IV.3 Misalignment Angle

By comparing the misalignment angles we can see how responses stay in the same plane with the head-movement plane, namely, how spatially accurate the vestibular system is. Important effects and dependencies of misalignment angles among groups are best depicted in **Figure IV-13**, **Figure IV-14** and **Figure IV-15**.

Yaw-horizontal plane

- The repeated measures ANOVA revealed **statistically significant** age-related changes in misalignment angles in yaw-plane [$F(2,30)=5.4$; $p<0.01$]. Although velocity gain did not show an age-related difference for yaw plane, things are different in this case.
- **Significant** effect of time [$F(3,90) = 6.4$; $p<0.001$] was found.
- Post Hoc Bonferroni Test revealed **a significant** difference between the middle group and the elderly group ($p<0.05$), between the young and elderly ($p<0.05$) but not between the young and middle ($p\sim1.000$).

Pitch-vertical plane

- The repeated measures ANOVA revealed **no statistically significant** age-related changes in misalignment angle in the pitch plane [F(2,27)=2.3; p=0.11].
- Only **significant** interaction of time and direction [F(3,81) = 3.4; p<0.05] on misalignment angles was found. It is clear that misalignment angle in the vertical plane does not change with age.

Roll-torsional plane

- The repeated measures ANOVA revealed **statistically significant** age-related changes in misalignment angles in the roll-plane [F(2,27)=4.6; p<0.05].
- **Significant** effect of time [F(2,54) = 4.2; p<0.05] was found.
- Post Hoc Bonferroni Test revealed **significant** difference between the middle group and the elderly group (p<0.05) but not between the young and middle (p=0.834) or the young and elderly (p=0.163).

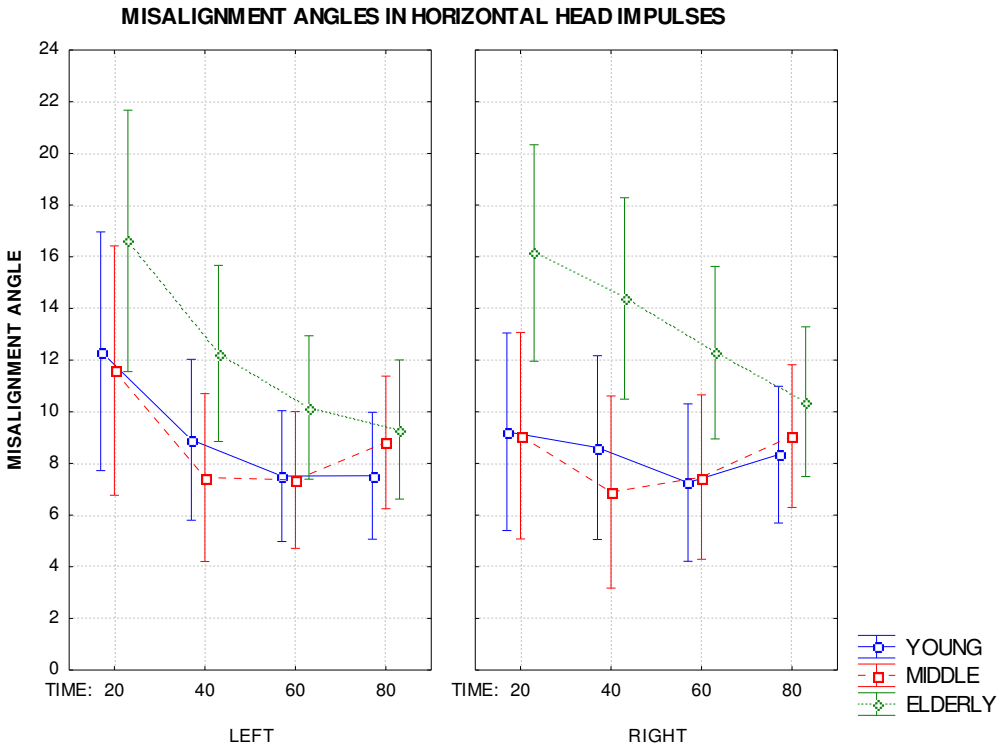

Figure IV-13: Misalignment angles for horizontal head impulses.
ANOVA plots for time points from 20 ms to 80 ms. Vertical bars denote 0,95 confidence intervals.

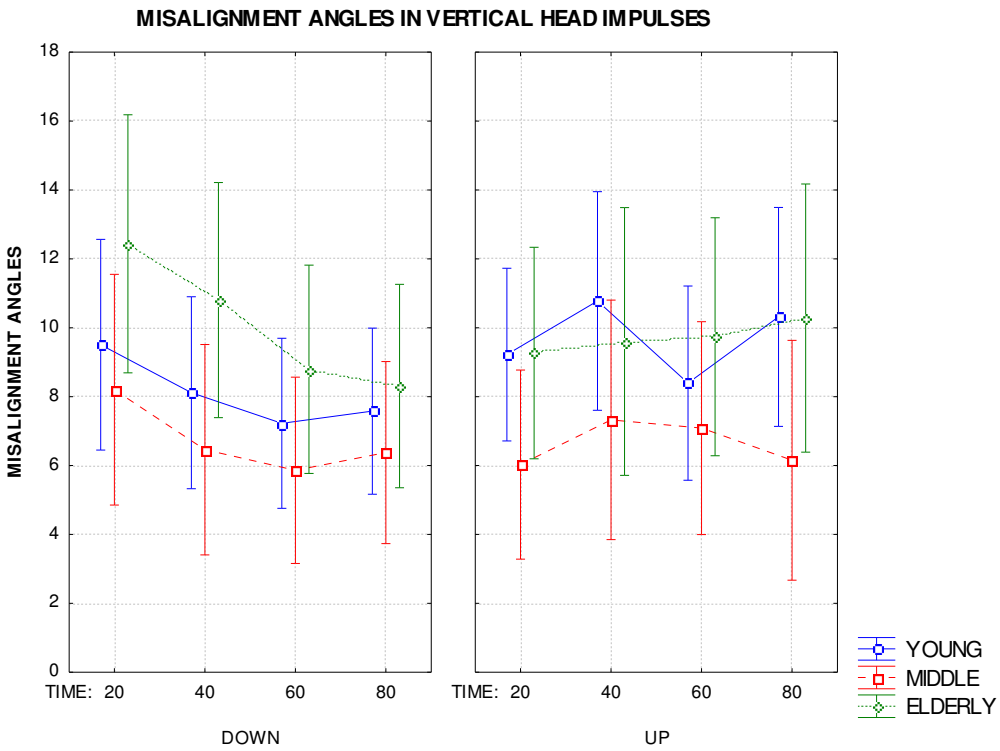

Figure IV-14 Misalignment angles for vertical head impulses.
ANOVA plots for time points from 20 ms to 80 ms. Vertical bars denote 0,95 confidence intervals.

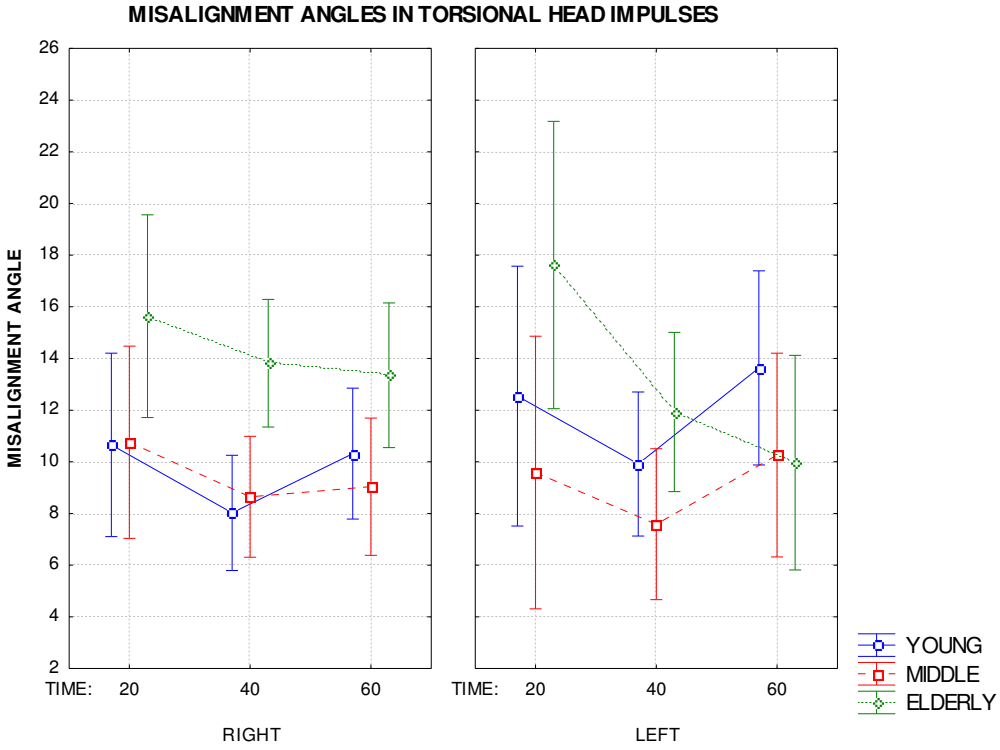

Figure IV-15: Misalignment angles for torsional head impulses.
ANOVA plots for time points from 20 ms to 60 ms. Vertical bars denote 0,95 confidence intervals.

IV.4 Gamma Gain

γ-gain covers both – amplitude and spatial alignment of the response. In our study this parameter should best describe the significant differences. Important effects and dependencies of γ-gains among groups are best depicted in **Figure IV-16**, **Figure IV-17** and **Figure IV-18**.

Yaw-horizontal plane

- The repeated measures ANOVA revealed **statistically significant** age-related changes in γ-gain in yaw-plane [$F(2,31)=3.7$; $p<0.05$]. It is quite obvious and important to show that misalignment angle is the value that changed significance in gain measurement for yaw plane.
- **Significant** effect of time [$F(3,93) = 36.5$; $p<0.0001$], significant effect of direction [$F(1,31)=4.8$; $p<0.05$], and interaction of time and direction [$F(3,93) = 6.6$; $p<0.0005$] on γ-gain was found.
- Post Hoc Bonferroni Test revealed **significant** difference between the young group and elderly group ($p<0.05$) but not between the middle and elderly ($p=0.104$) or between the young and middle ($p\sim1.000$).

Pitch-vertical plane

- The repeated measures ANOVA revealed **statistically highly significant** age-related changes in γ-gain in pitch-plane [$F(2,26)=13.6$; $p<0.0001$]. High significance is obtained thanks to important age-related differences in velocity gain in pitch plane.
- **Significant** effect of time [$F(3,78) = 14.6$; $p<0.0001$], and interaction of time and direction [$F(3,78) = 4.1$; $p<0.01$] on γ-gain was found.
- Post Hoc Bonferroni Test revealed **significant** difference between the young group and the elderly group ($p<0.01$), between the middle and elderly ($p<0.0001$) but not between the young and middle ($p=0.132$).

Roll-torsional plane

- The repeated measures ANOVA revealed **statistically highly significant** age-related changes in γ-gain in the roll-plane [$F(2,31)=9.8$; $p<0.001$]. Age-related significance in the roll plane is obvious in all compared aspects, reaching important differences in γ-gain.

- **Significant** interaction of direction and group [F(2,31) = 4.1; p<0.05] on γ-gain was found.
- Post Hoc Bonferroni Test revealed **significant** difference between the young group and the elderly group (p<0.005), between the middle and elderly (p<0.001) but not between the young and middle (p~1.000).

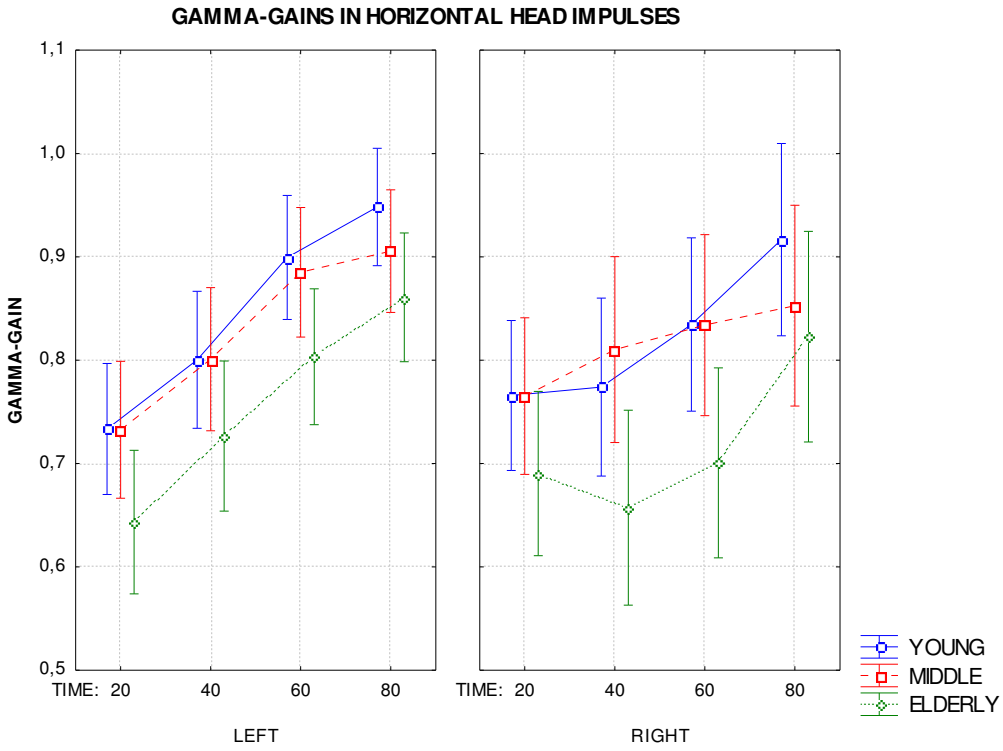

Figure IV-16: Gamma-gains for horizontal head impulses.
ANOVA plots for time points from 20 ms to 80 ms. Vertical bars denote 0,95 confidence intervals.

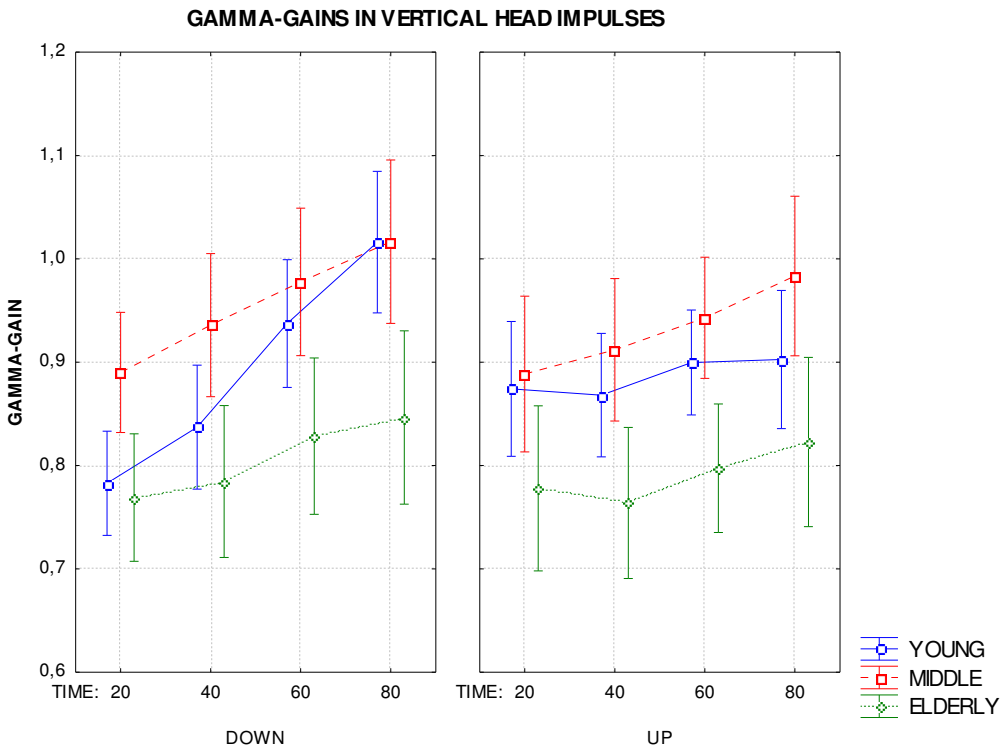

Figure IV-17: Gamma-gains for vertical head impulses.
ANOVA plots for time points from 20 ms to 80 ms. Vertical bars denote 0,95 confidence intervals.

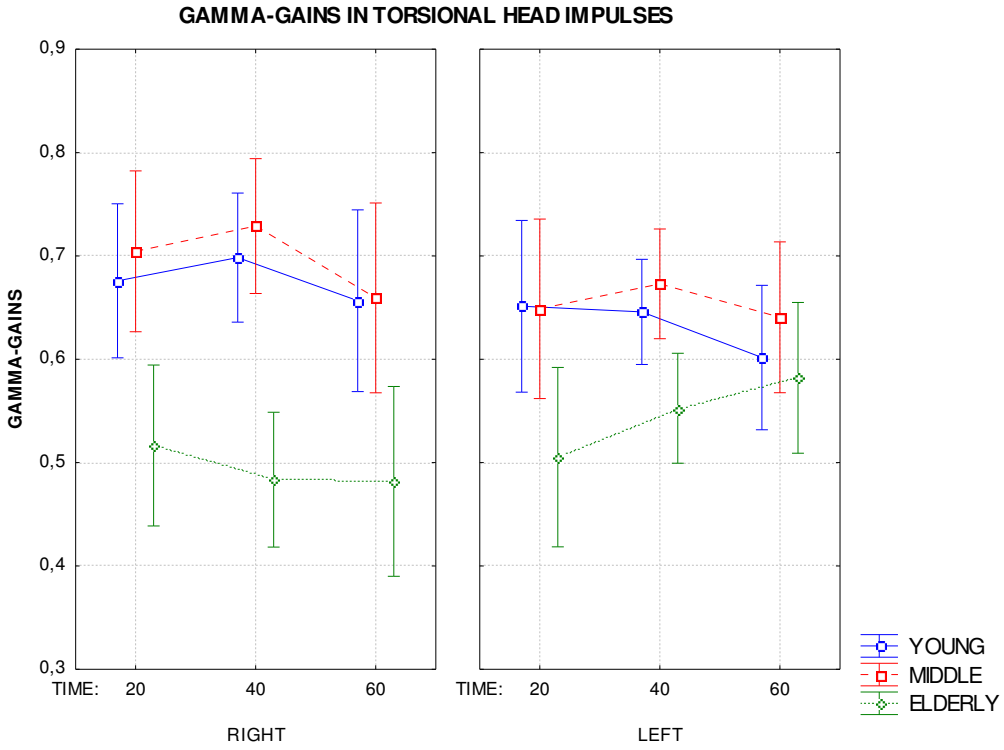

Figure IV-18: Gamma-gains for torsional head impulses.
ANOVA plots for time points from 20 ms to 60 ms. Vertical bars denote 0,95 confidence intervals.

IV.5 Additional Results and Observations

Multivariate Wilks' test of significance related to age as a continuous predictor showed significant age-dependent difference in the pitch plane γ-gains (p=0.001), the roll plane γ-gains (p=0.02), and in the yaw plane γ-gains (p=0.02). These results are in accordance with γ-gain significance values.

In evaluated aspects of the VOR response in the HIT, if an age-related difference was significant, Post Hoc Bonferroni test often showed significant difference between the middle age group and the elderly; calculated statistical significance between the young and elderly or the young and the middle groups was either on the border of significance often not reaching it at all (for exact values see **Table IV-A**, **Table IV-B** and **Table IV-C**, see also **Figure IV-19**).

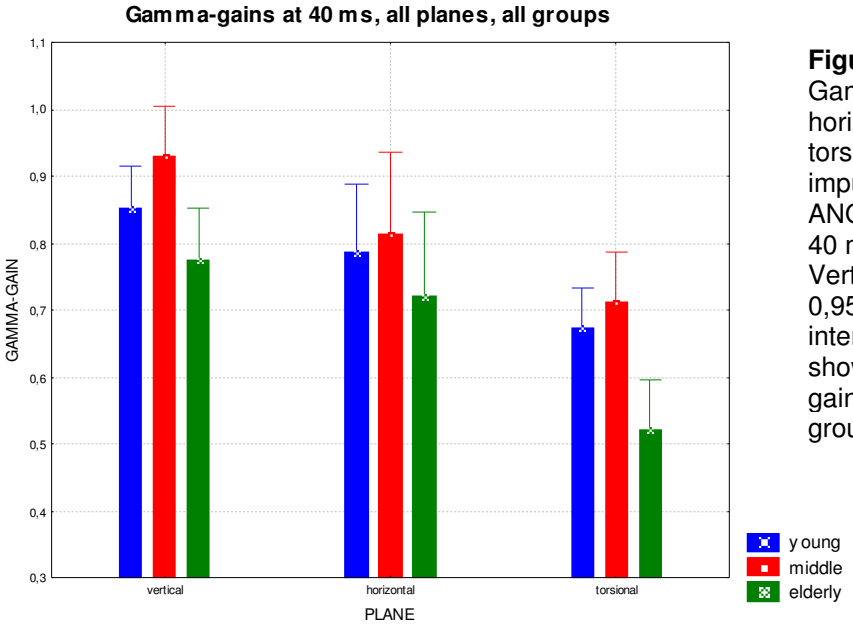

Figure IV-19: Gamma-gains for horizontal, vertical and torsional head impulses I. ANOVA plots for time 40 ms - all ages. Vertical bars denote 0,95 confidence intervals. Figure shows highes gamma-gains in the middle group.

It can be seen from the tracings that γ-gain values significantly increase with time. In the horizontal plane it starts around 0.7 for early responses and goes up to 0.9 for late responses in stimulation.

The repeated measures ANOVA revealed statistically highly significant differences between planes (and among ages) in γ-gains in 40ms [F(2, 126)=61,165, p=0,0000]. Low γ-gain is most prominent in the roll plane (see **Figure IV-20** and V.3 Additional Conclusions).

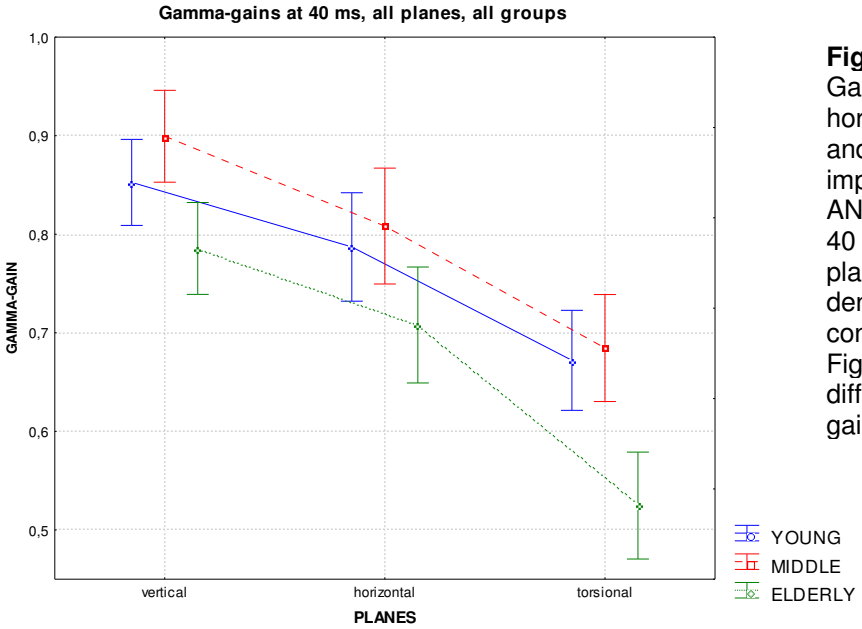

Figure IV-20: Gamma-gains for horizontal, vertical and torsional head impulses II. ANOVA plots for time 40 ms - all ages, all planes. Vertical bars denote 0,95 confidence intervals. Figure depicts different gamma-gains among plains.

V Discussion

V.1 General Results

My study examined 38 age different normal subjects to describe how aging and age-related changes affect performance of the vestibulo-ocular reflex. The VOR performance is usually tested during conditions that are different from mechanical aspects of normal locomotion (Muller, 1994;St George, Lord, & Fitzpatrick, 2003;Leigh RJ, 1999;Hirasaki, Moore, Raphan, & Cohen, 1999;Crane & Demer, 1997;Grossman, Leigh, Abel, Lanska, & Thurston, 1988;Grossman, Leigh, Bruce, Huebner, & Lanska, 1989;Wall, III, Black, & Hunt, 1984;Peterka, Black, & Schoenhoff, 1990;Paige, 1992;Peterka, Black, & Schoenhoff, 1990;Kim & Sharpe, 2001;Yagi, Sekine, & Shimizu, 1983;Paige, 1994). Evidently, this kind of testing paradigms does not disclose a real behavior of the VOR response, especially when age-associated relations are considered (Wiest, Demer, Tian, Crane, & Baloh, 2001;Hajioff, Barr-Hamilton et al., 2000;Hajioff, Barr-Hamilton et al., 2002). Some earlier studies proclaim that special kind of vestibular maneuver, called the head impulse test (Cremer, Halmagyi, Aw, Curthoys, McGarvie, Todd, Black, & Hannigan, 1998;Halmagyi, Curthoys, Cremer, Henderson, Todd, Staples, & D'Cruz, 1990), has parameters (acceleration, velocity, frequency spectrum) closest to parameters of common locomotion (Leigh & Brandt, 1993). The VOR performance shows short latencies, and is responsible for a specific spatial and temporal arrangement of the eye movements after the head impulse stimulation (Aw, Haslwanter, Halmagyi, Curthoys, Yavor, & Todd, 1996;Leigh RJ, 1999). Due to above, only first 80 ms of response were recorded using very accurate measuring system called search-coil system (Robinson, 1963).

Using this setup (dual search coil recording) and the head impulse stimulus (unpredictable manually delivered head rotations with angular acceleration over $1000°/s^2$) in three orthogonal planes – yaw-horizontal, pitch-vertical and roll-torsional, which match the planes of head movements during walking, my study demonstrates a functional ageing of the vestibular system.

Responses of the vestibular system were described according to amplitude of response and spatial alignment. First was defined as the velocity gain, latter as the misalignment angle; both parameters were included in computation of γ-gain. Additionally, my results are plane-specific, describing the VOR performance in different planes. Therefore, by comparing age-related results among three age different groups in three planes, following was found:

- γ-gain showed statistically significant differences among all groups in all tested planes of stimulation.
- most pronounced differences were in the roll-torsional and pitch-vertical planes.
- while difference in pitch plane is due to the velocity gain, a distinction in yaw and roll plane is obtained due to the misalignment angle difference.
- specifically, for γ-gain in horizontal plane a significant divergence is pronounced between the young and the old but not between the middle and elderly groups or between the young and middle groups.
- in roll and pitch plane, the difference is consistently statistically significant between the young and old, and the middle and old but not between the young and the middle groups.
- plane-specific differences in other parameters were comparable.
- expected significant effect of time in most of the planes and parameters was found, with a single exception being the roll plane.
- effect of direction, or interaction of direction and time was also predominantly found in the yaw and pitch planes in all parameters.
- test of significance with age as a continuous predictor showed significant age-dependent difference in the pitch plane γ-gain and roll plane γ-gain but not significant in the yaw plane.

In concert with the main findings outlined above, I was able to describe an age-related deterioration in measured characteristics of function of the vestibulo-ocular reflex with special effect in the roll and pitch planes.

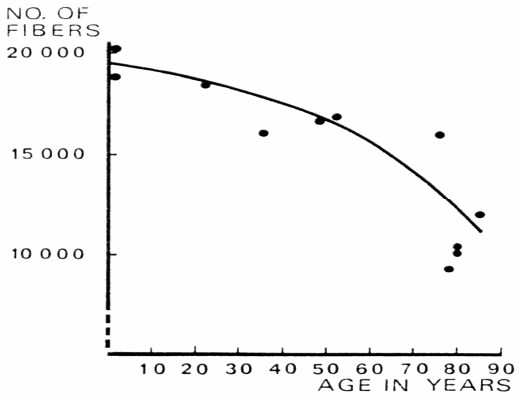

Figure V-1: Correlation between age and number of vestibular nerve fibers in the investigated individuals. (Bergstrom, 1973).

Earlier studies show varying age-related differences in gains, but indicate significantly decreased gain with increasing age. The gain trend has been more consistent at lower frequencies than in the higher ones. Stimuli used often differ from normal circumstances (Wall, III, Black, & Hunt, 1984;Peterka, Black, & Schoenhoff, 1990;Paige, 1992;Peterka,

Black, & Schoenhoff, 1990;Kim & Sharpe, 2001;Yagi, Sekine, & Shimizu, 1983). Recently, Tian and colleagues used a more appropriate stimulus with parameters close to natural (and close to the head impulse test) (Tian, Shubayev, Baloh, & Demer, 2001). In their study of eye movements in transient rotations at high acceleration: a significant gain decrease in yaw-horizontal stimulus in elderly was recorded—in compliance with my results.

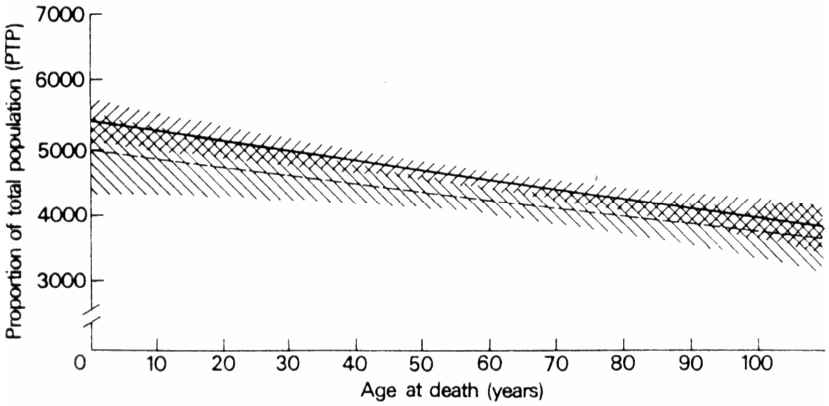

Figure V-2: Proportion of total population of Purkinje cells for males and females with 95% confidence limits on the mean response (Hall, Miller, & Corellis, 1975).

V.2 Functional vs. Anatomic Loss

Increase in age leads to observable histological changes in nearly all anatomic structures involved in the vestibulo-ocular reflex (Richter, 1980;Rosenhall, 1973;Bergstrom, 1973;Bergstrom, 1973;Bergstrom, 1973;Nagai, Goto, Goto, Kaneko, & Suzaki, 1999;Park, Tang, Lopez, & Ishiyama, 2001;Lopez, Honrubia, & Baloh, 1997;Tang, Lopez, & Baloh, 2001;Alvarez, Diaz, Suarez, Fernandez, Gonzalez, Navarro, & Tolivia, 2000;Hall, Miller, & Corellis, 1975;Chen & Hillman, 1999;Fattoretti, Bertoni-Freddari, Caselli, Paoloni, & Meier-Ruge, 1998;Hadj-Sahraoui, Frederic, Zanjani, Herrup, Delhaye-Bouchaud, & Mariani, 1997;Larsen, Skalicky, & Viidik, 2000).

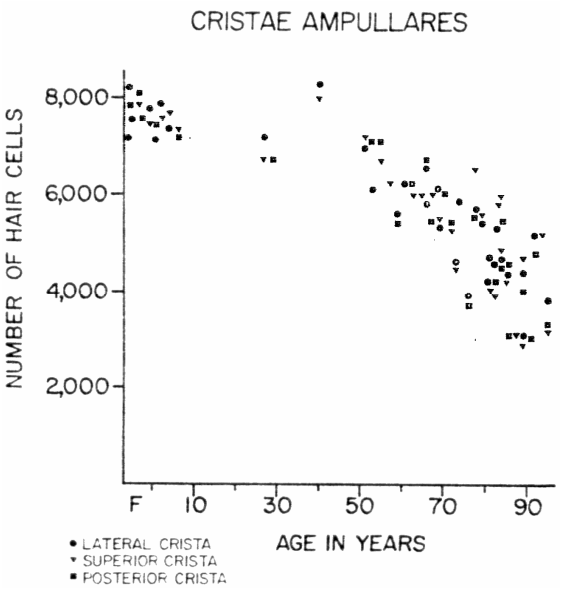

Figure V-3: Relationship between total number of hair cells of the cristae ampullares and age. There is a marked reduction of the hair cell populations with age. The reduction, exceeding what is seen in the maculae is about the same for all three cristae. Superior crista = crista anterior (Rosenhall, 1973).

Even if the anatomic loss is in accordance with my results, the pattern of histological changes differs. Most of the anatomical decrease is described as a gradient or a step-like neuronal or fiber deterioration with age (see **Figure V-1**, **Figure V-2**, **Figure V-3**, **Figure V-4**).

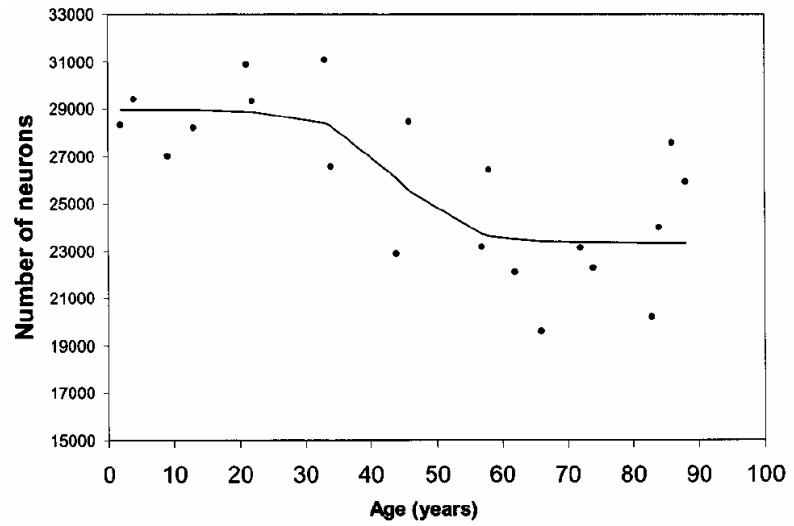

Figure V-4: Total number of neurons in the vestibular ganglion within temporal bone specimens of various individuals.
Plot based on logistics-based regression analysis shows a decline in the number of ganglion cells approximately between the ages of 20 to 70 years and most markedly, step-like drop, between 30 to 60 years of age (Park, Tang, Lopez, & Ishiyama, 2001).

Nonetheless, if the results of my study are considered and a relationship between the γ-gain and age is projected (best at time point 40ms where gain reached maximal values and no fast phases are yet present, see **Figure IV-1** - **Figure IV-9**), an inverse U-shaped curve indicating age dependency can be seen. The most pronounced increase of responses occurs between the third and the fifth decade of life. Reponses also show a slight increase for the fifth and a remarkable decrease from the sixth to the ninth decade. This pattern is best seen in the vertical plane responses, less in the torsional plane, and at the least is imprinted in the horizontal plane (see **Figure V-5**, **Figure V-6**, **Figure V-7**).

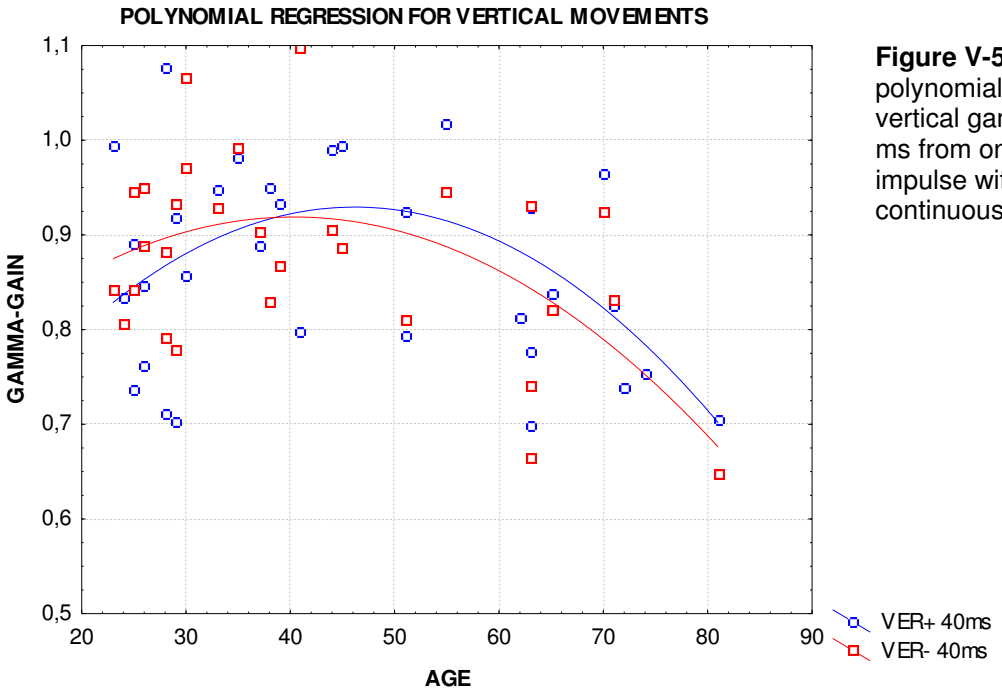

Figure V-5: Scatterplot with polynomial regression for vertical gamma-gains at 40 ms from onset of head impulse with age as continuous factor.

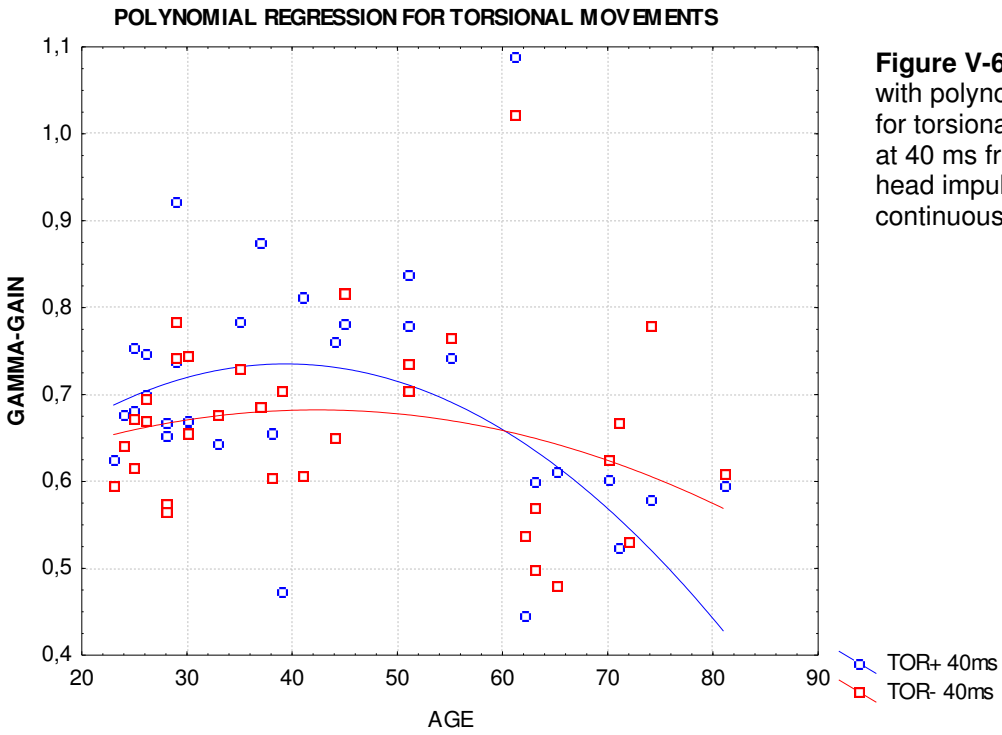

Figure V-6: Scatterplot with polynomial regression for torsional gamma-gains at 40 ms from onset of head impulse with age as continuous factor.

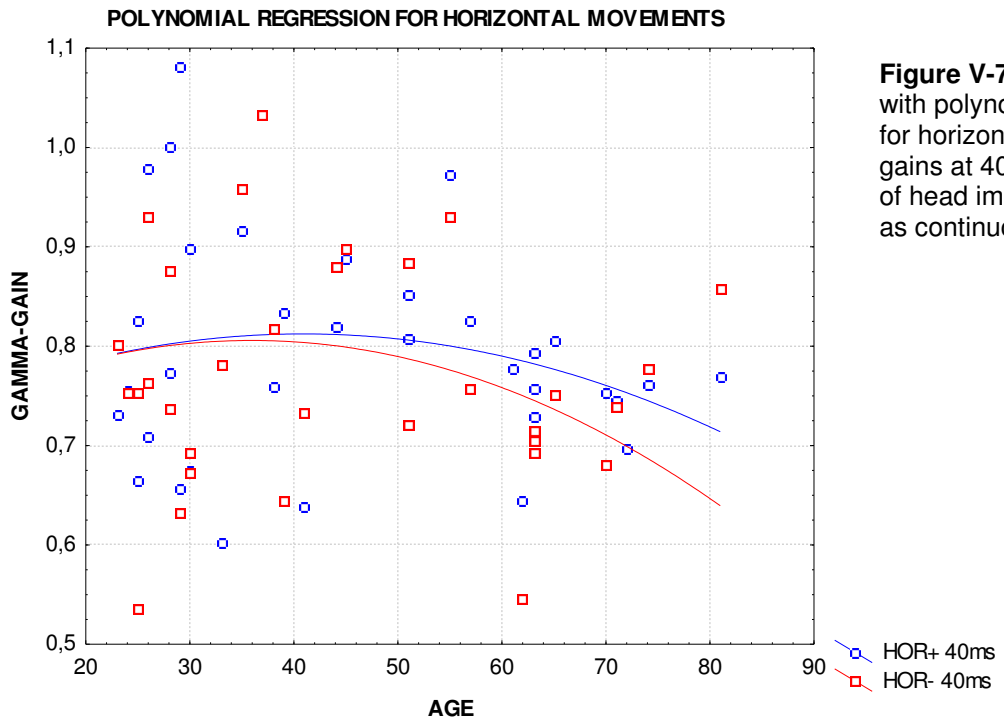

Figure V-7: Scatterplot with polynomial regression for horizontal gamma-gains at 40 ms from onset of head impulse with age as continuous factor.

Such curve has been shown before. Klaus Jahn and his colleagues working on galvanic stimulation of the vestibular nerve (Jahn, Naessl, Schneider, Strupp, Brandt, & Dieterich, 2003) presented similar results (see **Figure V-8**): increase of responses between the fourth and sixth decade, slight increase for the third and a decrease for the seventh decade.

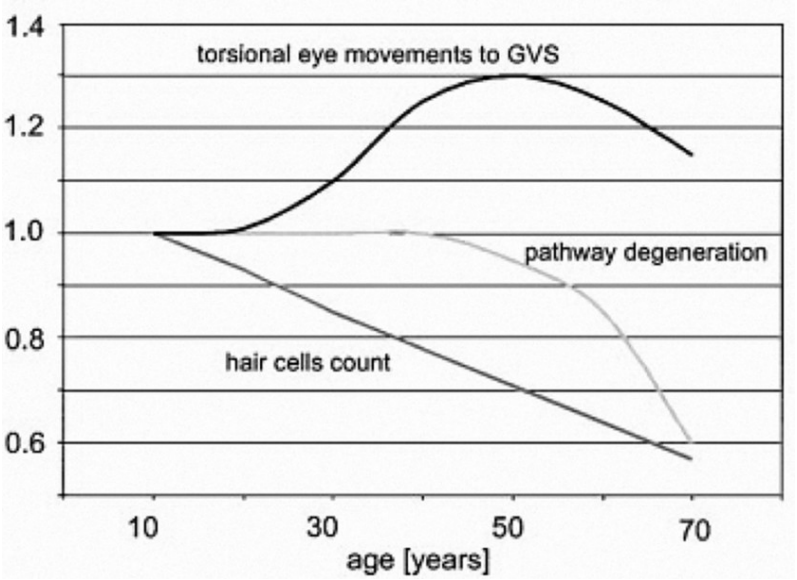

Figure V-8: The inverse U-shaped curve for age-dependency of torsional eye movement responses to GVS.
The curve shape for age-dependency between the eye movements and the GVS (black solid line) shows increase of responses between the fourth and sixth decade with slight increase for the third and a decrease for the seventh decade (Jahn, Naessl, Schneider, Strupp, Brandt, & Dieterich, 2003).

To interpret these findings, they had to consider the site of action of the GVS. It is generally accepted that the GVS stimulates the vestibular nerve rather than the hair cells. It acts at the spike trigger site of the primary vestibular afferents which extend 10±50 mm from the synapse to the first level of myelinization, and is thought to involve afferents from all

vestibular endorgans [semicircular canals (SCCs) and otolith] to a similar extent (Goldberg, Smith et al., 1984;Kleine & Grusser, 1996). Since otolith afferent stimulation induces a tonic ocular torsion (Suzuki, Tokumasu, & Goto, 1969), many studies attributed these responses to the activation of the otolith afferents (Inglis, Shupert et al., 1995;Day, Severac et al., 1997;Zink, Steddin et al., 1997;Watson, Brizuela et al., 1998). However, by modeling the expected responses (Wardman & Fitzpatrick, 2002) or mimicking GVS-induced eye movements by pure SCC stimulation (Schneider, Glasauer et al., 2002), it could be shown that the evoked eye movements can be attributed mainly to SCC activation. Evidence exists that the GVS stimulates predominantly irregular afferents which does not play a significant role in the three-neuron arc of the VOR (Goldberg, 2000). Higher currents can apparently stimulate regular afferents, which have higher thresholds, contribute maximally to the vestibulo-ocular reflex, and do not degenerate so apparently with age (Bergstrom, 1973;Bergstrom, 1973;Bergstrom, 1973;Nagai, Goto, Goto, Kaneko, & Suzaki, 1999;Jahn, Naessl, Schneider, Strupp, Brandt, & Dieterich, 2003;Goldberg, 2000). With respect to above, Jahn and co-workers proposed mechanism explaining the inverse U-shaped curve for age dependency of eye movement responses to the GVS:

The hair cell decline starts early and continues at a constant rate throughout life, whereas vestibular nerve and central neuron decline begins at midlife, increasing in rate at an older age. This has potential functional implications as to compensatory mechanisms. A schematic view of the proposed mechanism is illustrated in **Figure V-9.** Since hair cell loss precedes those seen in the vestibular nerve and the Scarpa's ganglion, the decrease in hair cell counts could be compensated by increased sensitivity of afferent nerve fibers or central mechanisms. Increased sensitivity could maintain normal function despite the reduced peripheral input. If this were true, the direct stimulation of vestibular nerve should cause larger responses than hair cell stimulation. As the GVS acts at the vestibular nerve, thereby bypassing the hair cells, electrical stimulation should be more efficient in subjects with beginning hair cell degeneration but increased vestibular afferent sensitivity, as seen in Jahn's data for age dependency. This holds only as long as the vestibular nerve and central structures remain unaffected. In more advanced ages, the degeneration of nerve fibers, ganglion cells and central neurons become evident. Thus, the compensatory increase in sensitivity breaks down and the GVS-induced eye movements decline. This is reflected in the inverse U-shaped curve for age dependency found in Jahn's study.

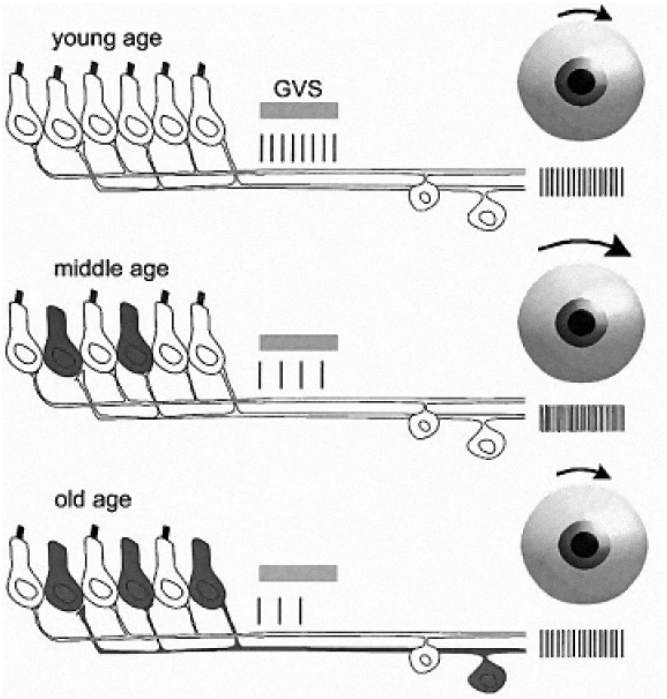

Figure V-9: The assumed mechanism of decline in old age.
Sensory hair cells and afferent pathways are shown for three different periods in life. During youth (upper panel), most hair cells are intact. Their excitatory synaptic transmission determines a resting discharge frequency that is increased by cathodal GVS and produces torsional eye movements. Resting discharge decreases with hair cell loss (middle age, middle panel). It is assumed that the vestibular system compensates for this by an increase in sensitivity. GVS of the nerve therefore leads to larger eye movement responses in middle age. When axon degeneration is added to hair cell loss (old age), the remaining structures can only partially compensate for the nerve fiber loss, despite their increased sensitivity to excitatory stimuli (lower panel) (Jahn, Naessl, Schneider, Strupp, Brandt, & Dieterich, 2003).

However innovative this conclusion is, results of my study open many questions and shatter the hypothesis presented above. As well as the GVS-induced eye movements, also my results of the head impulse responses show an inverse U-shaped curve for age dependency. Nevertheless, the site of action of the HITs is in the hair cells of the SCC in contrary to the nerve fiber endings of the SCC in the GVS. Therefore, proposed theory that increased central sensitivity to age-related hair cell decrease leads to inverse U-shaped response for the GVS should not be the case for the hair cell stimulation throughout the age span. Due to the above conclusion, it seems that the problem of increased responses in the middle age with a sudden decrease for the elderly and an increasing tendency for young is more complicated that could be explained only by dissociation between the hair cell loss, and the fiber and neuronal loss. Thin fibers, which we denote as carriers of the VOR information do not decrease significantly with age, contrary to thick myelinated fibers (Bergstrom, 1973;Bergstrom, 1973;Bergstrom, 1973;Nagai, Goto, Goto, Kaneko, & Suzaki, 1999). Additionally, Tang (Tang, Lopez, & Baloh, 2001) used a novel stereological investigation in the medial vestibular nucleus of various human individuals to prove that the neuronal decrease is gradient without any sudden drops (see **Figure V-10**). Thus, central overcompensation of predicted decrease of response, seen in both the GVS and HIT, must be driven by other changes then expected in Jahn's theory, and could be the same.

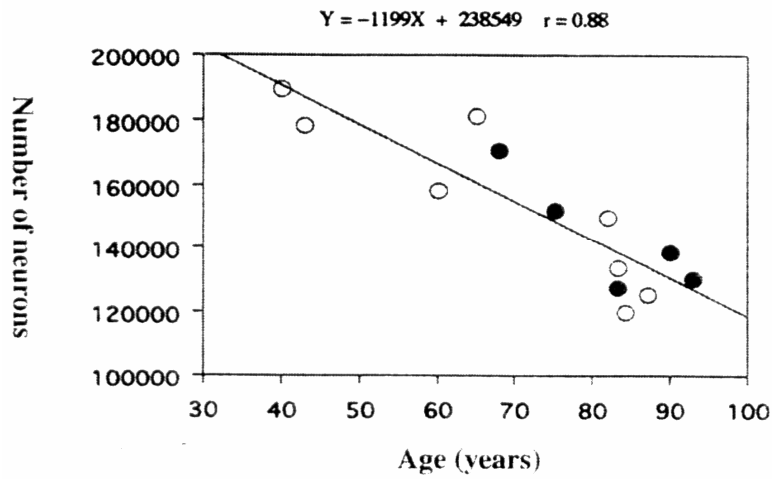

Figure V-10: Total number of neurons in the human medial vestibular nucleus of various individuals.
Regression analysis shows an age-related decline in the number of human medial vestibular nucleus neurons. Open circles: men; filled cycles: women (Tang, Lopez, & Baloh, 2001).

It is difficult to speculate about the reason, but at a first glance, the central mechanisms also loose their cells and so they have some limited capacity to facilitate inputs from peripheral vestibular structures. We can expect a critical threshold age after which these central mechanisms are not able to serve any more resulting in decrease of VOR performance – system collapses. Why there is and increase in responses in young and middle aged subjects, which is probably due to a central compensatory over-amplification, is not yet clear. Some answers could be provided by dynamics of the cerebellar Purkinje cells loss, cells crucially important in the VOR adaptation (Ito, 1984;Ito, 1972;Ito, 1982). There is a reported PC loss of 25 percent over the age span 0 to 100 years with a sudden decline after 60 years of age (with wide interindividual variation) (Hall, Miller, & Corellis, 1975). This could explain the part of decline in the curves but would be insufficient to understand why the overcompensation is reported. The part of increase in the curves more flat for the HIT responses and the peek shifting to earlier ages deserve more scrutiny. We could explain this by the involvement of a gradient hair cell loss, which changes the curve of the GVS to the pattern of the HIT response. Other studies where different VOR aspects were considered, e.g. the VOR time constant was measured, also published an inverse U-shaped age-related ratio with slightly increased response in subjects up to about 30 years and then decreased with increasing age. (Peterka, Black, & Schoenhoff, 1990). This confirms the involvement of the cerebellar structures in the age-related response.

Jahn recorded the roll responses. My results are best pronounced in the vertical eye responses but clearly seen also in roll recordings (see **Figure V-5**, **Figure V-6**, **Figure V-7**). Many of my results show similarities after stimulation in the roll and pitch planes (e.g. significance in γ-gain, test with age as a continuous predictor, particular differences between age-different groups etc.). This is probably due to this fact that vertical and torsional VORs

are driven by the same semicircular canals, respond with the same muscles, and it seems that even brainstem pathways for both the vertical and torsional VORs are very similar (Brandt & Dieterich, 1999;Leigh RJ, 1999) contrary to the horizontal VOR. Therefore, a functional loss and adaptive mechanisms could react on the vertical and torsional VOR similarly due to the same anatomical structure involved, while that stand in a contrast to the horizontal VOR. Inverse U-shaped curve of the roll responses has pattern closer to horizontal response. Similarly, significant age-related difference in the pitch plane is due to the velocity gain; distinction in the yaw and roll planes is obtained due to the misalignment angle difference. Reason for these presented observations remains unclear.

V.3 Additional Conclusions

In the roll plane, there was no significant effect of time found. We can speculate that this could be explained by the maximal magnitude of γ-gain in torsional eye movements which are only about 0.7 (of course with differences according to age) at the time point of 40ms from the onset of the head impulse. This complies with the results of previous studies that measured roll responses (Aw, Haslwanter, Halmagyi, Curthoys, Yavor, & Todd, 1996). Such low maximal γ-gain cannot produce significant effect of time, in other words, latency and starting amplitude in the roll, yaw and pitch responses are the same, but only in the roll plane do eye movements reach maximally 0.7 γ-gain. This is probably due to several reasons: roll head movements are of smaller amplitude during a run and a walk in comparison to movements in other planes, so, the roll eye movements are probably not as necessary in daily activities (Leigh RJ, 1999;Leigh & Brandt, 1993) (see **Figure I-8**). This is in accordance with lower sensitivity for torsional head movements in vertical ducts (Muller & Verhagen, 2002) and little velocity storage for the roll VOR (Leigh RJ, 1999).

Although there are evidences of extreme ocular tilts in pathological circumstances (up to 30º in acute unilateral brainstem disorders) (Dieterich M, 1992;Dieterich M, 1993;Halmagyi, Curthoys, Cremer, Henderson, Todd, Staples, & D'Cruz, 1990) counterrolling of the eyes in humans compensates up to maximum of 10º (Diamond & Markham, 1983;Jampel & Shi, 2002;Leigh RJ, 1999). Therefore, we can suggest that performing high acceleration maneuvers in the roll-torsional plane, which exceed 10 º of head tilt, would lead to very early correctional quick phases of the eyes.

Finally, roll eye movements are rotated according to the naso-occipital axis, mechanically against the other forces in the bulb orbit.

Finding the effect of direction or interaction of direction and time that was predominantly found in yaw and pitch plane in all parameters proves interesting. It points at the fact that the left-right and up-down responses differ in amplitude and alignment. This result was consistently found from in my earlier research (Brzezny, Glasauer, Bayer, Siebold, & Buttner, 2003;Brzezny, Glasauer, von Lindeiner, Hoshi, Kiss, Siebold, Jeřábek, & Buttner, 2003) and even the data were recorded later by other researchers. Throughout the three years of the study, the effect of direction was even more intensified. An up-down variance in oculomotor testing was referred before (Aw, Haslwanter, Halmagyi, Curthoys, Yavor, & Todd, 1996;Kim & Sharpe, 2001;Kim & Sharpe, 2001). Probably due to the three-dimensional orientation vectors of human semicircular canals which are leading to an asymmetry (Blanks, Curthoys, & Markham, 1975), a weaker upward head movement VOR is seen in comparison with a downward head movement VOR (upward gain of 0.85, downward gain of 1.15, see **Figure I-5**), more or less compensated centrally by the inhibitory pathways of the flocculus and the parafloccculus (Ito, Nisimaru, & Yamamoto, 1977).

Although my results comply with these presented above, the difference in other studies was not as significantly prominent. Additionally, the effect of direction in horizontal plane was never published, in spite of a possible speculation that the left-right difference might be due to dexterous providers of head impulses.

Hence, we have to look into a possible problem in the basic recording settings. According to personal communication with S.T.Aw from the Royal Prince Alfred Hospital in Sydney, Australia, from whom most of the settings were adopted, very similar findings were experienced in the beginning of their recordings. After attaching the coil to the bite-bar, the left-right and up-and-down differences were reduced. This is an important aspect that will be introduced in my future studies.

It is hard to explain why horizontal responses showed low significance in ANOVA test and no significance with age as a continuous predictor. There seems to be no significance in the velocity gain. This may lead us to conclude that with increasing age the amplitude reaction in horizontal plane remains quite stable, but the misalignment is increased.

V.4 Clinical and Public Health Implications

The vestibular system abnormalities are highly related to falls, typically, due to a bilateral loss of vestibular function in patients older than 65 (Whitney, Hudak et al., 2000;Herdman, Blatt et al., 2000). Mechanisms of vestibular dysfunction have been connected to reduced

adaptability of the vestibular system in elderly, and consequently linked to significantly increased frequency of falls (Di Fabio, Greany et al., 2002).

Work-related falls in people older than 45 years are more serious in comparison to younger individuals. Longer hospitalization rates and prolonged disability from such injuries has been described (Kemmlert & Lundholm, 2001). More than one third of individuals older than 65 report a fall some time during a year prior to an examination(Thapa, Brockman et al., 1996;Six, 1992). In the population older than 72 more than half suffers from falls. About 50 percent of falls result in serious consequences (Thapa, Brockman, Gideon, Fought, & Ray, 1996;Tinetti, Doucette et al., 1995;Kallin, Lundin-Olsson et al., 2002). Majority of patients with unfavorable outcomes require hospitalization in a nursing home, while death rate after falls is four times higher in the elderly when compared to the younger adults (Ellis & Trent, 2001;Ghodsi, Roudsari et al., 2003).

In the Czech Republic, reduction in falls by only 10 percent would reduce the incidence of hip fractures by more than 800 per year, and reduce all hospital admissions by more than 1000 per year. Quality of life would improve, together with reduction in financial and social burden. In this group of people serious reduction in activities of daily living, reduction of physical activities, and related rates of anxiety and depression represent an underestimated problem (Liddle & Gilleard, 1984;Vetter & Ford, 1989;Topinková & Neuwirth, 1995).

Falls are caused by internal and external factors. External factors, which include the factors of environment, can be adapted to decrease the risk. For example, sufficient labeling of dangerous places (stairs, etc.) might be helpful (Ghodsi, Roudsari, Abdollahi, & Shadman, 2003). The major internal factor is the general capacity to keep the equilibrium. This requires synergistic activity of different sensory systems. Aging affects all of them. Not surprisingly, age-related morphological changes of anatomical structures important for the sense of balance have been described. In geriatric patients, changes in the nervous system structures are additionally complicated by polymorbidity, and, unfortunately so often, polypharmacy (Topinková & Neuwirth, 1995;Ambler, 2000).

V.5 Closing Remarks

V.5.1 Multisensory Co-operation in Adaptational Strategies

Adding to our results, the contribution of other reflexes during compensatory eye movements should be finally taken into account. These other non-vestibular inputs could come from the skin, muscle or joint proprioceptors in the legs and torso, from torsion of the

pelvis, movements of the inner fluids, or, in particular, from a passive, cervico-ocular reflex. All those probably make a small contribution to the gaze stability during rapid head movements (Zee, 1977;Buttner-Ennever, 1999). There are some reports that labyrinthectomized monkeys are able to reach values near 0.80 of the VOR gain , e.g. during active had movements (Zee, 1977). In patients, a number of other strategies were suggested in order to improve the gaze stability including corrective saccades, slower voluntary compensatory movements, and recalibration of the relationship between the saccadic amplitude and retinal error during active target seeking. An effort of spatial localizing and predictive mechanisms play important roles in determining the adequacy of gaze stability (Zee, 1977):

It may be that patients avoid the visual blur that would inevitably accompany the retinal slip produced by head movements toward the affected side, by blinking and making refixation saccades. Some patients have found perhaps the simplest strategy of all for dealing with the ampullofugal rVOR deficit: they learn to restrict head movements toward the affected side. They learn to use only their eyes rather than their heads and eyes together to refixate objects of the interest within the orbital range of the affected site (Halmagyi, Curthoys, Cremer, Henderson, Todd, Staples, & D'Cruz, 1990). And finally, the compensatory mechanisms can even preprogram the system to prepare the eye to reach desired position before the expected movement, which eventually points the gaze in the correct direction.

V.5.2 Additional Aspects in Brain Ageing

More recent anatomical studies indicate that age-dependent changes of the extracellular brain matrix and glia have also eminent influence on neuronal performance and increased susceptibility of the aging brain to various insults. This disposition helps to explain a delimited functional brain reserve to various stress factors like metabolic changes in hypoxia. Since there is a great variability in amount of cellular loss in anatomic structures in elderly (Hall, Miller, & Corellis, 1975;Park, Tang, Lopez, & Ishiyama, 2001;Rosenhall, 1973), in smaller populations of young and old subjects, the age-related changes may remain undetected due to casual selection of these older subjects with a luck of having no stress situation in their life. Specific to this scenario is amount of cellular deterioration in the cerebellar structures in elderly which is probably dependent on earlier lifestyle and habits, and may be prevented or delayed by a physical exercise (Larsen, Skalicky, & Viidik, 2000;Larsen, Skalicky, & Viidik, 2000). Questions pertaining to this topic were not solicited from our tested subjects. One could propose that a small group of older subjects is not significant

enough to describe age-related changes due to large variability of the anatomic changes in elderly. This concept does not correlate with rather small results variabilities among the elderly in our study (compare **Figure V-1**, **Figure V-3**, **Figure V-4** and **Figure V-5** - **Figure V-7**).

A different study looking at varied lifestyles among a bigger group of subjects would be essential in understanding whether the function of vestibular structures deteriorates in a specific way, and how the cerebellar or other structures with varying interindividual anatomical decline are involved in particular planes of stimulation, including particularly the canal planes.

One more aspect with a potential to contribute to the decreased part of the age curves is that there are records of degenerative changes in human's eye muscles after 60 years of age (Vijayashankar & Brody, 1977;Vijayashankar & Brody, 1977;Muhlendyck, 1979). Changes in oculomotor nuclei relative to age have never been reported.

V.5.3 Head-Impulse Testing in Ageing and Unilateral Vestibular Lesions

According to measured labyrinthine caloric asymmetry in elderly, we would suggest a gradual functional difference between both sides, which resembles slight unilateral vestibulopathy. Patients with such condition show highly significant direction differences in precise eye-movements recordings in horizontal head impulses (Aw, Halmagyi, Haslwanter, Curthoys, Yavor, & Todd, 1996;Aw, Haslwanter, Halmagyi, Curthoys, Yavor, & Todd, 1996;Beynon, Jani et al., 1998;Carey, Hirvonen et al., 2002;Carey, Minor et al., 2002;Cremer, Halmagyi, Aw, Curthoys, McGarvie, Todd, Black, & Hannigan, 1998;Halmagyi, Curthoys, Cremer, Henderson, Todd, Staples, & D'Cruz, 1990;Halmagyi, Colebatch et al., 1994). Since head impulses seem to be the best test method especially for the chronic vestibular lesions (Schmid-Priscoveanu, Bohmer, Obzina, & Straumann, 2001), and the changes in elderly subjects are much alike changes in those lesions, it appears that head impulses should be the most suitable for defining the age-dependent changes. Therefore, it is not surprising that study by Tian and colleagues (Tian, Shubayev, Baloh, & Demer, 2001;Tian, Shubayev, Baloh, & Demer, 2001) which studied eye movements in transient rotations at high acceleration, recorded significant gain decrease in yaw-horizontal stimulus in elderly. My findings in horizontal plane correlated with this study; however, the results were not as prominent.

V.5.4 Future Research

Several suggestions for future research plans related to my study were presented above. Most prominently, the latency of response should be computed. Older subjects are consistently found to have prolonged latencies in the horizontal VOR, as well as in other reflexes or in evoked potentials measurements(Tian, Shubayev, Baloh, & Demer, 2001;Zumsteg & Wieser, 2002). Moreover, it is not surprising to find prolonged VOR latencies among older subjects. The bigger reason for the prolonged latencies lies in the age-related myelin loss in the central and peripheral neuronal structures (Attarian, Azulay et al., 2001;Bergstrom, 1973;Bergstrom, 1973;Capasso, Torrieri et al., 2002;Ebner, Dengler et al., 1981;Koprdová, 1998;Poinoosawmy, Fontana et al., 1997;Vite, McGowan et al., 2001). Lastly, an approach focused on accounting for different lifestyles should also be considered in the future work.

VI Reference List

1. Bergstrom, B. (1973). Morphology of the vestibular nerve. II. The number of myelinated vestibular nerve fibers in man at various ages. *Acta Otolaryngol.* 76, 173-179.

2. Land, M. F. (1999). Motion and vision: why animals move their eyes. *J.Comp Physiol [A]* 185, 341-352.

3. Leigh RJ, Z. D. (1999). "The Neurology of Eye Movements." Oxford University Press,Inc., Oxford.

4. Angelaki, D. E. (2003). Three-dimensional ocular kinematics during eccentric rotations: evidence for functional rather than mechanical constraints. *J.Neurophysiol.* 89, 2685-2696.

5. Allen, J. L. (2003). "Bride of the Mistletoe." The Project Gutenberg.

6. Engbert, R. and Kliegl, R. (2003). Microsaccades uncover the orientation of covert attention. *Vision Res.* 43, 1035-1045.

7. Gerrits, H. J. and Vendrik, A. J. (1970). Artificial movements of a stabilized image. *Vision Res.* 10, 1443-1456.

8. Martinez-Conde, S., Macknik, S. L., and Hubel, D. H. (2002). The function of bursts of spikes during visual fixation in the awake primate lateral geniculate nucleus and primary visual cortex. *Proc.Natl.Acad.Sci.U.S.A* 99, 13920-13925.

9. Moller, F., Laursen, M. L., Tygesen, J., and Sjolie, A. K. (2002). Binocular quantification and characterization of microsaccades. *Graefes Arch.Clin.Exp.Ophthalmol.* 240, 765-770.

10. James, P. K. (1991). The Sence of Balance. *In* "Principles of Neural Science" (E. R. Kandel, J. H. Schwartz, and T. M. Jessell, Eds.), pp. 500-511. Elsevier, New York.

11. Druga, R. and Petrovický, R. (1991). "Smyslové orgány, kůže a kožní ústrojí." Karolinum.

12. Feneis, H. (1974). "Anatomisches Bildwörterbuch." Georg Thieme Verlag, Suttgart.

13. Muller, M. and Verhagen, J. H. (2002). Optimization of the mechanical performance of a two-duct semicircular duct system--part 3: the positioning of the ducts in the head. *J.Theor.Biol.* 216, 443-459.

14. Blanks, R. H., Curthoys, I. S., and Markham, C. H. (1975). Planar relationships of the semicircular canals in man. *Acta Otolaryngol.* 80, 185-196.

15. Cremer, P. D., Halmagyi, G. M., Aw, S. T., Curthoys, I. S., McGarvie, L. A., Todd, M. J., Black, R. A., and Hannigan, I. P. (1998). Semicircular canal plane head impulses detect absent function of individual semicircular canals. *Brain* 121 (Pt 4), 699-716.

16. Rother, T., Schrock-Pauli, C., Karmody, C. S., and Bachor, E. (2003). 3-D reconstruction of the vestibular endorgans in pediatric temporal bones. *Hear.Res.* 185, 22-34.

17. Takagi, A., Sando, I., and Takahashi, H. (1989). Computer-aided three-dimensional reconstruction and measurement of semicircular canals and their cristae in man. *Acta Otolaryngol.* 107, 362-365.

18. Milhaud, P. G., Nicolas, M. T., Bartolami, S., Cabanis, M. T., and Sans, A. (1999). Vestibular semicircular canal epithelium of the rat in culture on filter support: polarity and barrier properties. *Pflugers Arch.* 437, 823-830.

19. Sterkers, O., Ferrary, E., and Amiel, C. (1988). Production of inner ear fluids. *Physiol Rev.* 68, 1083-1128.

20. Muller, M. and Verhagen, J. H. (2002). Optimization of the mechanical performance of a two-duct semicircular duct system--part 1: dynamics and duct dimensions. *J.Theor.Biol.* 216, 409-424.

21. Muller, M. and Verhagen, J. H. (2002). Optimization of the mechanical performance of a two-duct semicircular duct system--part 2: excitation of endolymph movements. *J.Theor.Biol.* 216, 425-442.

22. Steinhausen, W. (1933). Über die Beobachtungen der Cupula in den Bogengangsampullen des Labyrinthes des lebenden Hechts. *Pflugers Arch.* 232, 500-512.

23. Hillman, D. E. and McLaren, J. W. (1979). Displacement configuration of semicircular canal cupulae. *Neuroscience* 4, 1989-2000.

24. Rusch, A. and Thurm, U. (1989). Cupula displacement, hair bundle deflection, and physiological responses in the transparent semicircular canal of young eel. *Pflugers Arch.* 413, 533-545.

25. Jijiwa, H., Watanabe, N., Hattori, T., Matuda, F., Hashiba, M., Mizuno, Y., Shindo, M., and Watanabe, S. (2001). Does the endolymph pass through the base of the cupula? *Acta Astronaut.* 49, 365-369.

26. Dohlman, G. F. (1971). The attachment of the cupulae, otolith and tectorial membranes to the sensory cell areas. *Acta Otolaryngol.* 71, 89-105.

27. Muller, M. (1994). Semicircular Duct Dimensions and Sensitivity of the Vertebrate Vestibular System. *Journal of Theoretical Biology* 167, 239-256.

28. Dohlman, G. F. (1981). Critical review of the concept of cupula function. *Acta Otolaryngol.Suppl* 376, 1-30.

29. Holt, J. R., Corey, D. P., and Eatock, R. A. (1997). Mechanoelectrical Transduction and Adaptation in Hair Cells of the Mouse Utricle, a Low-Frequency Vestibular Organ. *Journal of Neuroscience* 17, 8739-8748.

30. Lopez, I., Honrubia, V., Chul Lee, S., Schoeman, G., and Beykirch, K. (1997). Quantification of the process of hair cell loss and recovery in the chinchilla crista ampullaris after gentamicin treatment. *International Journal of Developmental Neuroscience* 15, 447-461.

31. Eatock, R. A., Rusch, A., Lysakowski, A., and Saeki, M. (1998). Hair cells in mammalian utricles. *Otolaryngol.Head Neck Surg.* 119, 172-181.

32. Kevetter, G. A., Blumberg, K. R., and Correia, M. J. (2000). Hair cell and supporting cell density and distribution in the normal and regenerating posterior crista ampullaris of the pigeon. *International Journal of Developmental Neuroscience* 18, 855-867.

33. Goldberg, J. M. (2000). Afferent diversity and the organization of central vestibular pathways. *Exp.Brain Res.* 130, 277-297.

34. Matsui, J. I. and Cotanche, D. A. (2004). Sensory hair cell death and regeneration: two halves of the same equation. *Curr.Opin.Otolaryngol.Head Neck Surg.* 12, 418-425.

35. Jaeger, R., Takagi, A., and Haslwanter, T. (2002). Modeling the relation between head orientations and otolith responses in humans. *Hear.Res.* 173, 29-42.

36. Lins, U., Farina, M., Kurc, M., Riordan, G., Thalmann, R., Thalmann, I., and Kachar, B. (2000). The Otoconia of the Guinea Pig Utricle: Internal Structure, Surface Exposure, and Interactions with the Filament Matrix. *Journal of Structural Biology* 131, 67-78.

37. Wiederhold, M. L., Harrison, J. L., and Gao, W. (2003). A critical period for gravitational effects on otolith formation. *J.Vestib.Res.* 13, 205-214.

38. Ibsch, M., Anken, R., Beier, M., and Rahmann, H. (2004). Endolymphatic calcium supply for fish otolith growth takes place via the proximal portion of the otocyst. *Cell Tissue Res.* 317, 333-336.

39. Anken, R. H., Beier, M., and Rahmann, H. (2004). Hypergravity decreases carbonic anhydrase-reactivity in inner ear maculae of fish. *J.Exp.Zoolog.Part A Comp Exp.Biol.* 301, 815.

40. Kondrachuk, A. V. (2000). Computer simulation of the mechanical stimulation of the saccular membrane of bullfrog. *Hearing Research* 143, 130-138.

41. Grant, J. W., Huang, C. C., and Cotton, J. R. (1994). Theoretical mechanical frequency response of the otolithic organs. *J.Vestib.Res.* 4, 137-151.

42. Kachar, B., Parakkal, M., and Fex, J. (1990). Structural basis for mechanical transduction in the frog vestibular sensory apparatus: I. The otolithic membrane. *Hear.Res.* 45, 179-190.

43. Ross, M. D., Komorowski, T. E., Rogers, C. M., Pote, K. G., and Donovan, K. M. (1987). Macular suprastructure, stereociliary bonding and kinociliary/stereociliary coupling in rat utricular macula. *Acta Otolaryngol.* 104, 56-65.

44. Curthoys, I. S., BETTS, G. A., BURGESS, A. M., MacDOUGALL, H. G., CARTWRIGHT, A. D., and Halmagyi, G. M. (1999). The Planes of the Utricular and Saccular Maculae of the Guinea Pig. *Annals of the New York Academy of Sciences* 871, 27-34.

45. Sato, H., Sando, I., and Takahashi, H. (1992). Computer-aided three-dimensional measurement of the human vestibular apparatus. *Otolaryngol.Head Neck Surg.* 107, 405-409.

46. Takagi, A. and Sando, I. (1988). Computer-aided three-dimensional reconstruction and measurement of the vestibular end-organs. *Otolaryngol.Head Neck Surg.* 98, 195-202.

47. Rosenhall, U. (1972). Vestibular macular mapping in man. *Ann.Otol.Rhinol.Laryngol.* 81, 339-351.

48. Kong, W. J., Hussl, B., Thumfart, W. F., and Schrott-Fischer, A. (1998). Ultrastructural localization of ChAT-like immunoreactivity in the human vestibular periphery. *Hear.Res.* 119, 96-103.

49. Bergstrom, B. (1973). Morphology of the vestibular nerve. I. Anatomical studies of the vestibular nerve in man. *Acta Otolaryngol.* 76, 162-172.

50. Nagai, Y., Goto, N., Goto, J., Kaneko, Y., and Suzaki, H. (1999). Morphometric nerve fiber analysis and aging process of the human vestibular nerve. *Okajimas Folia Anat.Jpn.* 76, 95-100.

51. Bergstrom, B. (1973). Morphology of the vestibular nerve. 3. Analysis of the calibers of the myelinated vestibular nerve fibers in man at various ages. *Acta Otolaryngol.* 76, 331-338.

52. Suarez, C., Diaz, C., Tolivia, J., Alvarez, J. C., Gonzalez, d. R., and Navarro, A. (1997). Morphometric analysis of the human vestibular nuclei. *Anat.Rec.* 247, 271-288.

53. Buttner-Ennever, J. A. (1999). A review of otolith pathways to brainstem and cerebellum. *Ann.N.Y.Acad.Sci.* 871, 51-64.

54. Glasauer, S., Dieterich, M., and Brandt, T. (2001). Central positional nystagmus simulated by a mathematical ocular motor model of otolith-dependent modification of Listing's plane. *J.Neurophysiol.* 86, 1546-1554.

55. Glasauer, S., Dieterich, M., and Brandt, T. (2001). Modeling the role of the interstitial nucleus of Cajal in otolithic control of static eye position. *Acta Otolaryngol Suppl* 545, 105-7.

56. Suzuki, J. I., Tokumasu, K., and Goto, K. (1969). Eye movements from single utricular nerve stimulation in the cat. *Acta Otolaryngol* 68, 350-62.

57. Marlinski, V., Plotnik, M., and Goldberg, J. M. (2004). Efferent actions in the chinchilla vestibular labyrinth. *J.Assoc.Res.Otolaryngol.* 5, 126-143.

58. Rabbitt, R. D. (1999). Directional coding of three-dimensional movements by the vestibular semicircular canals. *Biol.Cybern.* 80, 417-431.

59. St George, R., Lord, SR., and Fitzpatrick, RC. SYCOPHYSICAL TESTS OF THE VESTIBULAR OCULAR REFLEX. the 6th IBRO Wordl Congress of Neuroscience , (abstract). 2003.

60. Grossman, G. E., Leigh, R. J., Abel, L. A., Lanska, D. J., and Thurston, S. E. (1988). Frequency and velocity of rotational head perturbations during locomotion. *Exp.Brain Res.* 70, 470-476.

61. Grossman, G. E., Leigh, R. J., Bruce, E. N., Huebner, W. P., and Lanska, D. J. (1989). Performance of the human vestibuloocular reflex during locomotion. *J.Neurophysiol.* 62, 264-272.

62. Leigh, R. J. and Brandt, T. (1993). A reevaluation of the vestibulo-ocular reflex: new ideas of its purpose, properties, neural substrate, and disorders. *Neurology* 43, 1288-1295.

63. Ito, M., Nisimaru, N., and Yamamoto, M. (1977). Specific patterns of neuronal connexions involved in the control of the rabbit's vestibulo-ocular reflexes by the cerebellar flocculus. *J.Physiol* 265, 833-854.

64. Glasauer, S., von Lindeiner, H., Siebold, C., and Buttner, U. (2004). Vertical vestibular responses to head impulses are symmetric in downbeat nystagmus. *Neurology* 63, 621-625.

65. Cohen, B., Henn, V., Raphan, T., and Dennett, D. (1981). Velocity storage, nystagmus, and visual-vestibular interactions in humans. *Ann N.Y.Acad Sci* 374, 421-433.

66. Gresty, M. A., Bronstein, A. M., Brandt, T., and Dieterich, M. (1992). Neurology of otolith function. Peripheral and central disorders. *Brain* 115 (Pt 3), 647-673.

67. Minor, L. B. and Goldberg, J. M. (1991). Vestibular-nerve inputs to the vestibulo-ocular reflex: a functional-ablation study in the squirrel monkey. *J.Neurosci.* 11, 1636-1648.

68. Aw, S. T., Haslwanter, T., Halmagyi, G. M., Curthoys, I. S., Yavor, R. A., and Todd, M. J. (1996). Three-dimensional vector analysis of the human vestibuloocular reflex in response to high-acceleration head rotations. I. Responses in normal subjects. *J.Neurophysiol.* 76, 4009-4020.

69. Brzezny, R., Glasauer, S., Bayer, O., Siebold, Ch., and Buttner, U. Head Impulses in Three Orthogonal Planes of Space - The Influence of Age. Ann N Y Acad Sci. 1004, 473-477. 2003.

70. Brzezny, R., Glasauer, S., von Lindeiner, H., Hoshi, M., Kiss, M., Siebold, Ch., Jeřábek, J., and Buttner, U. AGE-RELATED CHANGES IN THREE-DIMENSIONAL HUMAN VESTIBULO-OCULAR REFLEX IN RESPONSE TO HIGH-ACCELERATION HEAD ROTATIONS. the 6th IBRO Wordl Congress of Neuroscience , (abstract). 2003.

71. Mulavara, A. P. and Bloomberg, J. J. (2002). Identifying head-trunk and lower limb contributions to gaze stabilization during locomotion. *J.Vestib.Res.* 12, 255-269.

72. Hirasaki, E., Moore, S. T., Raphan, T., and Cohen, B. (1999). Effects of walking velocity on vertical head and body movements during locomotion. *Exp.Brain Res.* 127, 117-130.

73. Crane, B. T. and Demer, J. L. (1997). Human gaze stabilization during natural activities: translation, rotation, magnification, and target distance effects. *J.Neurophysiol.* 78, 2129-2144.

74. Viirre, E., Tweed, D., Milner, K., and Vilis, T. (1986). A reexamination of the gain of the vestibuloocular reflex. *J.Neurophysiol.* 56, 439-450.

75. Crane, B. T. and Demer, J. L. (1998). Human horizontal vestibulo-ocular reflex initiation: effects of acceleration, target distance, and unilateral deafferentation. *J.Neurophysiol.* 80, 1151-1166.

76. Curthoys, I. S. (2000). Vestibular compensation and substitution. [Review]. *Current Opinion in Neurology* 13, 27-30.

77. Halmagyi, G. M., Black, R. A., Thurtell, M. J., and Curthoys, I. S. (2003). The human horizontal vestibulo-ocular reflex in response to active and passive head impulses after unilateral vestibular deafferentation. *Ann N.Y.Acad Sci* 1004, 325-336.

78. Segal, B. N. and Katsarkas, A. (1988). Long-term deficits of goal-directed vestibulo-ocular function following total unilateral loss of peripheral vestibular function. *Acta Otolaryngol.* 106, 102-110.

79. Ito, M. (1972). Neural design of the cerebellar motor control system. *Brain Res.* 40, 81-84.

80. Ito, M. (1982). Cerebellar control of the vestibulo-ocular reflex--around the flocculus hypothesis. *Annu.Rev.Neurosci.* 5, 275-296.

81. Carthwright, A. D., Curthoys, I. S., and Gilchrist, D. P. (1999). Testable predictions from realistic neural network simulations of vestibular compensation: integrating the behavioural and physiological data. *Biol.Cybern.* 81, 73-87.

82. Chioran, G. M. and Yee, R. D. (1991). Analysis of electro-oculographic artifact during vertical saccadic eye movements. *Graefes Arch.Clin.Exp.Ophthalmol.* 229, 237-241.

83. Schmid-Priscoveanu, A., Bohmer, A., Obzina, H., and Straumann, D. (2001). Caloric and search-coil head-impulse testing in patients after vestibular neuritis. *J.Assoc.Res.Otolaryngol.* 2, 72-78.

84. van der Geest, J. N. and Frens, M. A. (2002). Recording eye movements with video-oculography and scleral search coils: a direct comparison of two methods. *J Neurosci.Methods* 114, 185-195.

85. Irving, E. L., Zacher, J. E., Allison, R. S., and Callender, M. G. (2003). Effects of scleral search coil wear on visual function. *Invest Ophthalmol.Vis.Sci.* 44, 1933-1938.

86. Murphy, P. J., Duncan, A. L., Glennie, A. J., and Knox, P. C. (2001). The effect of scleral search coil lens wear on the eye. *Br.J.Ophthalmol.* 85, 332-335.

87. Collewijn, H., van der, M. F., and Jansen, T. C. (1975). Precise recording of human eye movements. *Vision Res.* 15, 447-450.

88. Robinson, D. A. A method of measuring eye movement using a scleral search coil in a magnetic field. IEEE Trans.Biomed.Eng. 10, 137-145. 1963.

89. Demer, J. L., Crane, B. T., Tian, J. R., and Wiest, G. (2001). New tests of vestibular function. *Ann N Y Acad Sci* 942, 428-45.

90. Brandt, T. (1998). "Vertigo: Its Multisensory Syndromes." Springer-Verlag Telos, New York.

91. Halmagyi, G. M., Curthoys, I. S., Cremer, P. D., Henderson, C. J., Todd, M. J., Staples, M. J., and D'Cruz, D. M. (1990). The human horizontal vestibulo-ocular reflex in

response to high- acceleration stimulation before and after unilateral vestibular neurectomy. *Exp.Brain Res.* 81, 479-490.

92. Day, B. L. (1999). Galvanic vestibular stimulation: new uses for an old tool. *The Journal of Physiology Online* 517, 631.

93. Fitzpatrick, R. C., Wardman, D. L., and Taylor, J. L. (1999). Effects of galvanic vestibular stimulation during human walking. *The Journal of Physiology Online* 517, 931-939.

94. Jahn, K., Naessl, A., Schneider, E., Strupp, M., Brandt, T., and Dieterich, M. (2003). Inverse U-shaped curve for age dependency of torsional eye movement responses to galvanic vestibular stimulation. *Brain* 126, 1579-1589.

95. Baloh, R. W. and Demer, J. (1991). Gravity and the vertical vestibulo-ocular reflex. *Exp.Brain Res.* 83, 427-433.

96. Demer, J. L. (1992). Mechanisms of human vertical visual-vestibular interaction. *J.Neurophysiol.* 68, 2128-2146.

97. Allum, J. H., Yamane, M., and Pfaltz, C. R. (1988). Long-term modifications of vertical and horizontal vestibulo-ocular reflex dynamics in man. I. After acute unilateral peripheral vestibular paralysis. *Acta Otolaryngol.* 105, 328-337.

98. Wiest, G., Demer, J. L., Tian, J., Crane, B. T., and Baloh, R. W. (2001). Vestibular function in severe bilateral vestibulopathy. *J.Neurol.Neurosurg.Psychiatry* 71, 53-57.

99. Aw, S. T., Halmagyi, G. M., Curthoys, I. S., Todd, M. J., and Yavor, R. A. (1994). Unilateral vestibular deafferentation causes permanent impairment of the human vertical vestibulo-ocular reflex in the pitch plane. *Exp.Brain Res.* 102, 121-130.

100. Aw, S. T., Halmagyi, G. M., Haslwanter, T., Curthoys, I. S., Yavor, R. A., and Todd, M. J. (1996). Three-dimensional vector analysis of the human vestibuloocular reflex in response to high-acceleration head rotations. II. responses in subjects with unilateral vestibular loss and selective semicircular canal occlusion. *J.Neurophysiol.* 76, 4021-4030.

101. Sastry, P. S. and Rao, K. S. (2000). Apoptosis and the nervous system. *J.Neurochem.* 74, 1-20.

102. Haug, H., Knebel, G., Mecke, E., Orun, C., and Sass, N. L. (1981). The aging of cortical cytoarchitectonics in the light of stereological investigations. *Prog.Clin.Biol.Res.* 59B, 193-197.

103. Flood, D. and Coleman, P. (1987). Neuron numbers and sizes in aging brain: comparisons of human, monkey and rodent data. *Neurobiol Aging* 9, 453-63.

104. Simic, G., Bexheti, S., Kelovic, Z., Kos, M., Grbic, K., Hof, PR., and Kostovic, I. Hemispheric asymmetry, modular variability and age-related changes in the human entorhinal cortex. Neuroscience . 2004.

105. Alvarez, J. C., Diaz, C., Suarez, C., Fernandez, J. A., Gonzalez, d. R., Navarro, A., and Tolivia, J. (2000). Aging and the human vestibular nuclei: morphometric analysis. *Mech.Ageing Dev.* 114, 149-172.

106. Lopez, I., Honrubia, V., and Baloh, R. W. (1997). Aging and the human vestibular nucleus. *J.Vestib.Res.* 7, 77-85.

107. Tang, Y., Lopez, I., and Baloh, R. W. (2001). Age-related change of the neuronal number in the human medial vestibular nucleus: a stereological investigation. *J.Vestib.Res.* 11, 357-363.

108. Chen, S. and Hillman, D. E. (1999). Dying-back of Purkinje cell dendrites with synapse loss in aging rats. *J.Neurocytol.* 28, 187-196.

109. Fattoretti, P., Bertoni-Freddari, C., Caselli, U., Paoloni, R., and Meier-Ruge, W. (1998). Impaired succinic dehydrogenase activity of rat Purkinje cell mitochondria during aging. *Mech.Ageing Dev.* 101, 175-182.

110. Hadj-Sahraoui, N., Frederic, F., Zanjani, H., Herrup, K., Delhaye-Bouchaud, N., and Mariani, J. (1997). Purkinje cell loss in heterozygous staggerer mutant mice during aging. *Brain Res.Dev.Brain Res.* 98, 1-8.

111. Hall, T. C., Miller, A. K. H., and Corellis, J. A. N. Variations in the human Purkinje cell population according to age and sex. Neuropathol.appl.Neurobiol. 267-292. 1975.

112. Larsen, J. O., Skalicky, M., and Viidik, A. (2000). Does long-term physical exercise counteract age-related Purkinje cell loss? A stereological study of rat cerebellum. *J.Comp Neurol.* 428, 213-222.

113. Rutten, B. P., Korr, H., Steinbusch, H. W., and Schmitz, C. (2003). The aging brain: less neurons could be better. *Mech.Ageing Dev.* 124, 349-355.

114. Hajra, K. M. and Liu, J. R. (2004). Apoptosome dysfunction in human cancer. *Apoptosis.* 9, 691-704.

115. Seidman, M. D. (2000). Effects of dietary restriction and antioxidants on presbyacusis. *Laryngoscope* 110, 727-738.

116. Richter, E. (1980). Quantitative study of human Scarpa's ganglion and vestibular sensory epithelia. *Acta Otolaryngol.* 90, 199-208.

117. Rosenhall, U. (1973). Degenerative patterns in the aging human vestibular neuro-epithelia. *Acta Otolaryngol.* 76, 208-220.

118. Park, J. J., Tang, Y., Lopez, I., and Ishiyama, A. (2001). Age-related change in the number of neurons in the human vestibular ganglion. *J.Comp Neurol.* 431, 437-443.

119. Ito, M. Cerebellum and Neural Control. 1984. New York, Raven Press.

120. Wall, C., III, Black, F. O., and Hunt, A. E. (1984). Effects of age, sex and stimulus parameters upon vestibulo-ocular responses to sinusoidal rotation. *Acta Otolaryngol.* 98, 270-278.

121. Peterka, R. J., Black, F. O., and Schoenhoff, M. B. (1990). Age-related changes in human vestibulo-ocular reflexes: sinusoidal rotation and caloric tests. *J.Vestib.Res.* 1, 49-59.

122. Paige, G. D. (1992). Senescence of human visual-vestibular interactions. 1. Vestibulo-ocular reflex and adaptive plasticity with aging. *J.Vestib.Res.* 2, 133-151.

123. Peterka, R. J., Black, F. O., and Schoenhoff, M. B. (1990). Age-related changes in human vestibulo-ocular and optokinetic reflexes: pseudorandom rotation tests. *J.Vestib.Res.* 1, 61-71.

124. Paige, G. D. (1994). Senescence of human visual-vestibular interactions: smooth pursuit, optokinetic, and vestibular control of eye movements with aging. *Exp.Brain Res.* 98, 355-372.

125. Kim, J. S. and Sharpe, J. A. (2001). The vertical vestibulo-ocular reflex, and its interaction with vision during active head motion: effects of aging. *J.Vestib.Res.* 11, 3-12.

126. Yagi, T., Sekine, S., and Shimizu, M. (1983). Age-dependent changes in the gains of the vestibulo-ocular reflex in humans. *Adv.Otorhinolaryngol.* 30, 9-12.

127. Tian, J. R., Shubayev, I., Baloh, R. W., and Demer, J. L. (2001). Impairments in the initial horizontal vestibulo-ocular reflex of older humans. *Exp.Brain Res.* 137, 309-322.

128. Welgampola, M. S. and Colebatch, J. G. (2001). Vestibulocollic reflexes: normal values and the effect of age. *Clinical Neurophysiology* 112, 1971-1979.

129. Welgampola, M. S. and Colebatch, J. G. (2002). Selective effects of ageing on vestibular-dependent lower limb responses following galvanic stimulation. *Clinical Neurophysiology* 113, 528-534.

130. Kelders, W. P., Kleinrensink, G. J., van der Geest, J. N., Feenstra, L., de Zeeuw, C. I., and Frens, M. A. (2003). Compensatory increase of the cervico-ocular reflex with age in healthy humans. *J Physiol* 553, 311-317.

131. Remmel, R. S. (1984). An inexpensive eye movement monitor using the scleral search coil technique. *IEEE Trans.Biomed.Eng* 31, 388-390.

132. http://www.angelfire.com/scifi2/remmel.labs/monitor.html . 2006.

133. Straumann, D., Zee, D. S., and Solomon, D. (2000). Three-dimensional kinematics of ocular drift in humans with cerebellar atrophy. *J.Neurophysiol.* 83, 1125-1140.

134. Van Rijn, L. J., Van der, S. J., and Collewijn, H. (1994). Instability of ocular torsion during fixation: cyclovergence is more stable than cycloversion. *Vision Res.* 34, 1077-1087.

135. Hays, A. V., Richmond, B. J., and Optican, L. M. A UNIX-based multiple process system for real-time data acquisition and control. 2, 1-10. 1982. WESCON Conf Proc.

136. Haustein, W. (1989). Considerations on Listing's Law and the primary position by means of a matrix description of eye position control. *Biol.Cybern.* 60, 411-420.

137. Haslwanter, T. (1995). Mathematics of three-dimensional eye rotations. *Vision Res.* 35, 1727-1739.

138. Savitzky, A. and Golay, M. J. E. (1964). Smoothing and differentiation of data by simplified least squares procedures. *Anal.Chem.* 36, 1627-1639.

139. Hepp, K. (1990). On Listing's Law. *Commun.Math.Phys.* 132, 285-295.

140. Tweed, D., Sievering, D., Misslisch, H., Fetter, M., Zee, D., and Koenig, E. (1994). Rotational kinematics of the human vestibuloocular reflex. I. Gain matrices. *J.Neurophysiol.* 72, 2467-2479.

141. StatSoft, Inc. STATISTICA (data analysis software system). (6). 2003. StatSoft,Inc.

142. Hajioff, D., Barr-Hamilton, R. M., Colledge, N. R., Lewis, S. J., and Wilson, J. A. (2000). Re-evaluation of normative electronystagmography data in healthy ageing. *Clin.Otolaryngol.* 25, 249-252.

143. Hajioff, D., Barr-Hamilton, R. M., Colledge, N. R., Lewis, S. J., and Wilson, J. A. (2002). Is electronystagmography of diagnostic value in the elderly? *Clin.Otolaryngol.* 27, 27-31.

144. Goldberg, J. M., Smith, C. E., and Fernandez, C. (1984). Relation between discharge regularity and responses to externally applied galvanic currents in vestibular nerve afferents of the squirrel monkey. *J.Neurophysiol.* 51, 1236-1256.

145. Kleine, J. F. and Grusser, O. J. (1996). Responses of rat primary afferent vestibular neurons to galvanic polarization of the labyrinth. *Ann N.Y.Acad Sci* 781, 639-641.

146. Inglis, J. T., Shupert, C. L., Hlavacka, F., and Horak, F. B. (1995). Effect of galvanic vestibular stimulation on human postural responses during support surface translations. *J.Neurophysiol.* 73, 896-901.

147. Day, B. L., Severac, C. A., Bartolomei, L., Pastor, M. A., and Lyon, I. N. (1997). Human body-segment tilts induced by galvanic stimulation: a vestibularly driven balance protection mechanism. *J.Physiol* 500 (Pt 3), 661-672.

148. Zink, R., Steddin, S., Weiss, A., Brandt, T., and Dieterich, M. (1997). Galvanic vestibular stimulation in humans: effects on otolith function in roll. *Neurosci.Lett.* 232, 171-174.

149. Watson, S. R., Brizuela, A. E., Curthoys, I. S., Colebatch, J. G., MacDOUGALL, H. G., and Halmagyi, G. M. (1998). Maintained ocular torsion produced by bilateral and unilateral galvanic (DC) vestibular stimulation in humans. *Exp.Brain Res.* 122, 453-458.

150. Wardman, D. L. and Fitzpatrick, R. C. (2002). What does galvanic vestibular stimulation stimulate? *Adv.Exp.Med.Biol.* 508, 119-128.

151. Schneider, E., Glasauer, S., and Dieterich, M. (2002). Comparison of human ocular torsion patterns during natural and galvanic vestibular stimulation. *J.Neurophysiol.* 87, 2064-2073.

152. Brandt, T. and Dieterich, M. (1999). Does the vestibulo-ocular reflex use the same pathways for functions in roll and pitch planes? *Electroencephalogr.Clin.Neurophysiol.Suppl* 50, 221-225.

153. Dieterich M, B. T. (1992). Wallenberg's Syndrome:Lateropulsion, Cyclorotation, and Subjective Visual Vetical in Thirty-Six Patients. *Ann Neurol* 31, 399-408.

154. Dieterich M, B. T. (1993). Ocular torsion and tilt of subjective visual vertical are sensitive brainstem signs. *Ann Neurol* 33, 282-9.

155. Diamond, S. G. and Markham, C. H. (1983). Ocular counterrolling as an indicator of vestibular otolith function. *Neurology* 33, 1460-1469.

156. Jampel, R. S. and Shi, D. X. (2002). The absence of so-called compensatory ocular countertorsion: the response of the eyes to head tilt. *Arch.Ophthalmol.* 120, 1331-1340.

157. Whitney, S. L., Hudak, M. T., and Marchetti, G. F. (2000). The dynamic gait index relates to self-reported fall history in individuals with vestibular dysfunction. *J Vestib.Res.* 10, 99-105.

158. Herdman, S. J., Blatt, P., Schubert, M. C., and Tusa, R. J. (2000). Falls in patients with vestibular deficits. *Am.J.Otol.* 21, 847-851.

159. Di Fabio, R. P., Greany, J. F., Emasithi, A., and Wyman, J. F. (2002). Eye-head coordination during postural perturbation as a predictor of falls in community-dwelling elderly women. *Arch.Phys.Med.Rehabil.* 83, 942-951.

160. Kemmlert, K. and Lundholm, L. (2001). Slips, trips and falls in different work groups--with reference to age and from a preventive perspective. *Appl.Ergon.* 32, 149-153.

161. Thapa, P. B., Brockman, K. G., Gideon, P., Fought, R. L., and Ray, W. A. (1996). Injurious falls in nonambulatory nursing home residents: a comparative study of circumstances, incidence, and risk factors. *J Am.Geriatr Soc.* 44, 273-278.

162. Six, P. (1992). [Epidemiology of falls and hip fractures]. *Schweiz.Rundsch.Med.Prax.* 81, 1378-1382.

163. Tinetti, M. E., Doucette, J., Claus, E., and Marottoli, R. (1995). Risk factors for serious injury during falls by older persons in the community. *J Am.Geriatr.Soc.* 43, 1214-1221.

164. Kallin, K., Lundin-Olsson, L., Jensen, J., Nyberg, L., and Gustafson, Y. (2002). Predisposing and precipitating factors for falls among older people in residential care. *Public Health* 116, 263-271.

165. Ellis, A. A. and Trent, R. B. (2001). Do the risks and consequences of hospitalized fall injuries among older adults in California vary by type of fall? *J Gerontol.A Biol.Sci.Med.Sci.* 56, M686-M692.

166. Ghodsi, S. M., Roudsari, B. S., Abdollahi, M., and Shadman, M. (2003). Fall-related injuries in the elderly in Tehran. *Injury* 34, 809-814.

167. Liddle, J. and Gilleard, C. The emotional consequences of falls for patients and their families. Age Ageing 23 (suppl 4), 17. 1984.

168. Vetter, N. and Ford, D. Anxiety and depression scores in elderly fallers. Int J Geriatr Psychiatry 4, 158-63. 1989.

169. Topinková, E. and Neuwirth, J. Geriatrie pro praktického lékaře. 1995. Praha, Grada Publishing.

170. Ambler, Z. Neurologické poruchy ve vyšším věku. Základní principy jejich farmakoterapie. 2000. Praha, Triton.

171. Zee, DS. (1977). Disorders of Eye-Head Coordination. *In* "Eye Movements" (BA. Brooks and FJ. Bajandas, Eds.), pp. 9-39. Plenum Press, New York.

172. Vijayashankar, N. and Brody, H. (1977). A study of aging in the human abducens nucleus. *J.Comp Neurol.* 173, 433-438.

173. Vijayashankar, N. and Brody, H. (1977). Aging in the human brain stem. A study of the nucleus of the trochlear nerve. *Acta Anat.(Basel)* 99, 169-172.

174. Muhlendyck, H. (1979). [Age-dependent changes in transverse sections of muscle fibres from the exterior eye muscles in man]. *Z.Gerontol.* 12, 46-59.

175. Beynon, G. J., Jani, P., and Baguley, D. M. (1998). A clinical evaluation of head impulse testing. *Clin.Otolaryngol.* 23, 117-122.

176. Carey, J. P., Hirvonen, T. P., Peng, G. C., ella Santina, C. C., Haslwanter, T., and T.P. Minor. Changes in the Angular VOR After A Single Dose of Intratympanic Gentamicin for Méniére's Disease. (XXII Bárány Society Meeting). 2002. Seattle.

177. Carey, J. P., Minor, L. B., Peng, G. C., Della Santina, C. C., Cremer, P. D., and Haslwanter, T. (2002). Changes in the Three-Dimensional Angular Vestibulo-Ocular Reflex following Intratympanic Gentamicin for Meniere's Disease. *J.Assoc.Res.Otolaryngol.* 3, 430-443.

178. Halmagyi, G. M., Colebatch, J. G., and Curthoys, I. S. (1994). New tests of vestibular function. *Baillieres Clin.Neurol.* 3, 485-500.

179. Zumsteg, D. and Wieser, H. G. (2002). Effects of aging and sex on middle-latency somatosensory evoked potentials: normative data. *Clin.Neurophysiol.* 113, 681-685.

180. Attarian, S., Azulay, J. P., Boucraut, J., Escande, N., and Pouget, J. (2001). Terminal latency index and modified F ratio in distinction of chronic demyelinating neuropathies. *Clin.Neurophysiol.* 112, 457-463.

181. Capasso, M., Torrieri, F., Di Muzio, A., De Angelis, M. V., Lugaresi, A., and Uncini, A. (2002). Can electrophysiology differentiate polyneuropathy with anti-MAG/SGPG antibodies from chronic inflammatory demyelinating polyneuropathy? *Clin.Neurophysiol.* 113, 346-353.

182. Ebner, A., Dengler, R., and Meier, C. (1981). Peripheral and central conduction times in hereditary pressure- sensitive neuropathy. *J.Neurol.* 226, 85-99.

183. Koprdová (1998). Chronické zápalové (dysimúnne) demyelinizačné polyneuropatie (CIDP). *Čes.a Slov.Neurol.Neurochir.* 61/94, 331–339.

184. Poinoosawmy, D., Fontana, L., Wu, J. X., Fitzke, F. W., and Hitchings, R. A. (1997). Variation of nerve fibre layer thickness measurements with age and ethnicity by scanning laser polarimetry. *Br.J.Ophthalmol.* 81, 350-354.

185. Vite, C. H., McGowan, J. C., Braund, K. G., Drobatz, K. J., Glickson, J. D., Wolfe, J. H., and Haskins, M. E. (2001). Histopathology, electrodiagnostic testing, and magnetic resonance imaging show significant peripheral and central nervous system myelin abnormalities in the cat model of alpha-mannosidosis. *J.Neuropathol.Exp.Neurol.* 60, 817-828.

VII Attachment A

Head impulse detection default options

```
function options=getheaddetectdefaultoptions();
options.plotresults=1;
options.velthresh=100; % deg/s
options.relvelthresh=0; % relative threshold, if zero take absolute threshold
options.absvelthresh=30;% deg/s
options.timebeforeidheadmax=10;% ms
options.velmaxthresh=100;% deg/s
options.accthreshmin=-200;% deg/s^2;
options.accthreshmax=2000;% deg/s^2;
options.absveldiff=20;% deg/s
options.timevelmaxafterstart=30; % ms
options.filterheadacc=0; % Hz
options.timemaxafterstart=100; %ms
options.timevelwindow=options.timemaxafterstart; % this deactivates the option
options.headveloutlier=1.5; % times STD of other results
options.headvelsigndt=100; % ms
options.detectdirectionmethod=0; % 0: detect by maximum velocity 1: detect at
options.detectdirectiontime ms % option for computegammagain
options.detectdirectiontime=40; % 40 ms % option for computegammagain
options.correctforoffset=0; % 0: do not correct for eye velocity offset % option for
computegammagain
options.checkheadvelsign=1; % check for sign change
options.shifteyetohead=0; % shift eye by x ms
```

Head impulse selection

```
plotresults=3;
saveplots=1; % saves plots and closes them in case plotresult=1,3, else leaves plots open
ggtimes=[0 20 40 60 80];
domedian=1;
subgroups={'Jung','Alt'};

thefiles={'HPHOR.MAT';'HPTOR.MAT';'HPVER.MAT'};%;'HPRALP.MAT';'HPLARP.MAT'};
if strcmp(getenv('computername'),'ADMINISTRATOR'),
    basedir=['H:\Huberta\Kontrollen'];
else
    basedir=['L:\USERS\RBrzezny\BackUp_Siebold_disk\I\Backup_Coiling\Huberta\Kontrollen'];
end
directories={...
        {'Alt\Schwartz',65};...
        {'Alt\Schoedel',71};...
        {'Alt\Salfeld',81};...
        {'Alt\Fritzen',63};...
        {'Alt\ennes',51};...
        {'Alt\Büttner',57};... % only hor ralp larp
        {'Alt\Diermeier',39};...
        {'Alt\Egerle',55};...
        {'Alt\Jauer',63};...
        {'Alt\Kinzl',61};... % no -V data
        {'Alt\Koch',72};... % only a single good head impulse for VER+ with a quickphase (?)
        {'Alt\Konrad',72};... % no -V data
        {'Alt\KunertRudolf',62};... % no -V data
        %'Alt\Loew';... % bad calibration or big coilslip
        {'Alt\Loncar',63};...
        {'Alt\Mehltretter',71};...
        {'Alt\Muecke',44};...
        {'Alt\Oberhardt',70};...
        {'Alt\Tanriverdi',51};... % no -V data
        {'Alt\Weber',74};... % bad vertical head impulses
        {'Jung\Eggert',41};...
        {'Jung\Nedvidek',38};...
        {'Jung\Theil',35};...
        {'Jung\Häberle',25};...
        {'Jung\Mesko',26};...
        {'Jung\Golla',28};...
        {'Jung\Lindeiner',28};...
        {'Jung\Wassilowsky',29};...
        {'Jung\Gekeler',30};...
        {'Jung\Tchelidze',30};...
        {'Jung\Lehnen',25};...
        {'Jung\Finczicki',26};...
        {'Jung\KBartl',37};...
        {'Jung\Krell',23};...
        {'Jung\SBardins',29};...
        {'Jung\Strohmeyer',40};...
        {'Jung\Meitzner',33};...
        {'Jung\Steinbach',24};...
        {'Jung\Wiegner',45};...
};clear age
for i=1:size(directories,1),
    age(i)=directories{i}{2};
    directories{i}=directories{i}{1};
end
%newage=age(setdiff([1:22],[2 22]));
savefile='GYOXM';
doheaddetectcore

studyprefix='YO';
groupidx='Alt';
woffidx=[2,3,1];
doheaddetectsavesta
```

Head impulse detection core

```
subjects=[];
if ~exist('headimpoptions'),
    headimpoptions=getheaddetectdefaultoptions;
    headimpoptions.plotresults=plotresults;
    headimpoptions.velthresh=50; % deg/s
    headimpoptions.velmaxthresh=70; % deg/s
    headimpoptions.accthreshmin=-1000;% deg/s^2;
    headimpoptions.accthreshmax=1000;% deg/s^2;
    headimpoptions.timebeforeidheadmax=10;% ms
    headimpoptions.filterheadacc=0; % Hz
    headimpoptions.timevelmaxafterstart=20; % ms
    headimpoptions.timemaxafterstart=150; %ms
    headimpoptions.absveldiff=15;% deg/s
    headimpoptions.absvelthresh=20;% deg/s
    headimpoptions.headvelsigndt=100; % ms
    headimpoptions.correctforoffset=2; % correct for eye velocity offset ?
end
if ~exist('ggtimes'),
    firstgamma=10; % entspricht Gamma 30 (Aw et al.)
    anothergamma=40;
    secondgamma=60; %
    thirdgamma=80; % entspricht Gamma 100 (Aw et al.)
    ggtimes=[firstgamma anothergamma secondgamma thirdgamma];
end
if ~exist('domedian'),
    domedian=0;
end
if ~exist('subgroups'),
    subgroups={};
end
if ~exist('repmeas'),
    repmeas={};
end
gg=[];dd=[];gaa=[];lg=[];gaall=[];ggall=[];ddall=[];woall=[];lgall=[];

dirbuffer=directories;
if ~isempty(repmeas),
    if ~exist('repcount'),
        repcount=1;
    else
        repcount=repcount+1;
    end
    for i=1:size(directories,1),
        directories{i}=[directories{i} '\' repmeas{repcount}];
    end
    savebuf=savefile;
    savefile=[savefile repmeas{repcount}];
    subjects={};
end

if ((plotresults==1)|(plotresults==3)) & saveplots,
    close all
end
if plotresults==2,
    close all
    for i=1:size(subgroups,2),
        figure
    end
end

nd=size(directories,1);
for i=1:nd,
    subjects=strvcat(subjects,dirbuffer{i});
    ggres=[];dres=[];wres=[];gares=[];lres=[];
    for j=1:size(thefiles,1),
        filename=fullfile(basedir,directories{i},thefiles{j});
        disp(filename)
        plotinfigure=0;
        if ~isempty(subgroups),
            for k=1:size(subgroups,2),
                if ~isempty(findstr(subgroups{k},filename)),
                    plotinfigure=k;
                end
            end
        end
        if saveplots,
```

```
[gr,dr,ga,lag,woff]=computegammagain(filename,ggtimes,plotresults,plotinfigure,j,headimpoption
s);
        else

[gr,dr,ga,lag,woff]=computegammagain(filename,ggtimes,plotresults,plotinfigure,saveplots,headi
mpoptions);
        end
        if ~isempty(gr),
            ggres=[ggres; gr];
            dres=[dres; dr];
            gares=[gares; ga];
            wres=[wres; j woff];
            lres=[lres; lag];
            if (plotresults==1) & saveplots,
                [plotpath plotfname]=fileparts(filename);
                for k=1:numel(get(0,'Children')),
                    plotfilename=fullfile(plotpath,[plotfname int2str(k) 'X.fig']);
                    saveas(k,plotfilename,'fig')
                end
                close all
            end
        else
            wres=[wres; j NaN NaN NaN];
        end
    end;
    % compute means
    ggbi=getmeans(i,ggres,ggtimes,domedian);
    dbi=getmeans(i,dres,ggtimes,domedian);
    gabi=getmeans(i,gares,ggtimes,domedian);
    lgbi=getmeans(i,lres,0,domedian);
    wres=[repmat(i,size(wres,1),1) wres];
    gg=[gg;ggbi];
    dd=[dd;dbi];
    gaa=[gaa;gabi];
    lg=[lg;lgbi];
    woall=[woall; wres];
    lgall=[lgall; [repmat(3,size(lres,1),1) lres]];
    ggall=[ggall; [repmat(3,size(ggres,1),1) ggres]];
    ddall=[ddall; [repmat(3,size(dres,1),1) dres]];
    gaall=[gaall; [repmat(3,size(gares,1),1) gares]];
end;
varnames=['TOR+';'TOR-';'RA  ';'LP  ';'VER+';'VER-';'LA  ';'RP  ';'HOR+';'HOR-'];
for i=1:numel(ggtimes),
    ggsubject=reshape(gg(:,2+i)',10,nd)';
    ddsubject=reshape(dd(:,2+i)',10,nd)';
    gasubject=reshape(gaa(:,2+i)',10,nd)';
    if ~isempty(savefile),
        tblwrite(ggsubject,varnames,subjects,fullfile(basedir,[savefile int2str(ggtimes(i))
'.TXT']),'\t')
        tblwrite(ddsubject,varnames,subjects,fullfile(basedir,[savefile int2str(ggtimes(i))
'D.TXT']),'\t')
        tblwrite(gasubject,varnames,subjects,fullfile(basedir,[savefile int2str(ggtimes(i))
'G.TXT']),'\t')
    end
end;
tblwrite(reshape(lg(:,3)',10,nd)',varnames,subjects,fullfile(basedir,[savefile 'L.TXT']),'\t')

if ~isempty(savefile),
    save(fullfile(basedir,[savefile
'.mat']),'gg','dd','gaa','lg','ggall','ddall','gaall','lgall','woall','ggtimes','subjects');
end
ggall=[];
ddall=[];
gaall=[];
lgall=[];
if size(subjects,1)==1,
    for i=1:10,
        ggall(i,:)=gg(find(gg(:,2)==i),3:end-1);
        ddall(i,:)=dd(find(dd(:,2)==i),3:end-1);
        gaall(i,:)=gaa(find(gaa(:,2)==i),3:end-1);
        lgall(i,:)=lg(find(lg(:,2)==i),3:end-1);
    end
else
    for i=1:10,
        ggall(i,:)=nanmean(gg(find(gg(:,2)==i),3:end-1));
        ddall(i,:)=nanmean(dd(find(dd(:,2)==i),3:end-1));
        gaall(i,:)=nanmean(gaa(find(gaa(:,2)==i),3:end-1));
```

```
        lgall(i,:)=nanmean(lg(find(lg(:,2)==i),3:end-1));
    end
end
if ~isempty(savefile),
    rownames={};
    for i=1:numel(ggtimes),
        rownames=strvcat(rownames,int2str(ggtimes(i)));
    end
    tblwrite(ggall',varnames,rownames,fullfile(basedir,[savefile 'ALL.TXT']),'\t')
    tblwrite(ddall',varnames,rownames,fullfile(basedir,[savefile 'DALL.TXT']),'\t')
    tblwrite(gaall',varnames,rownames,fullfile(basedir,[savefile 'GALL.TXT']),'\t')
    tblwrite(lgall',varnames,'LAG',fullfile(basedir,[savefile 'LALL.TXT']),'\t')
end

if plotresults==2,
    for i=1:size(subgroups,2),
        figure(i)
        subplot(2,2,1)
        title('downward')
        subplot(2,2,2)
        title('upward')
        for j=1:2,
            subplot(2,2,j)
            xlim([-20 80])
            ylim([-400 400])
            xlabel('time (ms)')
            ylabel('velocity (deg/s)')
            hold off
        end
        for j=3:4,
            subplot(2,2,j)
            xlabel('horizontal (deg/s)')
            ylabel('vertical (deg/s)')
            xlim([-400 400])
            ylim([-400 400])
            hold off
        end
    end
end

if ~isempty(repmeas),
    directories=dirbuffer;
    savefile=savebuf;
    ggr{repcount}=gg;
    ddr{repcount}=dd;
    gar{repcount}=gaa;
    lgr{repcount}=lg;
    wor{repcount}=woall;
    if repcount<size(repmeas,1),
        doheaddetectcore
    else
        clear repcount
    end
end
```

Head impulse detection

```
function
[MarkerArray,idheadimp,idheadstart]=detectheadimp(Data,headvelchan,eyevelchan,options,headvel3
dchan);
% function
[MarkerArray,idheadimp,idheadstart]=detectheadimp(Data,headvelchan,eyevelchan,options,headvel3
dchan);
% headvelchan=strmatch('LeftEyeVel',DataNames,'exact');
%plotresults=0;
if nargin<3,
    error('MATLAB:badopt','DETECTHEDIMP: Not enough input arguments');
end
% if nargin>4,
%     error('MATLAB:badopt','DETECTHEDIMP: Calling arguments');
% end
if nargin<4,
    options=getheaddetectdefaultoptions;
elseif isempty(options),
    options=getheaddetectdefaultoptions;
end
if nargin<5,
    headvel3dchan=[];
end

firstX=-50;
lastX=100;
headvel=Data(:,headvelchan);
eyevel=Data(:,eyevelchan);
headacc=diff3(headvel)*1000;
if options.filterheadacc>0,
    headacc=filtgauss(headacc,1000,options.filterheadacc);
end
% find regions with velocity>velthresh
idx=find(headvel>options.velthresh);
% find start of regions
idxb=[1; find(diff(idx)-1); length(idx)];
idheadimp=[];
MarkerArray=[];
for i=1:length(idxb)-1,
    % construct index of head impulse region
    idxt=[idx(idxb(i)+1):idx(idxb(i+1))];   %idxtn=[idx(idxb(i)):idx(idxb(i)+1)];
    if idxt>20, % end of first interval before 20 ms,
        % get maximum velocity
        [index.maxvel(i),idvelmax]=max(headvel(idxt));
        % get lower threshold
        if options.relvelthresh==0
            lowvel=options.absvelthresh;
        else
            lowvel=options.relvelthresh*index.maxvel(i);
        end
        index.idheadmax(i)=idxt(idvelmax);
        % go down the hill until velocity falls below lower threshold
        j=idxt(1);
        while (j>1)&(headvel(j)>lowvel),
            j=j-1;
        end;
        % remember all that
        idthisone=[j:index.idheadmax(i)];
        idheadimp=[idheadimp,idthisone];
        index.idheadstart(i)=j;
        % get maximum velocity within window from start to options.timevelwindow
        idthisone=[j:j+options.timevelwindow];
        index.maxheadvelinwindow(i)=max(headvel(idthisone));
        % get acceleration minima and maxima from 30ms before start to maximum head velocity
        % default timebeforeidheadmax=10
        if j>30,
            idthisone=[j-30:index.idheadmax(i)-options.timebeforeidheadmax];
        else
            idthisone=[1:index.idheadmax(i)-options.timebeforeidheadmax];
        end
        % alternative would be : get acceleration minima and maxima from 30ms before start to
30 ms after
        % idthisone=[j-30:j+30];
        [index.maxacc(i),idaccmax]=max(headacc(idthisone));
        index.idheadacc(i)=idthisone(idaccmax);
        [index.minacc(i),idaccmin]=min(headacc(idthisone));
        index.idheadaccmin(i)=idthisone(idaccmin);
```

```
        % get max. absolute difference of eye and head velocity 50 ms before start
        if j>50,
            idthisone=[j-50:j];
        else
            idthisone=[1:j];
        end
        [index.eyemax(i),ideyemax]=max(abs(eyevel(idthisone)-headvel(idthisone)));
        % get max. head velocity 50 ms before start
        [index.headmaxbefore(i),idheadmaxbefore]=max(headvel(idthisone));
        if ~isempty(headvel3dchan),
            idthisone=index.idheadstart(i)+[0:options.headvelsigndt];
            if idthisone(end)>size(Data,1),
                idthisone=[index.idheadstart(i):size(Data,1)];
            end
            % get max head velocity channel
            [h,im]=max(max(abs(Data(idthisone,headvel3dchan))));
            % get sign change in the maximal component

index.headvelsign(i)=sign(max(Data(idthisone,headvel3dchan(im)))*min(Data(idthisone,headvel3dc
han(im))));
        else
            index.headvelsign(i)=1;
        end
    end;
end;
index.idxnum=numel(index.idheadstart);
reason{numel(index.idxnum)}='initialcount';
% throw away first pulse if it starts earlier than 30 ms after start of
% data
if index.idheadstart(1)<30,
    idx1=2:numel(index.idheadacc);
    index=reindex(index,idx1);
    reason{numel(index.idxnum)}='firststartsearly';
end
% find all impulses with maximum within 100 ms
idx1=find(index.idheadmax-index.idheadstart<options.timemaxafterstart);
index=reindex(index,idx1);
reason{numel(index.idxnum)}='timemaxafterstart';
% find all impulses with maximum AFTER 30 ms
idx1=find(index.idheadmax-index.idheadstart>options.timevelmaxafterstart);
index=reindex(index,idx1);
reason{numel(index.idxnum)}='timevelmaxafterstart';
% find all impulses with maximum larger than 100 deg/s
% default: velmaxthresh=100;
idx1=find(index.maxvel>options.velmaxthresh);
index=reindex(index,idx1);
reason{numel(index.idxnum)}='velmaxthresh';
% find all impulses with maximum in window larger than 100 deg/s
% default: velmaxthresh=100; to deactivate this option, set
options.timevelwindow=options.timemaxafterstart
idx1=find(index.maxheadvelinwindow>options.velmaxthresh);
index=reindex(index,idx1);
reason{numel(index.idxnum)}='timevelwindow';
% find all impulses with max. acceleration>accthreshmax and min. acceleration>accthreshmin
% default accthreshmax=2000;
% default accthreshmin=-200;
idx1=find((index.maxacc>options.accthreshmax)&(index.minacc>options.accthreshmin));
index=reindex(index,idx1);
reason{numel(index.idxnum)}='accthreshmax-min';
% find impulses with head velocity before start smaller than options.absvelthresh;
idx1=find(index.headmaxbefore<=options.absvelthresh);
index=reindex(index,idx1);
reason{numel(index.idxnum)}='absvelthresh';
% find all impulses with max. abs(eye-head) velocity< absveldiff
% default: absveldiff=20;
idx1=find(index.eyemax<options.absveldiff);
index=reindex(index,idx1);
reason{numel(index.idxnum)}='absveldiff';
% find all impulses with maxvel not being an outlier
if ~isempty(index.maxvel),
    idx1=find(abs(median(index.maxvel)-
index.maxvel)<=options.headveloutlier*iqr(index.maxvel));
    index=reindex(index,idx1);
    reason{numel(index.idxnum)}='headveloutlier';
    % find all head impulses where head velocity does not change sign
    if ~isempty(headvel3dchan) & options.checkheadvelsign,
        idx1=find(index.headvelsign>0);
        index=reindex(index,idx1);
```

```
        reason{numel(index.idxnum)}='checkheadvelsign';
    end
    for i=1:numel(index.idxnum),
        disp([num2str(index.idxnum(i)) ': ' reason{i}]);
    end
    %disp(index.idxnum)

    idheadimp=[];
    for i=1:numel(index.idheadstart),
        MarkerArray(i*2-1,1)=headvelchan;
        MarkerArray(i*2-1,2)=index.idheadstart(i);
        MarkerArray(i*2-1,3)=headvel(index.idheadstart(i));
        MarkerArray(i*2-1,4)=headvel(index.idheadstart(i));
        MarkerArray(i*2,1)=headvelchan;
        MarkerArray(i*2,2)=index.idheadmax(i);
        MarkerArray(i*2,3)=index.maxvel(i);
        MarkerArray(i*2,4)=index.maxvel(i);
        idheadimp=[idheadimp,[index.idheadstart(i):index.idheadmax(i)]];
    end;
    idheadstart=index.idheadstart;
    if options.plotresults==1,
        %     nplot=4;
        %     subplot(nplot,1,1);
        subplot(3,1,1)
        plot([1:numel(headvel)]/1000,headvel,idheadimp/1000,headvel(idheadimp),'.r');
        refline(0,options.velthresh)
        refline(0,options.velmaxthresh)
        xlabel('time (s)')
        ylabel('head velocity (deg/s)')
        %subplot(nplot,1,2);
        subplot(3,2,3)
        if isempty(index.idheadstart),
            h=[];
        else
            h=repmat(index.idheadstart,lastX-
firstX+1,1)+repmat([firstX:lastX]',1,numel(index.idheadstart));
            h(find(h<1))=1;
            plot(firstX:lastX,headvel(h),index.idheadmax-
index.idheadstart,headvel(index.idheadmax),'ro');
        end
        xlabel('time (ms)')
        ylabel('head velocity (deg/s)')
        subplot(3,2,5)
        if ~isempty(index.idheadstart),
            plot(firstX:lastX,eyevel(h));
        end
        xlabel('time (ms)')
        ylabel('eye velocity (deg/s)')
        %subplot(nplot,1,3);
        subplot(3,2,4)
        if ~isempty(index.idheadstart),
            plot(firstX:lastX,headvel(h)./repmat(index.maxvel,lastX-firstX+1,1));
        end
        xlabel('time (ms)')
        ylabel('head velocity (%)')
        %subplot(nplot,1,4);
        %     h=repmat(idheadacc,lastX-firstX+1,1)+repmat([firstX:lastX]'-
30,1,numel(idheadacc));
        %     plot([firstX:lastX]-30,headvel(h));
        subplot(3,2,6)
        if ~isempty(index.idheadstart),
            plot(firstX:lastX,headacc(h));
        end
        refline(0,options.accthreshmax)
        refline(0,options.accthreshmin)
        xlabel('time (ms)')
        ylabel('head acceleration (deg/s^2)')
        % reset to first plot
        subplot(3,1,1)
    end
else % no valid data found
    for i=1:numel(index.idxnum),
        disp([num2str(index.idxnum(i)) ': ' reason{i}]);
    end
    MarkerArray=[];
    idheadimp=[];
    idheadstart=[];
end
```

```
% load(filename);
% save(filename,'DataNames','DataUnits','SamplingRate','Data','MarkerArray',...
%     'EventMatrix','Comment','Diagnosis','Start_Time','Date',...
%     'AcquisitionProgram','Subject','Examinator','RecordingDevice',...
%     'OriginalFile','FilterFrequency','StartTime');
return

function index=reindex(index,idx1);
index.idheadacc=index.idheadacc(idx1);
index.idheadaccmin=index.idheadaccmin(idx1);
index.idheadstart=index.idheadstart(idx1);
index.idheadmax=index.idheadmax(idx1);
index.maxvel=index.maxvel(idx1);
index.maxacc=index.maxacc(idx1);
index.minacc=index.minacc(idx1);
index.eyemax=index.eyemax(idx1);
index.headvelsign=index.headvelsign(idx1);
index.headmaxbefore=index.headmaxbefore(idx1);
index.maxheadvelinwindow=index.maxheadvelinwindow(idx1);
index.idxnum=[index.idxnum numel(index.idheadstart)];
return
```

Gamma gain computation

```
function
[ggres,dres,gares,lag,woffset]=computegammagain(filename,ggarray,plotresults,plotinfigure,save
plots,options);
% function
%
[ggres,dres,gares,woffset]=computegammagain(filename,ggarray,plotresults,plotinfigure,saveplot
s,options);
% compute gamma gains, misalignment angles, and gain for one file containing head impulses
% ggarray gives time in ms after onset for gamma gain computation
% plotresults=1: do the plots
% plotresults=0: do no plots
% saveplots=0: do not save plot
% direction of head impulse is detected automatically

if nargin<4,
    plotinfigure=0;
end
if nargin<5,
    saveplots=0;
end

if exist(filename,'file'),
    load(filename)
else
    ggres=[];dres=[];gares=[];woffset=[];lag=[];
    return
end
% get channels
cnames={'LeftEyeTor';... %head in space position
 'LeftEyeHor';... %head in space position
 'LeftEyeVer';... %head in space position
 'EyeVelX';... %eye in head vel
 'EyeVelY';... %eye in head vel
 'EyeVelZ';... %eye in head vel
 'LeftEyeVelX';... %head in space vel
 'LeftEyeVelY';... %head in space vel
 'LeftEyeVelZ'}; %head in space vel
for i=1:size(cnames,1),
    Ch_Array(i) = strmatch(cnames{i},DataNames,'exact');
end
% generate scalar component for head velocity
whs=[zeros(size(Data,1),1) Data(:,Ch_Array(7):Ch_Array(9))];
% transform to head coordinates
whh=quatm(invquat([Data(:,Ch_Array(1)) Data(:,Ch_Array(3))
Data(:,Ch_Array(2))]),quatm(whs,[Data(:,Ch_Array(1)) Data(:,Ch_Array(3))
Data(:,Ch_Array(2))]));
clear whs
% throw away scalar component
whh=whh(:,2:4);
if options.shifteyetohead~=0,
    Data(:,Ch_Array(4:6))=circshift(Data(:,Ch_Array(4:6)),options.shifteyetohead);
end
% get eye in head velocity
weh=Data(:,Ch_Array(4):Ch_Array(6));
% get qc for canal transform, ruft m-file canalcoord auf
canalcoord;
% transform to canal coordinates
whc=quatprod(invquat(qc),quatprod([zeros(size(whh,1),1) whh],qc));
wec=quatprod(invquat(qc),quatprod([zeros(size(weh,1),1) weh],qc));
% throw away scalar component
whc=whc(:,2:4);
wec=wec(:,2:4);

% compute gamma gain
[gg,ga]=gammagain(whh,weh);
delta=acos(gg./ga)*180/pi;

if plotresults==1,
    figure
end
[MarkerArray,idheadimp,idheadstart]=detectheadimp(Data,strmatch('LeftEyeVel',DataNames,'exact'
),strmatch('RightEyeVel',DataNames,'exact'),options,[Ch_Array(7):Ch_Array(9)]);
if plotresults==1,
    title(filename)
end
```

```
firstX=-20;
lastX=80;
ggres=[];dres=[];gares=[];lag=[];woffset=[];
if ~isempty(idheadstart),
    idx100=repmat(idheadstart,lastX-firstX,1)+repmat([firstX:lastX-1]',1,numel(idheadstart));

    if options.correctforoffset>0, % correct for eye velocity offsets prior to head impulse
        if options.correctforoffset==1,
            wehhh=weh(idx100(1:10,:),:)-whh(idx100(1:10,:),:); % difference between eye and
head velocity from 20 to 10 ms before start
            woffset=median(wehhh); % median value of eye velocity offset
            disp(['Offset : ' num2str(woffset)]);
            weh=weh-repmat(woffset,size(weh,1),1); % offset-free eye velocity
        else
            idxvel0=find(Data(:,strmatch('LeftEyeVel',DataNames,'exact'))<5); % head moves
less than 5 deg/s
            woffset=median(weh(idxvel0,:));
            disp(['Offset : ' num2str(woffset)]);
            weh=weh-repmat(woffset,size(weh,1),1); % offset-free eye velocity
        end
        % recompute gamma gain with new values
        [gg,ga]=gammagain(whh,weh);
        delta=acos(gg./ga)*180/pi;
    else
        woffset=[0 0 0];
    end

    % ggres=zeros(numel(idheadstart),1+numel(ggarray));
    for i=1:numel(idheadstart),
        % wrong !!! 25.11.02 SG
        % idthisone=[idheadstart(i)-firstX:idheadstart(i)+lastX];
        idthisone=idx100(:,i); % same as:
idthisone=[idheadstart(i)+firstX:idheadstart(i)+lastX-1];
        idthisone=idthisone(find(idthisone>0)); % check that all are above zero
        % get minima and maxima
        whminmax=[abs(max(whh(idthisone,:)));...
                abs(min(whh(idthisone,:)));...
                abs(max(whc(idthisone,:)));...
                abs(min(whc(idthisone,:)))];
        % alternative: get vector at 40 ms
        whminmaxa=[whh(idthisone(options.detectdirectiontime-firstX),:);...
                -whh(idthisone(options.detectdirectiontime-firstX),:);...
                whc(idthisone(options.detectdirectiontime-firstX),:);...
                -whc(idthisone(options.detectdirectiontime-firstX),:)];

        % get maximum of these to see which impulse was given
        if options.detectdirectionmethod==1
            [m,ggres(i,1)]=max(whminmaxa(:));
        else
            [m,ggres(i,1)]=max(whminmax(:));
        end
        dres(i,1)=ggres(i,1);
        gares(i,1)=ggres(i,1);

        lag(i,1)=ggres(i,1);
        switch lag(i,1),
            case {5,6}
                [c,lags]=crosscorr(Data(idthisone,strmatch('LeftEyeVer',DataNames,'exact')),-
Data(idthisone,strmatch('EyeVer',DataNames,'exact')),20:61);
            case {1,2}
                [c,lags]=crosscorr(Data(idthisone,strmatch('LeftEyeTor',DataNames,'exact')),-
Data(idthisone,strmatch('EyeTor',DataNames,'exact')),20:61);
            case {9,10,11,12}
                [c,lags]=crosscorr(Data(idthisone,strmatch('LeftEyeHor',DataNames,'exact')),-
Data(idthisone,strmatch('EyeHor',DataNames,'exact')),20:61);
            otherwise
                c=[];lags=[];
        end
        if ~isempty(c),
            c=c(find(abs(lags)<15));
            lags=lags(find(abs(lags)<15));
            [mx,cx]=max(c);
            lag(i,2)=lags(cx);
            %plot(lags,c,lags(cx),mx,'o'),hold on
        else
            lag(i,2)=NaN;
        end
%       next lines are run below in vectorized code
```

```
%         for j=1:numel(ggarray),
%             % wrong !!! 25.11.02 SG
%             % ggres(i,1+j)=gg(idheadstart(i)-firstX+ggarray(j));
%             ggres(i,1+j)=gg(idheadstart(i)+ggarray(j));
%         end

        %     1:torpos
        %     2:torneg
        %     3:RA
        %     4:LP
        %     5:verpos
        %     6:verneg
        %     7:LA
        %     8:RP
        %     9,11:horpos
        %     10,12:horneg
    end
    if numel(idheadstart)==1,
        ggres=[ggres
gg(repmat(idheadstart,1,numel(ggarray))+repmat(ggarray,numel(idheadstart),1))'];
        dres=[dres
delta(repmat(idheadstart,1,numel(ggarray))+repmat(ggarray,numel(idheadstart),1))'];
        gares=[gares
ga(repmat(idheadstart,1,numel(ggarray))+repmat(ggarray,numel(idheadstart),1))'];
    else
        ggres=[ggres
gg(repmat(idheadstart',1,numel(ggarray))+repmat(ggarray,numel(idheadstart),1))];
        dres=[dres
delta(repmat(idheadstart',1,numel(ggarray))+repmat(ggarray,numel(idheadstart),1))];
        gares=[gares
ga(repmat(idheadstart',1,numel(ggarray))+repmat(ggarray,numel(idheadstart),1))];
    end

    titles={'TOR','VER','HOR','RALP','LARP'};
    nums=[numel(find((ggres(:,1)==1)|(ggres(:,1)==2))) ...
            numel(find((ggres(:,1)==5)|(ggres(:,1)==6))) ...
            numel(find((ggres(:,1)>=9)&(ggres(:,1)<=12))) ...
            numel(find((ggres(:,1)==3)|(ggres(:,1)==4))) ...
            numel(find((ggres(:,1)==7)|(ggres(:,1)==8))) ...
        ];
    [m,i]=max(nums); % maximum in this plane
    if i<4, % tor ver hor
        wh=whh(:,i);
        we=weh(:,i);
    else % RALP LARP
        wh=whc(:,i-3);
        we=wec(:,i-3);
    end

    if plotresults==1,
        % make sure no index is below zero!
        idx100(find(idx100<=0))=1;
        figure
        subplot(2,2,1)
        plot(firstX:lastX-1,gg(idx100))
        xlabel('time (ms)')
        ylabel('gamma gain')
        xlim([firstX lastX-1])
        ylim([-0.25 1.25])
        title(titles{i})
        for j=1:numel(ggarray),
            line([ggarray(j) ggarray(j)],[-0.25 1.25]);
        end
        refline(0)
        refline(0,1)
        subplot(2,2,2)
        plot(firstX:lastX-1,delta(idx100))
        xlabel('time (ms)')
        ylabel('misaligment (deg)')
        xlim([firstX lastX-1])
        ylim([0 45])
        for j=1:numel(ggarray),
            line([ggarray(j) ggarray(j)],[0 45]);
        end
        refline(0)
        subplot(2,2,3)
        plot(wh(idx100),we(idx100),'.')
        xlabel('head (deg/s)')
```

```
        ylabel('eye (deg/s)')
        refline(-1)
        refline(0)
        subplot(4,2,6)
        plot(firstX:lastX-1,wh(idx100))
        xlabel('time (ms)')
        ylabel('head (deg/s)')
        xlim([firstX lastX-1])
        refline(0)
        subplot(4,2,8)
        plot(firstX:lastX-1,we(idx100))
        xlabel('time (ms)')
        ylabel('eye (deg/s)')
        xlim([firstX lastX-1])
        refline(0)
    elseif (plotresults==2)&(plotinfigure~=0),
        idx100(find(idx100<=0))=1;
        figure(plotinfigure)
        whh(idx100(end,:),:)=NaN;
        weh(idx100(end,:),:)=NaN;
        idvertdn=find(ggres(:,1)==5);
        idvertup=find(ggres(:,1)==6);
        if ~isempty(idvertdn),
            subplot(2,2,3)
            whp=whh(idx100(:,idvertdn),:);
            wep=weh(idx100(:,idvertdn),:);
            plot(whp(:,3),whp(:,2),'-b',wep(:,3),wep(:,2),'-r');
            hold on
            subplot(2,2,1)
            whp=reshape(whh(idx100(:,idvertdn),2),[],numel(idvertdn));
            wep=reshape(weh(idx100(:,idvertdn),2),[],numel(idvertdn));;
            plot(firstX:lastX-1,whp,'-b',firstX:lastX-1,wep,'-r');
            hold on
        end
        if ~isempty(idvertup),
            subplot(2,2,4)
            whp=whh(idx100(:,idvertup),:);
            wep=weh(idx100(:,idvertup),:);
            plot(whp(:,3),whp(:,2),'-b',wep(:,3),wep(:,2),'-r');
            hold on
            subplot(2,2,2)
            whp=reshape(whh(idx100(:,idvertup),2),[],numel(idvertup));
            wep=reshape(weh(idx100(:,idvertup),2),[],numel(idvertup));;
            plot(firstX:lastX-1,whp,'-b',firstX:lastX-1,wep,'-r');
            hold on
        end
    elseif (plotresults==3),
        idx100(find(idx100<=0))=1;
        whh(idx100(end,:),:)=NaN;
        weh(idx100(end,:),:)=NaN;
        gg(idx100(end,:),:)=NaN;
        idvertdn=find(ggres(:,1)==5);
        idvertup=find(ggres(:,1)==6);
        idvertle=find((ggres(:,1)==9)|(ggres(:,1)==11));
        idvertri=find((ggres(:,1)==10)|(ggres(:,1)==12));
        idverttop=find(ggres(:,1)==1);
        idvertton=find(ggres(:,1)==2);
        idvertra=find(ggres(:,1)==3);
        idvertlp=find(ggres(:,1)==4);
        idvertla=find(ggres(:,1)==7);
        idvertrp=find(ggres(:,1)==8);
        if ~isempty([idvertdn; idvertup]),
            figure
            if ~isempty(idvertup),
                subplot(3,2,5)
                whp=whh(idx100(:,idvertup),:);
                wep=weh(idx100(:,idvertup),:);
                plot(whp(:,3),whp(:,2),'-b',wep(:,3),wep(:,2),'-r');
                subplot(3,2,1)
                whp=reshape(whh(idx100(:,idvertup),2),[],numel(idvertup));
                wep=reshape(weh(idx100(:,idvertup),2),[],numel(idvertup));;
                plot(firstX:lastX-1,whp,'-b',firstX:lastX-1,wep,'-r');
                subplot(3,2,3)
                ggp=reshape(gg(idx100(:,idvertup)),[],numel(idvertup));
                plot(firstX:lastX-1,ggp,'-k');
            end
            if ~isempty(idvertdn),
                subplot(3,2,6)
```

```
            whp=whh(idx100(:,idvertdn),:);
            wep=weh(idx100(:,idvertdn),:);
            plot(whp(:,3),whp(:,2),'-b',wep(:,3),wep(:,2),'-r');
            subplot(3,2,2)
            whp=reshape(whh(idx100(:,idvertdn),2),[],numel(idvertdn));
            wep=reshape(weh(idx100(:,idvertdn),2),[],numel(idvertdn));;
            plot(firstX:lastX-1,whp,'-b',firstX:lastX-1,wep,'-r');
            subplot(3,2,4)
            ggp=reshape(gg(idx100(:,idvertdn)),[],numel(idvertdn));
            plot(firstX:lastX-1,ggp,'-k');
        end
        for j=1:2,
            subplot(3,2,j)
            xlim([-20 80])
            ylim([-400 400])
            xlabel('time (ms)')
            ylabel('velocity (deg/s)')
            h=refline(0,0);set(h,'linestyle','--','Color',[0 0 0]);
            hold off
        end
        for j=3:4,
            subplot(3,2,j)
            xlim([-20 80])
            ylim([-0.1 1.4])
            xlabel('time (ms)')
            ylabel('\gamma-gain')
            h=refline(0,1);set(h,'linestyle','--','Color',[0 0 0]);
            h=refline(0,0);set(h,'linestyle','--','Color',[0 0 0]);
            hold off
        end
        for j=5:6,
            subplot(3,2,j)
            xlabel('horizontal (deg/s)')
            ylabel('vertical (deg/s)')
            xlim([-400 400])
            ylim([-400 400])
            hold off
        end
        subplot(3,2,1)
        title('upward')
        subplot(3,2,2)
        title('downward')
        fpos=get(gcf,'Position');
        set(gcf,'Name',filename,'Position',[fpos(1) fpos(2)-fpos(4) fpos(3) 2*fpos(4)]);
        if saveplots>0,
            [plotpath plotfname]=fileparts(filename);
            plotfilename=fullfile(plotpath,['HPVERT' int2str(saveplots) '.fig']);
            saveas(gcf,plotfilename,'fig')
            close(gcf);
        end
    end
    if ~isempty([idverttop; idvertton]),
        figure
        if ~isempty(idverttop),
            subplot(3,2,5)
            whp=whh(idx100(:,idverttop),:);
            wep=weh(idx100(:,idverttop),:);
            plot(whp(:,1),whp(:,2),'-b',wep(:,1),wep(:,2),'-r');
            subplot(3,2,1)
            whp=reshape(whh(idx100(:,idverttop),1),[],numel(idverttop));
            wep=reshape(weh(idx100(:,idverttop),1),[],numel(idverttop));;
            plot(firstX:lastX-1,whp,'-b',firstX:lastX-1,wep,'-r');
            subplot(3,2,3)
            ggp=reshape(gg(idx100(:,idverttop)),[],numel(idverttop));
            plot(firstX:lastX-1,ggp,'-k');
        end
        if ~isempty(idvertton),
            subplot(3,2,6)
            whp=whh(idx100(:,idvertton),:);
            wep=weh(idx100(:,idvertton),:);
            plot(whp(:,1),whp(:,2),'-b',wep(:,1),wep(:,2),'-r');
            subplot(3,2,2)
            whp=reshape(whh(idx100(:,idvertton),1),[],numel(idvertton));
            wep=reshape(weh(idx100(:,idvertton),1),[],numel(idvertton));;
            plot(firstX:lastX-1,whp,'-b',firstX:lastX-1,wep,'-r');
            subplot(3,2,4)
            ggp=reshape(gg(idx100(:,idvertton)),[],numel(idvertton));
            plot(firstX:lastX-1,ggp,'-k');
```

```
        end
        for j=1:2,
            subplot(3,2,j)
            xlim([-20 80])
            ylim([-400 400])
            xlabel('time (ms)')
            ylabel('velocity (deg/s)')
            h=refline(0,0);set(h,'linestyle','--','Color',[0 0 0]);
            hold off
        end
        for j=3:4,
            subplot(3,2,j)
            xlim([-20 80])
            ylim([-0.1 1.4])
            xlabel('time (ms)')
            ylabel('\gamma-gain')
            h=refline(0,1);set(h,'linestyle','--','Color',[0 0 0]);
            h=refline(0,0);set(h,'linestyle','--','Color',[0 0 0]);
            hold off
        end
        for j=5:6,
            subplot(3,2,j)
            xlabel('torsional (deg/s)')
            ylabel('vertical (deg/s)')
            xlim([-400 400])
            ylim([-400 400])
            hold off
        end
        subplot(3,2,1)
        title('torsion positive')
        subplot(3,2,2)
        title('torsion negative')
        fpos=get(gcf,'Position');
        set(gcf,'Name',filename,'Position',[fpos(1) fpos(2)-fpos(4) fpos(3) 2*fpos(4)]);
        if saveplots>0,
            [plotpath plotfname]=fileparts(filename);
            plotfilename=fullfile(plotpath,['HPTORS' int2str(saveplots) '.fig']);
            saveas(gcf,plotfilename,'fig')
            close(gcf);
        end
    end
    if ~isempty([idvertra; idvertlp]),
        figure
        if ~isempty(idvertra),
            subplot(3,2,5)
            whp=whh(idx100(:,idvertra),:);
            wep=weh(idx100(:,idvertra),:);
            plot(whp(:,1),whp(:,2),'-b',wep(:,1),wep(:,2),'-r');
            subplot(3,2,1)
            whp=reshape(whc(idx100(:,idvertra),1),[],numel(idvertra));
            wep=reshape(wec(idx100(:,idvertra),1),[],numel(idvertra));;
            plot(firstX:lastX-1,whp,'-b',firstX:lastX-1,wep,'-r');
            subplot(3,2,3)
            ggp=reshape(gg(idx100(:,idvertra)),[],numel(idvertra));
            plot(firstX:lastX-1,ggp,'-k');
        end
        if ~isempty(idvertlp),
            subplot(3,2,6)
            whp=whh(idx100(:,idvertlp),:);
            wep=weh(idx100(:,idvertlp),:);
            plot(whp(:,1),whp(:,2),'-b',wep(:,1),wep(:,2),'-r');
            subplot(3,2,2)
            whp=reshape(whc(idx100(:,idvertlp),1),[],numel(idvertlp));
            wep=reshape(wec(idx100(:,idvertlp),1),[],numel(idvertlp));;
            plot(firstX:lastX-1,whp,'-b',firstX:lastX-1,wep,'-r');
            subplot(3,2,4)
            ggp=reshape(gg(idx100(:,idvertlp)),[],numel(idvertlp));
            plot(firstX:lastX-1,ggp,'-k');
        end
        for j=1:2,
            subplot(3,2,j)
            xlim([-20 80])
            ylim([-400 400])
            xlabel('time (ms)')
            ylabel('velocity (deg/s)')
            h=refline(0,0);set(h,'linestyle','--','Color',[0 0 0]);
            hold off
        end
```

```
    for j=3:4,
        subplot(3,2,j)
        xlim([-20 80])
        ylim([-0.1 1.4])
        xlabel('time (ms)')
        ylabel('\gamma-gain')
        h=refline(0,1);set(h,'linestyle','--','Color',[0 0 0]);
        h=refline(0,0);set(h,'linestyle','--','Color',[0 0 0]);
        hold off
    end
    for j=5:6,
        subplot(3,2,j)
        xlabel('torsional (deg/s)')
        ylabel('vertical (deg/s)')
        xlim([-400 400])
        ylim([-400 400])
        hold off
    end
    subplot(3,2,1)
    title('RA')
    subplot(3,2,2)
    title('LP')
    fpos=get(gcf,'Position');
    set(gcf,'Name',filename,'Position',[fpos(1) fpos(2)-fpos(4) fpos(3) 2*fpos(4)]);
    if saveplots>0,
        [plotpath plotfname]=fileparts(filename);
        plotfilename=fullfile(plotpath,['HPRALP' int2str(saveplots) '.fig']);
        saveas(gcf,plotfilename,'fig')
        close(gcf);
    end
end
if ~isempty([idvertla; idvertrp]),
    figure
    if ~isempty(idvertla),
        subplot(3,2,5)
        whp=whh(idx100(:,idvertla),:);
        wep=weh(idx100(:,idvertla),:);
        plot(whp(:,1),whp(:,2),'-b',wep(:,1),wep(:,2),'-r');
        subplot(3,2,1)
        whp=reshape(whc(idx100(:,idvertla),2),[],numel(idvertla));
        wep=reshape(wec(idx100(:,idvertla),2),[],numel(idvertla));;
        plot(firstX:lastX-1,whp,'-b',firstX:lastX-1,wep,'-r');
        subplot(3,2,3)
        ggp=reshape(gg(idx100(:,idvertla)),[],numel(idvertla));
        plot(firstX:lastX-1,ggp,'-k');
    end
    if ~isempty(idvertrp),
        subplot(3,2,6)
        whp=whh(idx100(:,idvertrp),:);
        wep=weh(idx100(:,idvertrp),:);
        plot(whp(:,1),whp(:,2),'-b',wep(:,1),wep(:,2),'-r');
        subplot(3,2,2)
        whp=reshape(whc(idx100(:,idvertrp),2),[],numel(idvertrp));
        wep=reshape(wec(idx100(:,idvertrp),2),[],numel(idvertrp));;
        plot(firstX:lastX-1,whp,'-b',firstX:lastX-1,wep,'-r');
        subplot(3,2,4)
        ggp=reshape(gg(idx100(:,idvertrp)),[],numel(idvertrp));
        plot(firstX:lastX-1,ggp,'-k');
    end
    for j=1:2,
        subplot(3,2,j)
        xlim([-20 80])
        ylim([-400 400])
        xlabel('time (ms)')
        ylabel('velocity (deg/s)')
        h=refline(0,0);set(h,'linestyle','--','Color',[0 0 0]);
        hold off
    end
    for j=3:4,
        subplot(3,2,j)
        xlim([-20 80])
        ylim([-0.1 1.4])
        xlabel('time (ms)')
        ylabel('\gamma-gain')
        h=refline(0,1);set(h,'linestyle','--','Color',[0 0 0]);
        h=refline(0,0);set(h,'linestyle','--','Color',[0 0 0]);
        hold off
    end
```

```
    for j=5:6,
        subplot(3,2,j)
        xlabel('torsional (deg/s)')
        ylabel('vertical (deg/s)')
        xlim([-400 400])
        ylim([-400 400])
        hold off
    end
    subplot(3,2,1)
    title('LA')
    subplot(3,2,2)
    title('RP')
    fpos=get(gcf,'Position');
    set(gcf,'Name',filename,'Position',[fpos(1) fpos(2)-fpos(4) fpos(3) 2*fpos(4)]);
    if saveplots>0,
        [plotpath plotfname]=fileparts(filename);
        plotfilename=fullfile(plotpath,['HPLARP' int2str(saveplots) '.fig']);
        saveas(gcf,plotfilename,'fig')
        close(gcf);
    end
end
if ~isempty([idvertle; idvertri]),
    figure
    if ~isempty(idvertle),
        subplot(3,2,5)
        whp=whh(idx100(:,idvertle),:);
        wep=weh(idx100(:,idvertle),:);
        plot(whp(:,3),whp(:,2),'-b',wep(:,3),wep(:,2),'-r');
        subplot(3,2,1)
        whp=reshape(whh(idx100(:,idvertle),3),[],numel(idvertle));
        wep=reshape(weh(idx100(:,idvertle),3),[],numel(idvertle));;
        plot(firstX:lastX-1,whp,'-b',firstX:lastX-1,wep,'-r');
        subplot(3,2,3)
        ggp=reshape(gg(idx100(:,idvertle)),[],numel(idvertle));
        plot(firstX:lastX-1,ggp,'-k');
    end
    if ~isempty(idvertri),
        subplot(3,2,6)
        whp=whh(idx100(:,idvertri),:);
        wep=weh(idx100(:,idvertri),:);
        plot(whp(:,3),whp(:,2),'-b',wep(:,3),wep(:,2),'-r');
        subplot(3,2,2)
        whp=reshape(whh(idx100(:,idvertri),3),[],numel(idvertri));
        wep=reshape(weh(idx100(:,idvertri),3),[],numel(idvertri));;
        plot(firstX:lastX-1,whp,'-b',firstX:lastX-1,wep,'-r');
        subplot(3,2,4)
        ggp=reshape(gg(idx100(:,idvertri)),[],numel(idvertri));
        plot(firstX:lastX-1,ggp,'-k');
    end
    for j=1:2,
        subplot(3,2,j)
        xlim([-20 80])
        ylim([-400 400])
        xlabel('time (ms)')
        ylabel('velocity (deg/s)')
        h=refline(0,0);set(h,'linestyle','--','Color',[0 0 0]);
        hold off
    end
    for j=3:4,
        subplot(3,2,j)
        xlim([-20 80])
        ylim([-0.1 1.4])
        xlabel('time (ms)')
        ylabel('\gamma-gain')
        h=refline(0,1);set(h,'linestyle','--','Color',[0 0 0]);
        h=refline(0,0);set(h,'linestyle','--','Color',[0 0 0]);
        hold off
    end
    for j=5:6,
        subplot(3,2,j)
        xlabel('horizontal (deg/s)')
        ylabel('vertical (deg/s)')
        xlim([-400 400])
        ylim([-400 400])
        hold off
    end
    subplot(3,2,1)
    title('leftward')
```

```
            subplot(3,2,2)
            title('rightward')
            fpos=get(gcf,'Position');
            set(gcf,'Name',filename,'Position',[fpos(1) fpos(2)-fpos(4) fpos(3) 2*fpos(4)]);
            if saveplots>0,
                [plotpath plotfname]=fileparts(filename);
                plotfilename=fullfile(plotpath,['HPHORZ' int2str(saveplots) '.fig']);
                saveas(gcf,plotfilename,'fig')
                close(gcf);
            end
        end
    end
end
```

Gamma gain computation core

```
function [gg,ga]=gammagain(whh,weh,dt)
% function [gg,ga]=gammagain(whh,weh,dt)
% gg: gain gamma, see Aw et al J Neurophysiol 1996
% ga: gain |weh|/|whh|
% dt: if present, shift weh by n points to the left before calculating the
%     gains (uses CIRCSHIFT)
if nargin>2,
    if size(weh,1)==3,
        weh=circshift(weh',-dt)';
    else
        weh=circshift(weh,-dt);
    end
end
gg=(dot(-weh',whh')./dot(whh',whh'))';
ga=(dot(weh',weh')./dot(whh',whh'))'.^0.5;
```

Cross corection

```
function [c,lags]=crosscorr(x,y,range);
if nargin<3,
    range=round(max(size(x))*0.25):round(max(size(x))*0.75);
end
c=range*NaN;
lags=range*NaN;
for i=1:numel(range),
    r2=range+i-round(numel(range)/2);
    if isempty(find((r2<=0)|(r2>numel(y)))),
        cc=corrcoef(x(range),y(range+i-round(numel(range)/2)));
        c(i)=cc(2,1);
        lags(i)=i-round(numel(range)/2);
    end
end
```

Computation of means

```
function ggbi=getmeans(i,ggres,ggtimes,domedian);

if nargin<4,
    domedian=1; % compute means
end

ggbi=zeros(10,3+numel(ggtimes))*NaN;
if ~isempty(ggres),
    for j=1:8,
        idx=find(ggres(:,1)==j);
        if ~isempty(idx),
            if numel(idx)==1,
                ggbi(j,3:end-1)=ggres(idx,2:end);
            elseif domedian,
                ggbi(j,3:end-1)=median(ggres(idx,2:end));
            else
                ggbi(j,3:end-1)=mean(ggres(idx,2:end));
            end
            ggbi(j,end)=numel(idx);
        end
    end
    idx=find((ggres(:,1)==9)|(ggres(:,1)==11));
    if ~isempty(idx),
        if numel(idx)==1,
            ggbi(9,3:end-1)=ggres(idx,2:end);
        elseif domedian,
            ggbi(9,3:end-1)=median(ggres(idx,2:end));
        else
            ggbi(9,3:end-1)=mean(ggres(idx,2:end));
        end
        ggbi(9,end)=numel(idx);
    end
    idx=find((ggres(:,1)==10)|(ggres(:,1)==12));
    if ~isempty(idx),
        if numel(idx)==1,
            ggbi(10,3:end-1)=ggres(idx,2:end);
        elseif domedian,
            ggbi(10,3:end-1)=median(ggres(idx,2:end));
        else
            ggbi(10,3:end-1)=mean(ggres(idx,2:end));
        end
        ggbi(10,end)=numel(idx);
    end
end
ggbi(1:10,1)=i;
ggbi(1:10,2)=[1:10]'
```

VIII Attachment B

List of Publications and Papers

Publications in Journals with Impact Factor

1. **R. Brzezny**, S. Glasauer, O. Bayer, C. Siebold, and U. Buettner, **Head Impulses in Three Orthogonal Planes of Space: Influence of Age**, Ann NY Acad Sci 2003; 1004: p.473-477
IF 2003 - 1.892

2. **R. Brzezny**, M. Vyhnálek, J. Jeřábek, **Centrální a periferní polohové závrativé stavy**, Čes. a slov. Neurol. Neurochir., 68/101, 2005, No. 3, p. 148–153.
IF 2005 - 0.07

3. **R. Brzezny**, M. Vyhnálek, R. Černý, J. Jeřábek, **Onemocnění otolitových struktur rovnovážného systému. I. Patofyziologie a symptomatologie**, Čes. a slov. Neurol. Neurochir., 69/102, 2006, No. 4, p. 259–266.
IF 2005 - 0.07

4. **R. Brzezny**, M. Vyhnálek, R. Černý, J. Jeřábek, **Onemocnění otolitových struktur rovnovážného systému. II. Diagnostika**, Čes. a slov. Neurol. Neurochir., 69/102, 2006, No. 4, p. 267–271.
IF 2005 - 0.07

Publications in Journals without Impact Factor

1. M. Vyhnálek, **R. Brzezny,** J. Jeřábek, **Oční pohyby u specifických vývojových dyslexií,** Čes. a slov. Psychiat., 102, 2006, No. 5, pp. 256–260.

Abstracts in Conference Proceedings Published in Journals with Impact Factor

1. **R. Brzezny**, O. Bayer, S. Glasauer, U. Büttner, **Age-Related Changes in Three Dimensional Vestibulo-Ocular Reflex**, J Vestib Res, 14, 2004, No. 2,3, p. 294.
IF 2004 - 0.726

2. R. Černý, M. Vyhnálek, **R. Brzezny**, J. Jeřábek, **Saccadic eye movements examination in dyslexia,** Clin Neurophysiol.**,** 115, 2004, 8, p. 1960.
IF 2004 - 2.538

3. J. Jeřábek, R. Černý, P. Vrabec, **R. Brzezny**, M. Vyhnálek, **Benign paroxysmal positional vertigo-differential diagnosis, treatment,** Clin Neurophysiol.**,** 115, 2004, 8, p. 1961.
IF 2004 - 2.538

Articles and Abstracts in Conference Proceedings

1. **R. Brzezny,** D. Novák, D. Cuesta Frau, V. Eck, R. Černý, **Analýza pomalé fáze očních pohybů,** Česko-slovenská vědecká konference Inteligentní systémy ve zdravotní péči, Praha, Česká rep., Září 2002

2. J. Hozman, J. Štěpán, R. Černý, **R. Brzezny, Možnosti použití videosystému s následnou digitalizací pro pořízení a zpracování obrazových dat v kraniokorpografii**, Česko-slovenská vědecká konference Inteligentní systémy ve zdravotní péči, Praha, Česká rep., Září 2002

3. D. Novák, D. Cuesta-Frau, **R. Brzezny,** R. Cerny, V. Eck, L.Lhotska, **Method For Clinical Analysis Of Eye Movements Induced By Rotational Test**, 2nd European Medical & Biological Engineering Conference, Vienna, Austria. December 2002

4. D.Novák, D. Cuesta-Frau, **R. Brzezny**, R. Cerny, V. Eck, **Detection of Saccadic Eye Movements and Slow Phase Velocity Determination,** Biosignal 2002. Brno, Czech Republic. June 2002

5. D. Cuesta, P. Mico, M. Aboy, D. Novak, **R. Brzezny**, L. Samblas, D. Pastor, S. Sancho, **Biosignal Laboratory: A Software Tool for Biomedical Signal Processing and Analysis ,** 25th Annual International Conference of the IEEE Engineering in Medicine And Biology Society, Cancun, Mexico. 17-21.9,2003

6. **R. Brzezny**, S. Glasauer, H. von Lindeiner, M. Hoshi, M. Kiss, Ch. Siebold, J. Jerabek, U. Büttner, **Age-related Changes in Three-dimensional Human Vestibuloocular Reflex in Response to High-Acceleration Head Rotations**, Sixth IBRO World Congress of Neuroscience, Prague, Czech Rep., July 2003

7. M. Vyhnálek, R. Černý, **R. Brzezny**, J. Jeřábek: **Saccadic eye movements in developmental dyslexia,** Sixth IBRO World Congress od Neuroscience. Prague, Czech Rep., July 2003

8. D. Cuesta-Frau, D.Novak, M. Aboy, **R. Brzezny**, R. Cerny, J. Jerabek, **A Database of Occulographic Signals European Association for Speech, Signal and Image Processing,** 17th International EURASIP Conference BIOSIGNAL 2004, Brno, Czech Republic. June 2004

9. D. Novak, P.Kordik, M.Macas, **R.Brzezny,** M.Vyhnalek, L.Lhotska, **School Children Dyslexia Analysis using Self Organizing Maps**, 26th Annual International Conference of the IEEE Engineering in Medicine and Biology Society, San Francisco, USA, September 1-5, 2004

10. J. Jeřábek, P. Vrabec, **R. Brzezny**, R. Černý, **Diferenciální diagnostika polohového vertiga**, Kongres klinické neurologie, Praha, Česká rep., Prosinec 2002

11. R. Černý, J. Jeřábek, **R. Brzezny**, M. Bojar, **Periferní vestibulární syndrom cévního původu**, Kongres klinické neurologie, Praha, Česká rep., Prosinec 2002

Presentations of Research Results at the Students' Scientific Conferences of the 2nd School of Medicine

1. **R. Brzezny**, R. Černý, J. Jeřábek, **Vliv vergence na vestibulookulární relfex,** Neurologická klinika dospělých, UK 2. LF a FN Motol, STUDENTSKÁ VĚDECKÁ KONFERENCE 2002, Univerzita Karlova v Praze, 2. lékařská fakulta, Praha, Česká rep., duben 2002

2. **R. Brzezny**, S.Glasauer, H. von Lindeiner, Ch. Siebold, J. Jeřábek, U. Büttner, **Testování vestibulární hypotézy patomechanismu downbeat nystagmu vertikálními head impulsy**, STUDENTSKÁ VĚDECKÁ KONFERENCE 2003, Univerzita Karlova v Praze, 2. lékařská fakulta, Praha, Česká rep., duben 2003

3. **R. Brzezny**, S.Glasauer, O. Bayer, Ch. Siebold, U. Büttner, J. Jeřábek, **Vliv věku na funkci vestibulo-okulárního reflexu**, STUDENTSKÁ VĚDECKÁ KONFERENCE 2004, Univerzita Karlova v Praze, 2. lékařská fakulta, Praha, Česká rep., duben 2004

4. **R. Brzezny** et al., **Klinická diagnostika otolitových poruch,** STUDENTSKÁ VĚDECKÁ KONFERENCE 2006, Univerzita Karlova v Praze, 2. lékařská fakulta, Praha, Česká rep., květen 2006.

5. K. Strohm, R. Černý, J. Jeřábek, **R. Brzezny**, **Vyšetření vestibulárního aparátu – sinusový harmonický akcelerační test,** STUDENTSKÁ VĚDECKÁ KONFERENCE 2006, Univerzita Karlova v Praze, 2. lékařská fakulta, Praha, Česká rep., květen 2006.

Selection of Other Presentations and Posters

1. **R. Brzezny**, O. Bayer, S.Hoffmann, S. Glasauer, U. Büttner, **Head-Fixed and Head-Free Gaze Movements in Cerebellar Patients**, 15. Okulomotoriktreffen München - Tübingen – Zürich, München, Deutschland, Januar 2005

2. **R. Brzezny**, J. Steindler, M. Bláha, D. Štercl,L. Pekař, **Neurofyziologická peroperační monitorace operací páteře – indikační kritéria a kasuistiky**. Metastatická onemocnění páteře, Karviná,Česká rep., listopad 2005

3. P. Janouš, L. Pekař, **R. Brzezny**, J. Steindler, **Je mozečková ischemie absolutní indikací k operaci?**, Kunců v memoriál 2006, Praha, Česká rep., březen 2006

4. L. Pekař, **R. Brzezny**, J. Steindler, **DIAM – The Device for Intervertebral Assisted Motion**, The 13th International Meeting on Advanced Spine Techniques, Athens, Greece, July, 2006

5. J. Steindler, L. Pekař, **R. Brzezny**, **Clinical Experience with Minimally Invasive Microdiscectomy**, The 13th International Meeting on Advanced Spine Techniques, Athens, Greece, July, 2006

6. J. Steindler, L. Pekař, **R. Brzezny**, **METRx, – prvých sto nemocných po minimálně invazivní mikrodiskektomii lumbální páteře**, VII.výroční kongres České spondylochirurgické společnosti, Ostrava, Česká rep., září 2006

Research Reports

D. Novák, **R Brzezny**, M. Šorf, J. Jeřábek, R. Černý, **Analysis of Eye-Movement Slow Phase Velocity**. [Research Report]. Prague : CTU FEE, Department of Cybernetics, BIO Laboratory, 2001. BIO333-10/01. 18 p.